Technical Report

TR-09-20

Miniature canister corrosion experiment – results of operations to May 2008

N R Smart, A P Rance
Serco Technical and Assurance Services

July 2009

Svensk Kärnbränslehantering AB
Swedish Nuclear Fuel
and Waste Management Co

Box 250, SE-101 24 Stockholm
Phone +46 8 459 84 00

Miniature canister corrosion experiment – results of operations to May 2008

N R Smart, A P Rance
Serco Technical and Assurance Services

July 2009

Executive Summary

To ensure the safe encapsulation of spent nuclear fuel rods for geological disposal, SKB of Sweden are considering using the Copper-Iron Canister, which consists of an outer copper canister and a cast iron insert. Over the years a programme of laboratory work has been carried out to investigate a range of corrosion issues associated with the canister, including the possibility of expansion of the outer copper canister as a result of the anaerobic corrosion of the cast iron insert. Previous experimental work using stacks of test specimens has not shown any evidence of corrosion-induced expansion. However, as a further step in developing an understanding of the likely performance of the canister in a repository environment, Serco Technical and Assurance Services has set up a series of experiments in SKB's Äspö Hard Rock Laboratory (HRL) using inactive model canisters, in which leaks were deliberately introduced into the outer copper canister while surrounded by bentonite, with the aim of obtaining information about the internal corrosion evolution of the internal environment. The experiments use five small-scale model canisters that simulate the main features of the SKB canister design. The main aim of the work is to examine how corrosion of the cast iron insert will evolve if a leak is present in the outer copper canister.

This report describes how the experiments were set up and presents the results obtained from the start of the experiments in late 2006 up to May 2008. The model canisters consist of an outer copper body fabricated from 150 mm OD copper tubing, of the same grade of copper as that used for the full size canisters, and end caps fabricated from the lid material used for the full-scale canister assemblies. The end caps were electron-beam welded. The canisters contain at least one 1 mm defect which was introduced in the copper body near the weld area.

Five boreholes were drilled at a 10 slope to the horizontal at locations in the Äspö Hard Rock Laboratory where a plentiful supply of water exists. Each borehole contains one model canister assembly. In order to expose the model canisters to water that has a representative chemistry, the canisters are surrounded by either compacted bentonite (one experiment), in which case the rate of water transport to the surface of the canister is low, or low density bentonite (three experiments), in which case the rate of water transport is high. In a fifth experiment the model canister is exposed directly to unconditioned groundwater. Each canister is surrounded by a supporting cage, which contains bentonite at the required density and a range of sensors (e.g. reference electrodes, E_h electrodes, copper and iron electrodes), weight loss corrosion coupons and stress corrosion test pieces (U-bends and WOL specimens). Two canisters are monitored using strain gauges. The electrical connections to the sensors are taken out through a flange at the entrance to the boreholes. Datalogging equipment is located near the boreholes and data are transferred to the local intranet system and the external internet for analysis.

The report presents the results of a set of water analyses which were carried out during 2007. Gas composition and microbial activity were also measured. These data show an increase in the iron concentration inside the support cage, together with a decrease in the pH. There was also an increase in the concentration of nickel and chromium inside the support cage. The decrease in pH and the increase in metal ion concentration may be due to microbial activity affecting the corrosion behaviour of the iron-based metals in the experiment (i.e. cast iron and/or stainless steel).

The electrochemical measurements provide an in situ E_h value which is compatible with published data. The E_h value inside the boreholes decreased with time as oxygen was consumed by microbial activity and reaction with minerals in the surrounding rock. Corrosion rates were obtained using a range of electrochemical methods. The copper corrosion rate had a maximum value of 3.5 $\mu m\ yr^{-1}$, which is consistent with data reported in the literature. The electrochemically measured corrosion rate of iron was considerably higher (> 1 $mm\ yr^{-1}$ in some cases) than expected on the basis of laboratory experiments in the absence of microbial activity. These corrosion rates will be corroborated using the weight loss coupons when the experiments are dismantled for examination in due course, on a timescale to be agreed.

Contents

1 Introduction

To ensure the safe encapsulation of spent nuclear fuel rods for geological disposal, SKB of Sweden are considering using the Copper-Iron Canister, which consists of an outer copper canister and a cast iron insert, as shown schematically in Figure 1-1. A programme of work has been carried out over a number of years to investigate a range of corrosion issues associated with the canister, including the possibility of expansion of the outer copper canister as a result of the anaerobic corrosion of the cast iron insert. Experimental work using stacks of copper and iron test specimens has not shown any evidence of corrosion-induced expansion /1/. However, as a further step in developing an understanding of the likely performance of the canister in a repository environment, Serco Technical and Assurance Services has set up a series of experiments in SKB's Äspö Hard Rock Laboratory (HRL) using inactive model canisters, in which leaks were deliberately introduced into the outer copper canister while surrounded by bentonite, with the aim of obtaining information about the internal corrosion evolution of the internal environment /2/.

The experiments used small-scale model canisters that simulate the main features of the SKB canister design. The main aim of the work was to examine how the corrosion of the cast iron insert will develop if a leak is introduced into the outer copper canister. This would address such issues as:

- Does water penetrate into the annulus through a small defect?
- How does corrosion product spread around the annulus from the leak point?
- Does the formation of corrosion product in a constricted annulus cause any expansive damage to the copper canister?
- What is the effect of water penetration on the insert lid seal?
- Is there any detectable corrosion at the copper welds?
- Are there any deleterious galvanic interactions between copper and cast iron?
- Does corrosion lead to failure of the lid on the iron insert?

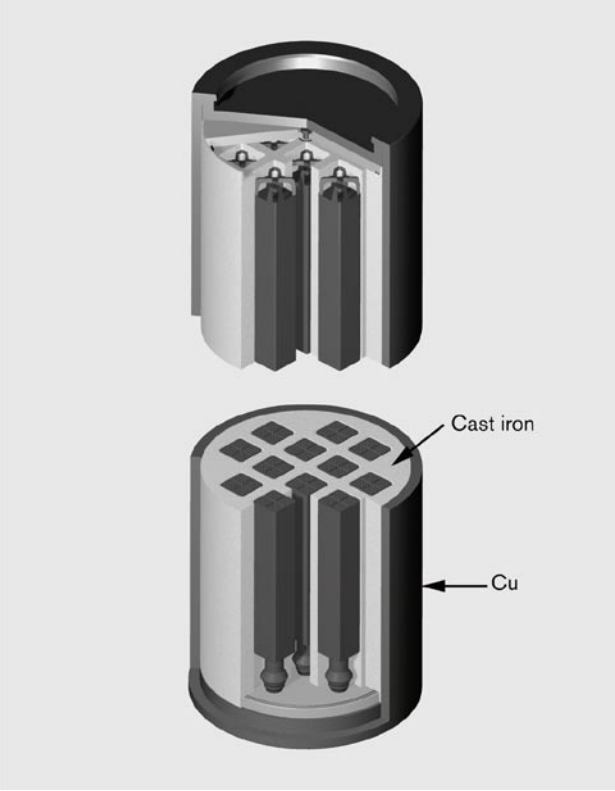

Figure 1-1. *Schematic diagram of SKB Copper-Iron Canister.*

These experiments were set up between September 2006 and February 2007. In addition to setting up the model canisters, corrosion experiments using separate corrosion coupons were also set up in the same boreholes as the ones used for the model canister experiments. A number of parameters were also measured in situ to define the test environment during the experiments. Initial set up work and sensor validation was carried out in the Serco laboratory at Culham, U.K. and subsequently, when the experimental techniques were developed, the experiments were set up at SKB's HRL at Äspö, Sweden by placing model canisters into specially prepared boreholes in a rock face of the laboratory. The work programme was carried out in a number of well-defined stages, as follows:

1. Design and planning.
2. Procurement.
3. Laboratory trials.
4. Installation of in-situ tests.
5. Monitoring.

The detailed design of the experiments is presented in reference /3/, which was prepared following discussions with staff at the SKB Äspö HRL, Clay Technology, Lund, Sweden and TWI, U.K. Installation was completed in the spring of 2007 and the programme has now entered the monitoring stage. The electrical wiring was upgraded in June 2007 to enable easier access to the connectors. The purpose of the present report is to describe the details of how the experiments were set up and to present the results obtained during the first year of operation, up to May 2008.

2 Overall design of experiment

In preliminary discussions with SKB a number of parameters were agreed regarding the overall design of the experiments, as follows:

- The experiments should be carried out at ambient temperature in the Äspö HRL (i.e. no secondary heating is used). The ambient temperature in the underground rock laboratory is 15°C.
- Several canisters should be set up, to allow a rolling programme of destructive examination. Each container is set up in its own individual borehole.
- A relatively thin permeable layer of bentonite should be placed around the canisters to condition the incoming groundwater, but also to allow sufficient water to permeate through the bentonite to reach the model canister.
- At least one 1 mm diameter hole should be made in the outer vessel of the model canisters.
- The inner canister should use a Viton gasket, so that the corrosion processes around such a gasket can be investigated.

In order to simulate the correct environment around the model canister a stainless steel cage was constructed around the canister, to contain bentonite. A small number of environmental sensors and corrosion test pieces were placed in the test environment around the model canisters.

3 Construction of model canister assemblies

3.1 Design of model canisters

A design for the model canisters was produced after considering the design of the full size canisters, as given in reference /4/. The design of the model canisters reflects the main features of the SKB canister design but does not have the fine details of the full size insert because they are unlikely to affect the corrosion performance of the model canisters. The main features of the model canister are:

- An outer copper cylindrical body.
- A copper lid and base, which is electron-beam welded to the body.
- A cast iron insert.
- The insert has a lid attached by a central bolt, with a Viton gasket around it.
- The insert contains four cylindrical holes simulating the fuel rod channels.
- There is a narrow annulus between the cast iron insert and the copper outer container.

The dimensions of the model canisters were determined by the size of the boreholes that can be produced in the Äspö HRL using standard equipment. At the underground laboratory the standard borehole sizes are 300 mm and 70 mm diameter. It was decided that 70 mm would be too small, so the model canister design was based on using a 300 mm diameter hole. This allowed the design to be based on the diameter of readily available copper tube (150 mm). In addition it was necessary to use a diameter of model canister that would allow bentonite to be placed around it inside a supporting cage.

The design of the model canister is shown in Figure 3-1 to Figure 3-4 and the components after manufacture are shown in Figure 3-5 and Figure 3-6. After machining from 150 mm outside diameter (OD) stock material with a 10 mm wall thickness, the OD of the copper canister was 145 mm, with an internal diameter (ID) of 130 mm and a wall thickness of 7.5 mm. This wall thickness is in scale with the 145 mm outer diameter. The diameter of the cast iron insert was nominally 129 mm, but it was machined to give a loose push fit into the outer copper canister, such that the width of the annulus was in the range 10–30 μm (based on actual measurements of the inner cast iron insert and the outer copper canister body). The annulus needed to be large enough to allow water entry, but narrow enough to allow the annulus to fill with corrosion product on a realistic timescale. Capillary action will encourage wetting of the surface of the cast iron. The surface of the insert will also be exposed to water vapour, which is sufficient to cause anaerobic corrosion /5/. The overall length of the model canister was 315 mm with a further protrusion of a centre insertion stub of 35 mm long at one end (see Figure 3-1 and Figure 3-2).

The 25 mm diameter centre stub on the lid was included to aid insertion and extraction of the canister and for the connection of electrical wiring to the canister. The inclusion of the stub on the tube cap end means that the material for the canister end caps was required to be 50 mm in thickness.

Although the cast iron insert for the full size canister uses a double O-ring design, it was agreed with SKB that it was only necessary to use a single O-ring in the model canister insert. The lid did not need to have a chamfer on it and a parallel-sided sliding push fit lid with a single O-ring was used. The insert had a flat bottom. On the full-scale canister the clearance between the top of the insert and the bottom of the lid will be ~ 2mm. In the model canister it was less than 0.5 mm. The central bolt also had an O-ring seal (this is not shown in the drawings in report TR-02-07).

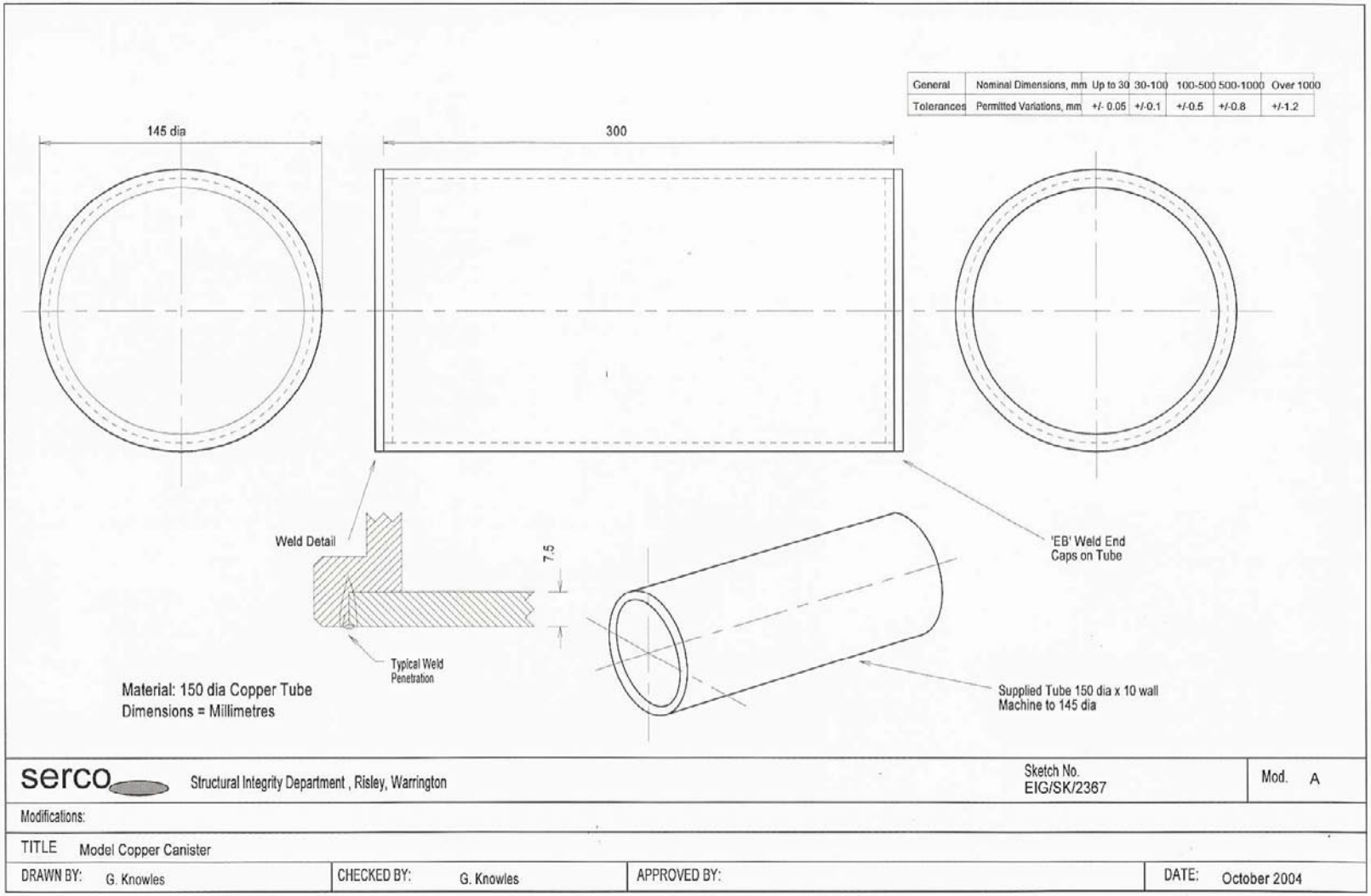

Figure 3-1. *Design of model canister – body of model canister.*

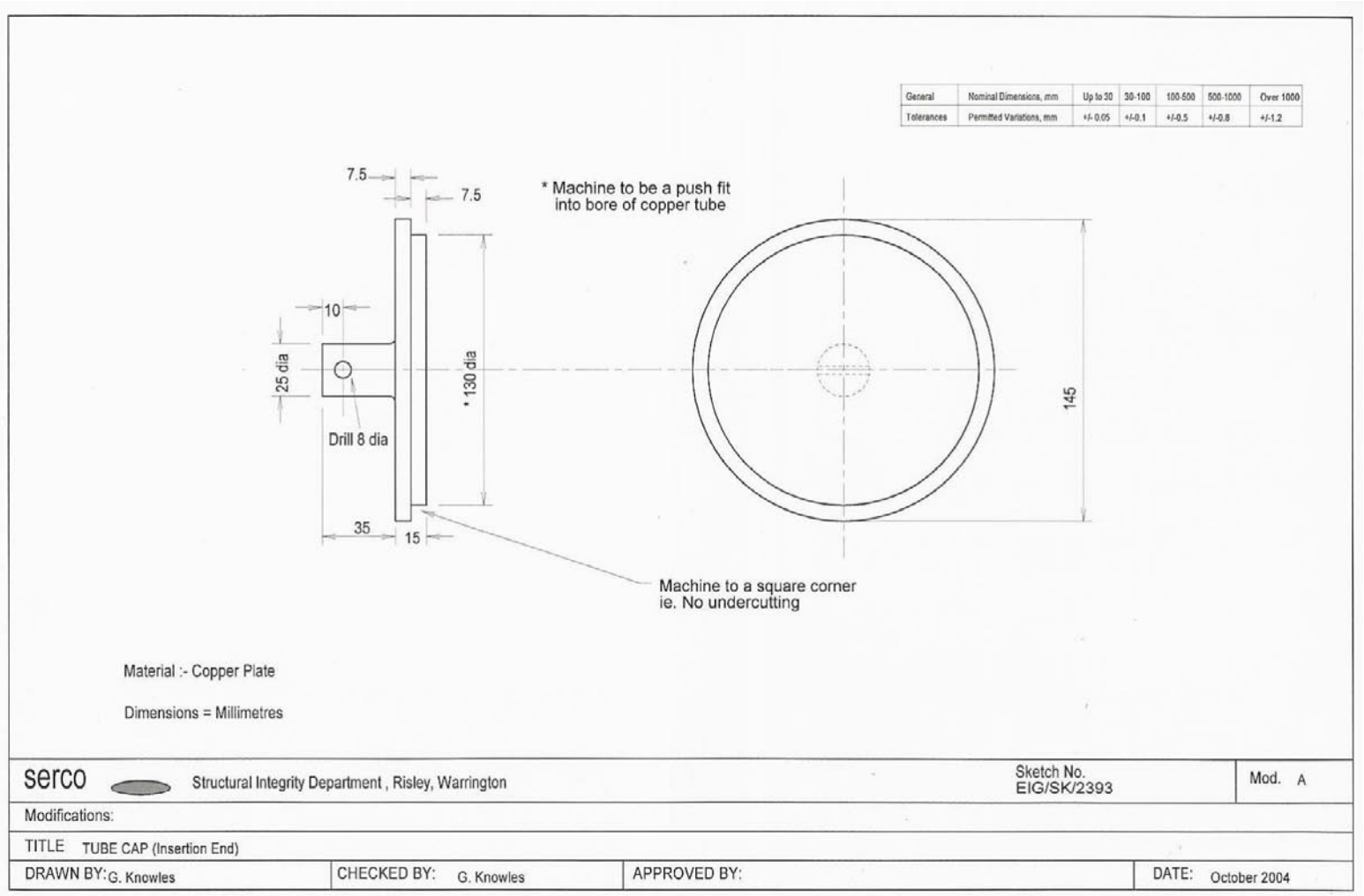

Figure 3-2. *Design of model canister – end cap with connector.*

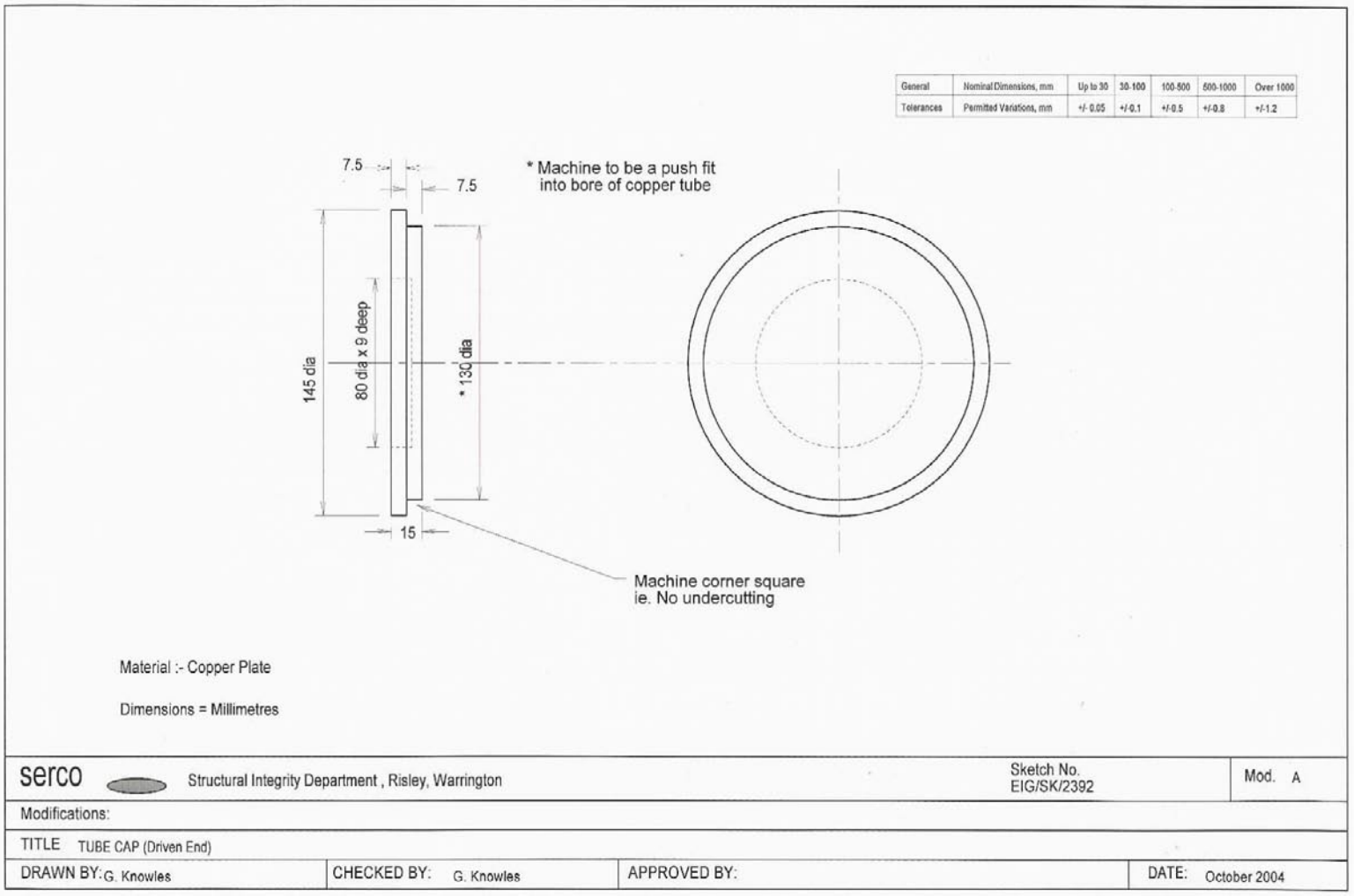

Figure 3-3. *Design of model canister – end cap without connector.*

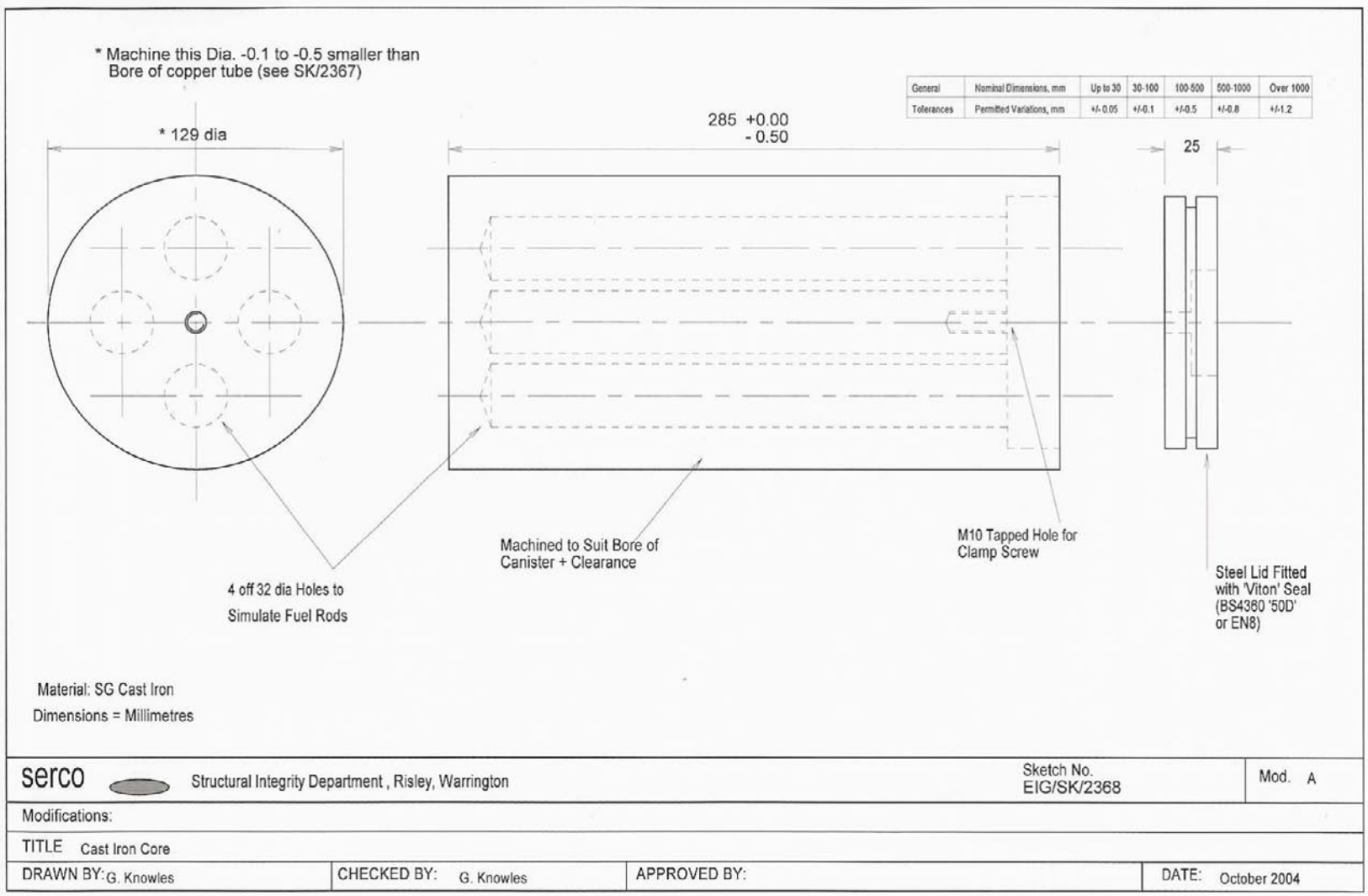

Figure 3-4. *Design of cast iron insert.*

Figure 3-5. *Copper components of miniature canisters.*

Figure 3-6. *Components of miniature canisters.*

3.2 Materials

3.2.1 Copper components

Outokumpu (Finland) supplied a piece of copper tube (EN 13600-CuOFE-R290-RND 150 x 10, Cu-OFE EN 1876:1988, UNS C10100 Ref. KTS001). This material had the composition shown in Table 3-1 with the mechanical properties shown in Table 3-2. It is the same grade of material as that used for the full size SKB canisters. It was 150 mm outside diameter and 10 mm wall thickness. The end caps for the model canisters were fabricated from full size lid material, supplied by SKB.

3.2.2 Ferrous components

The material used for the lid on the cast iron insert in the full size canister will be a steel: EN 10025 S355 (BS4360 50D; Swedish standard 14.21.72). The same material was used for the lid on the insert in the model canister. Its composition is shown in Table 3-3. The steel used for the liner of the fuel pin channels in the full size canister is EN 10015 S355 J2H, with the composition shown in Table 3-3. This material was used to line the four simulated fuel pin channels in the cast iron insert of the model canister. It was used as a push fit into the insert, rather than used as a former for casting the iron, as it would be in the fabrication of a full size canister /4/. The central bolt holding the steel lid to the insert was made from S355JR.

Table 3-1. Chemical composition of copper tube at two different positions (data from Outokumpu).

Cast no		Spec.	Meas. 105 2–3/1 Bottom	105 2–3/1 Top
Cu	% min	99.99	99.993	99.993
Ag	ppm max	25	14.4	14.3
As	“	5	1.3	1.3
Bi	“	1	<0.2	0.5
Cd	“	1	<0.4	<0.4
Fe	“	10	0.5	0.7
H	“	<0.6	0.46	0.39
Hg	“	1	<0.5	<0.5
Mn	“	0.5	<0.1	0.1
Ni	”	10	0.7	0.7
O	”	<5	1.7	2
P	”	30–70	32	38
Pb	“	5	<0.6	0.7
S	“	<8	7	6.9
Sb	“	4	2	2
Se	”	3	1	1.1
Sn	”	2	<0.7	<0.7
Te	”	2	<1	<1
Zn	”	1	<1	<1

Table 3-2. Mechanical properties of copper tube according to EN 10 002-1 (tensile test transversal direction, data from Outokumpu).

Pos.	Tensile strength, Rm, N/mm²	0.2% proof stress $Rp_{0.2}$ N/mm²	Elongation A5%	Hardness HV10	Initial grain size mm
	290–360	min 250	min 6		
1	319	307	14	101	0.250

Table 3-3. Typical composition of cast iron insert material (wt%).

Element	Cast Iron Insert (typical composition)	Steel end caps (actual analysis)	Steel tubes (actual analysis)
C	3.52	0.16	0.10
Si	2.66	0.18	0.17
Mn	0.092	1.47	0.46
S	0.006	0.007	0.006
P	0.037	0.016	0.011
Mg	0.067		
Cu	0.006		

3.2.3 O-rings

The material used for the O-ring seal on the insert and around the central securing bolt was Viton (general purpose, Grade A).

3.2.4 Cast Iron Insert

The cast iron insert assembly (Figure 3-4) was manufactured from BS2789 Grade 420/12 (equivalent to EN 1563 GJS 400-15 and Swedish grade SIS 140717 0717-00) material. The composition of the cast iron insert material is shown in Table 3-3. This material has a spheroidal graphite micro-structure. The insert had four equi-spaced drilled holes down its length to simulate fuel rod holes. These holes were lined with steel tubes of an equivalent grade to the Swedish EN 10015 S355 J2H specification.

The cast iron insert was fitted with a steel lid (BS4360 '50D') to seal the fuel rod holes. The lid was fitted with a Viton O ring seal to stop water ingress and was secured by a single central bolt fitted with a Viton seal under the head. The lid on the cast iron insert was sealed with air inside.

The surface area of the cast iron insert was ~0.14 m^2. It will corrode anaerobically to produce hydrogen, which at a gas generation rate of 2 $dm^3\ m^{-2}\ yr^{-1}$ /5/ would give a total evolved volume of gas of ~1.4 dm^3 of hydrogen, at STP, over a period of 5 years. At the hydraulic pressure exerted by the groundwater (i.e. ~40 bars at 400 m depth), this volume of gas will be reduced to 35 cm^3, compared to an annulus volume of 1.16 cm^3 for a 0.01 mm wide annulus, or 11.6 cm^3 for a 0.1 mm wide annulus.

3.3 Outer Canister Defects

The most probable through-wall defect in a full size canister would be a large surface defect, linked to a series of interlinking small pores, and the most likely position for such a defect would be near the weld itself. In the model canister experiments, 1 mm diameter defects were introduced into the wall of the model canister just below the welded region near the top cap. In most model canisters a single defect was used, but in two experiments two holes were introduced. The orientation of the defects was arranged slightly differently in each of the containers because the position of the hole in the canisters relative to its orientation could be important in relation to the ingress of water through the hole. The ingress of water through a defect in the copper canister into the annulus has been modelled /6/. The rate of ingress is determined by a number of factors including the size of the defect, the location of the defect, the rate of corrosion and hence the rate of generation of hydrogen by anaerobic corrosion, but most of all by the permeability of the external bentonite. The defect holes were machined by careful drilling prior to welding of the canister.

3.4 Assembly of model canisters and welding

On completion of all machining operations the copper components were cleaned in a solution of citric acid (5 wt%) to remove superficial surface staining. In order to ensure that the cast iron surfaces were as reactive as possible, they were pickled in hydrochloric acid and washed in demineralised water before mounting in the copper canisters. The components were assembled and sent to TWI to weld the lids and end caps on to the end of the canisters. The whole canister assembly was placed inside the vacuum chamber of the electron beam welding facility. The canister assembly was then evacuated overnight through the pre-drilled defects, ready for commencement of welding.

The welding was conducted by TWI at Abington, U.K. using the reduced pressure electron beam method. During welding it was necessary to have copper backing behind the welded joint rather than cast iron so that the copper was not welded to the cast iron. The lid was designed to take this into account. TWI carried out trial welds prior to welding the model canisters.

The small diameter defect holes in the outer wall of the canister allowed evacuation of the internal volume of the assembled canister, thus ensuring satisfactory welding. During welding the test piece was supported at one end in a rotating chuck and at the other end using a set of rollers. The weld speed was 500 mm/min. After welding, TWI carried out an NDT examination of the completed EB welds to confirm the integrity of the welds.

After welding, the defects in the walls of the copper canister were sealed with a rubber pad to minimise the ingress of air into the annulus between the copper outer canister and the cast iron insert. The pad was removed only when the copper canisters were placed into the support cages and the assemblies were introduced into the boreholes at Äspö.

3.5 Support cage

The experiments were carried out by mounting the miniature canisters inside a perforated stainless steel cage, which was designed to contain bentonite around the model canisters and to withstand its swelling pressure. The design of the support cages around the model canisters is shown in Figure 3-7 and the layout of the model canister inside the support cage is shown in Figure 3-8. The cage consisted of two perforated concentric tubes, between which bentonite of a low density was placed (Experiments 1 to 3). The bentonite was retained by the use of sintered stainless steel filters, which allowed the surrounding groundwater to penetrate into the inner cavity where the model canisters are situated. The concentric cylinders were manufactured from standard size stainless steel tubing. The filters were provided by Tridelta Siperm GmbH, Germany; they were 5 mm thick with a 10 μm pore size. End caps were attached at each end of the assembly using a series of bolts. The cylindrical filters were sealed at each end using flat polymeric gaskets (Viton). To ensure corrosion resistance the supporting cage was made from 316L stainless steel. It is likely that some localised corrosion of the stainless steel will occur while air is still present in the boreholes given the high chloride content of the surrounding groundwater although once the oxygen has been consumed localised corrosion should reduce. Sulphate Reducing Bacteria (SRBs) are a possible cause of corrosion of the stainless steel in the test environment.

Insulated pressure fittings (e.g. Conax fittings) were mounted in the plates at each end of the cage, to allow electrical connections to be taken out through the end caps of the cage assembly. The leads were taken out through tubular conduits to the borehole flange to prevent contact with the surrounding groundwater. Connections to the conduits were made using compression fittings (Swagelok).

The model canisters rested on circular PEEK plates so that they were not in direct electrical contact with the stainless steel support cage. Rings of insulating material were also placed around the canisters to prevent electrical contact.

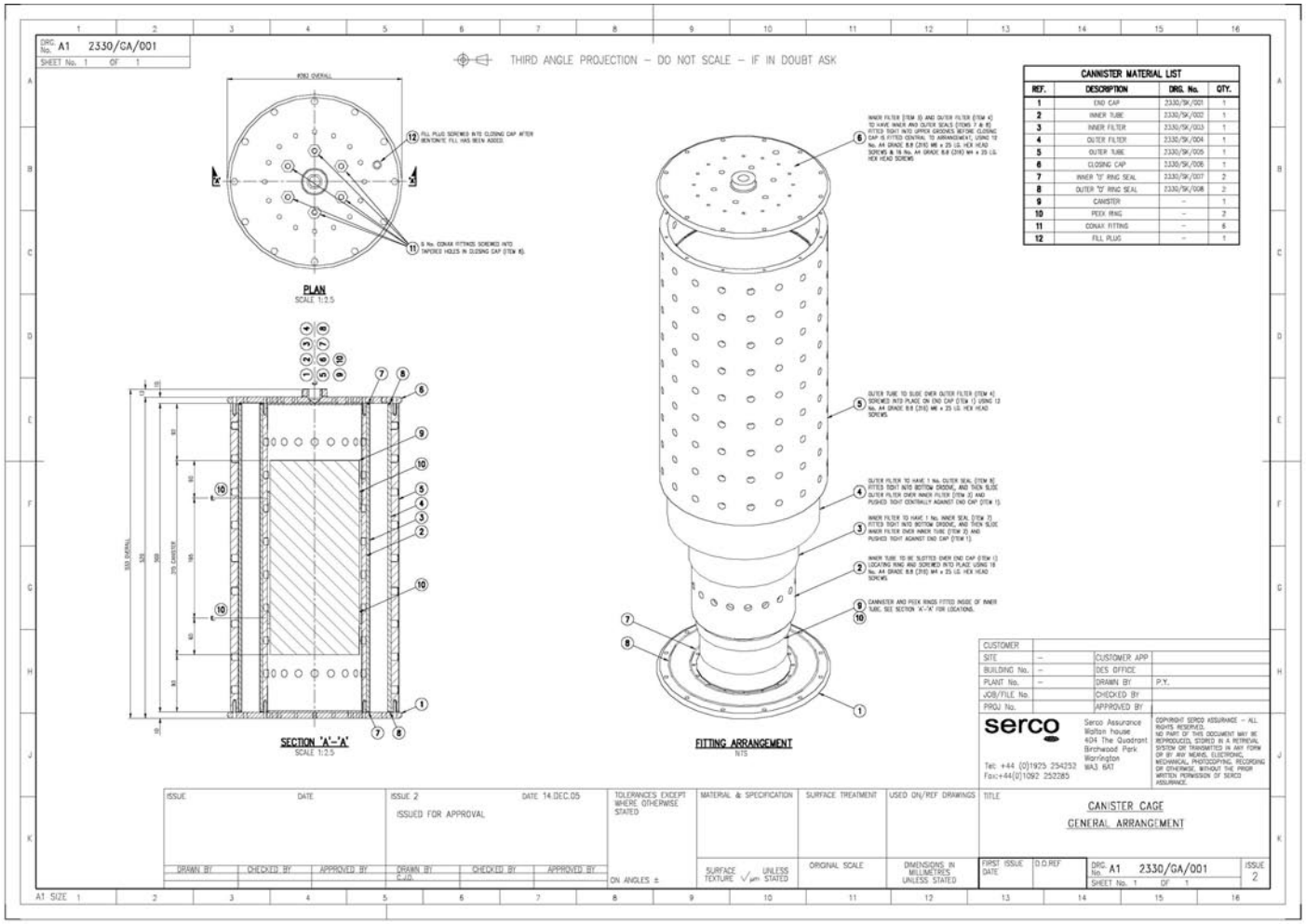

Figure 3-7. *Support cage – general arrangement.*

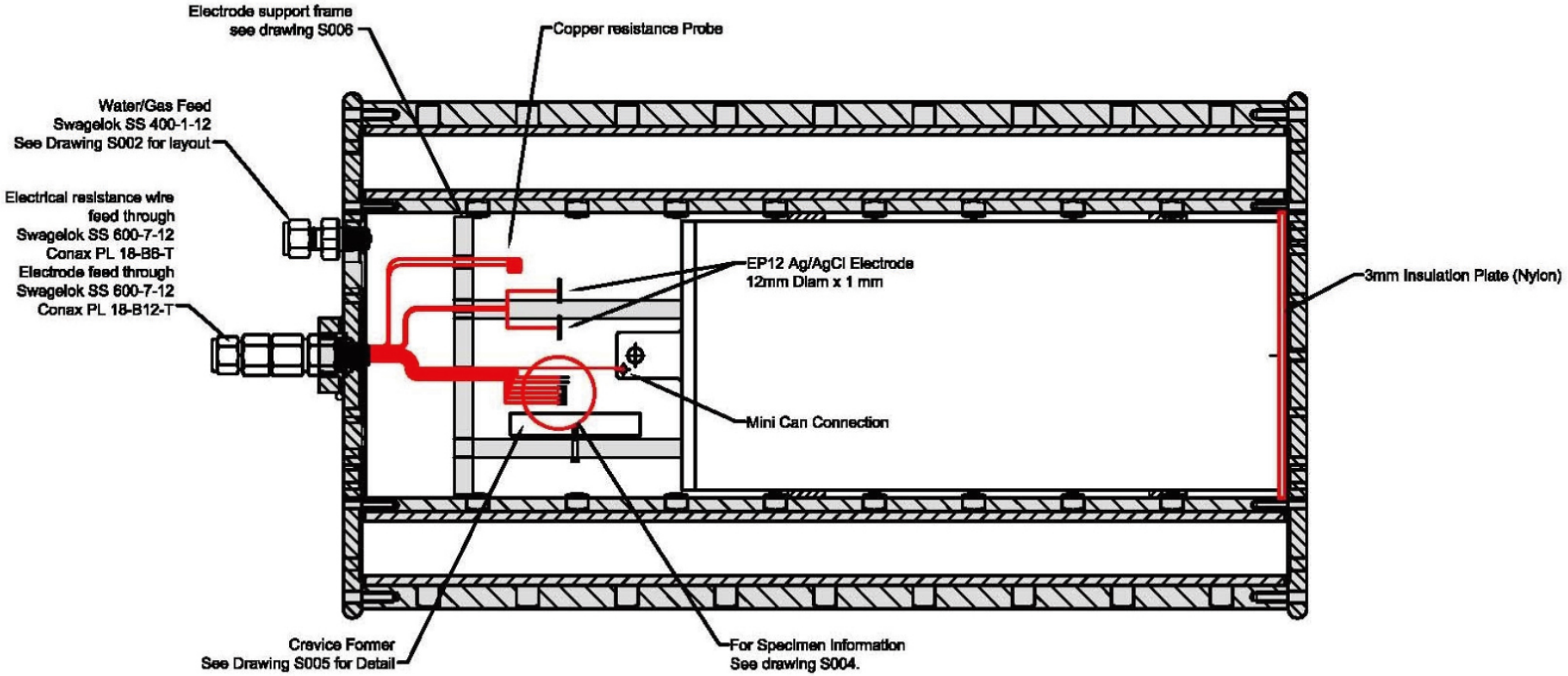

Figure 3-8. *Layout of model canister and sensors inside support cage.*

3.6 Test conditions

A summary of the test environments inside the five experiments is given in Table 3-4. In three out of the five proposed experiments a layer of bentonite was mounted inside an annulus between two concentric cylinders around the model canister. The purpose of the bentonite is to condition the chemistry of the incoming groundwater so that it is representative of the repository situation. The cage prevents direct contact between the bentonite and the surface of the canister in order to avoid blockage of the defect. The bentonite holder was filled with compacted bentonite pellets mixed with bentonite powder at a density designed to give a high permeability and low swelling pressure. The aim was to allow bentonite-conditioned groundwater to reach the model canister rapidly and to allow it to wet the annulus between the inner and outer canisters of the model canister.

In the fourth experiment the model canister was surrounded by compacted bentonite, to simulate as exactly as possible the real exposure conditions in the repository, although in this situation it is expected that the extent of corrosion will be limited by the supply of water through the compacted, low permeability bentonite /6/. In this experiment, where the model canister was directly surrounded by compacted bentonite, there was no inner cylinder and hence no annulus of bentonite, but rings of saturated compacted bentonite were machined to slide over the model canister, inside the outer cylinder. Clay Technology, Sweden machined the rings to size. The use of fully saturated bentonite should minimise the time required to achieve full saturation and hence the full swelling pressure of the bentonite. The thickness of the outer cylinder and the outer filter cylinder was selected to withstand the swelling pressure of compacted bentonite (7 MPa). Small holes or slots were machined in the compact bentonite as necessary to allow installation of electrodes, corrosion coupons and leads in the compacted bentonite and strain gauges on the surface of the model canister.

The fifth experiment was set up without any bentonite around the model canister, to examine whether a biofilm develops on the surface of the canister and to examine its effect on corrosion behaviour. For this experiment, where the canister is directly exposed to groundwater, the perforated steel cage was used to hold the model canister, but no bentonite was placed inside it. Consequently the groundwater will enter directly into the vicinity of the model canister.

Table 3-4. Summary of test conditions for model canister experiments.

Experiment number (borehole number)	Environment and defect details
1 (KA3386A02)	Low density, high permeability bentonite in annulus around model canister. Single defect near top weld, pointing vertically upwards.
2 (KA3386A03)	Low density, high permeability bentonite in annulus around model canister. Single defect near top weld, pointing vertically downwards.
3 (KA3386A04)	Low density, high permeability bentonite in annulus around model canister. Two defects, one near top weld, pointing vertically upwards, near bottom weld, pointing vertically downwards.
4 (KA3386A05)	Compacted bentonite. Single defect near top weld, pointing vertically downwards.
5 (KA3386A06)	No bentonite, direct contact of groundwater on model canister. Two defects, both near top weld, one pointing vertically upwards, the other vertically downwards.

4 Monitoring performance of model canisters

A number of parameters could be measured to monitor the experiment, including:

- Temperature and humidity,
- redox potential and electrochemical potential of the canister,
- pH and chloride concentration,
- strain at the canister surface, to detect whether any swelling of the canister due to internal corrosion is occurring,
- pressure,
- water composition.

However, in order to simplify the experiment it was agreed that only the essential parameters were to be measured, as discussed below.

4.1 Temperature and humidity

Temperature and humidity probes are already used on the prototype repository experiment /7–9/. However, it was decided that there was no need to measure the temperature, as it is fairly uniform throughout the HRL and the temperature is measured in other ongoing experiments. Similarly humidity is probably not relevant given that a high flow rate is required and that in most experiments, except the one in compacted bentonite, the canisters are surrounded by liquid water.

4.2 Electrochemical potential

In order to measure the overall corrosion potential of the model canisters and the redox potential of the environment it is necessary to employ stable reference electrodes. There are a number of commercial reference electrodes available and selected ones were tested in laboratory trials prior to installation in the model canister experiment, to ensure that they are stable and reliable. These electrodes were:

- Solid state silver-silver chloride reference disc electrodes (e.g. World precision instruments EP series).
- Liquid filled reference electrodes (e.g. World precision instruments EP series Dry-Ref reference electrodes) which are available encapsulated in a range of materials, including epoxy, Isoplast, PTFE, PVC, polypropylene).
- Long-life reference electrodes for cathodic protection (CP) purposes (e.g. Silvion reference electrodes). These are larger than the other types of reference electrode but have a long service life.

After carrying out the laboratory trials it was decided to use two small disc silver-silver chloride reference disc electrodes in each experiment, which were mounted inside the support cage, together with a large Silvion reference electrode outside the support cage, but inside the borehole as backup in case of any failures of the more delicate, less robust disc electrodes. These reference electrodes are shown in Figure 4-1.

The redox potential of the environment was measured by means of a gold wire and a platinum flag located near to the model canister inside the support cage and an Eh sensor located outside the supporting cage (Cumberland Electrochemical Ltd Pt/Ir mixed metal oxide, MOx, probe, which has been successfully used embedded in cementitious grout to monitor fluctuations in redox conditions).

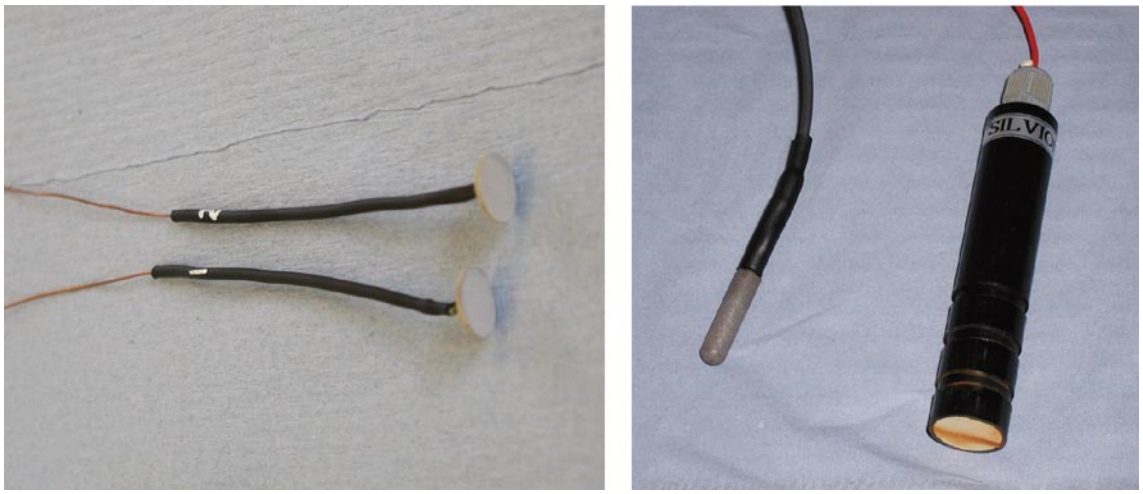

Figure 4-1. *Reference electrodes and Eh probes used in model canister experiments. Left – WPI Ag/AgCl reference electrode; Right (LHS) Mixed metal E_h probe, (RHS) Silvion silver-silver chloride reference electrode.*

Laboratory trials were carried out using the Eh probes, reference electrodes and strain gauges inside a Hastelloy autoclave containing Äspö groundwater, which was pressurised to 7 MPa with nitrogen to simulate the required hydraulic head. The electrodes were run for a few weeks to demonstrate that they run reliably under the required operational conditions. The sensors were supported from a nylon support rack inside the void above the model canister (Figure 4-2). All reference electrodes were calibrated before installation.

4.3 Water analysis

After installation water samples were taken for analysis at periodic intervals. Äspö staff carried out the required water analysis or sub-contracted the analysis to an appropriate laboratory. Water samples were extracted through stainless steel tubes that passed out through the borehole flange. For each borehole it was possible to extract samples from both within the support cage itself and from the borehole surrounding the model canister experiment. For the first few months (up to 22/5/2007) the sample volume was 6.5 litres per sample; thereafter the sample volume was reduced to 1.2 litres. There was a continuous bleed of gas from each borehole flange to prevent the development of a gas-filled space within the borehole. This gas is assumed to be nitrogen.

The concentration of dissolved gases was also determined by Microbial Analytics Sweden AB. The volume of the inner Minican compartment is approximately 1.5 litres and it was judged important to keep the sampling volume as small as possible, to avoid sample dilution. The samples were taken using PVB samplers that can take pressurized samples; the sampler was used for chemistry, gas and microbiological analyses. Each sampler has a volume of about 180 mL. The analyses were taken when the experiments had not been drained for water sampling for at least four weeks, to allow concentrations to build up.

The concentration of the following gases was analysed: H_2, He, O_2, N_2, Ar, CH_4, CO_2, CO, C_2H_6, C_2H_4, C_2H_2, C_3H_8, C_3H_6. The microbial analysis was used to measure the following:

1. The total number of microorganisms.
2. The number of aerobic cultivable bacteria.
3. Biomass measured as adenosine-three-phosphate.
4. The most probable number of the following types of bacteria were determined: sulphate reducing and autotrophic acetogens. These bacteria were chosen because they are likely to have the strongest effect on the corrosion behaviour of metals.

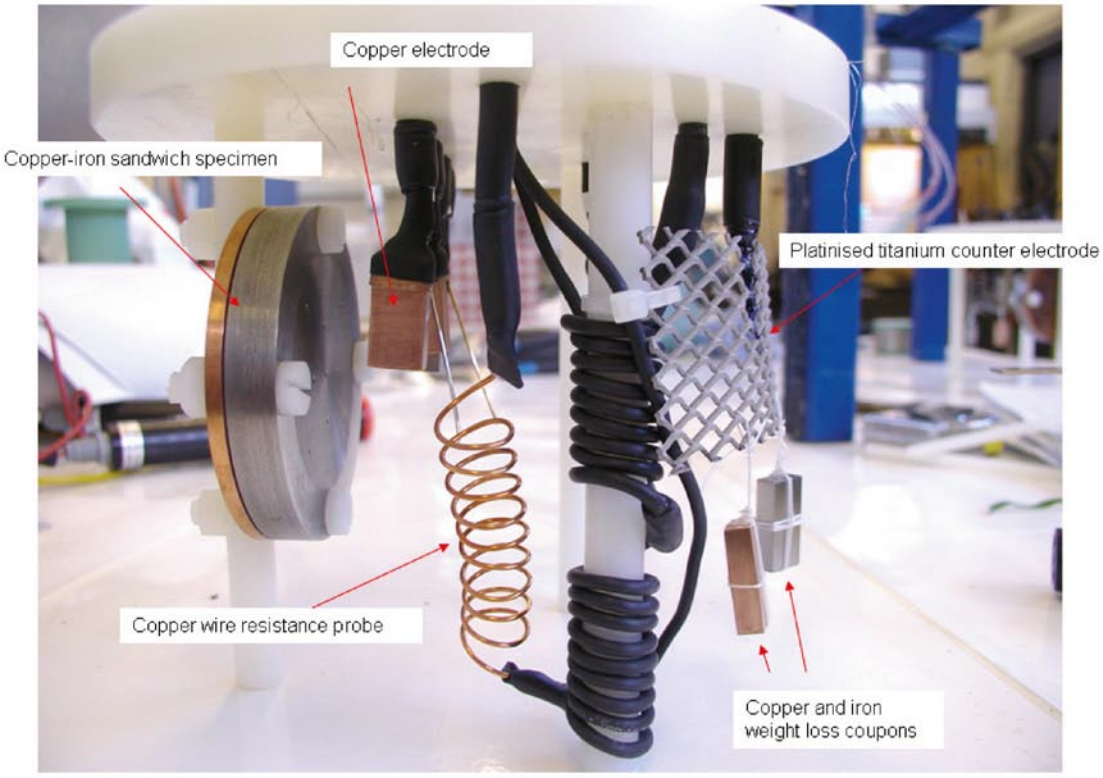

a)

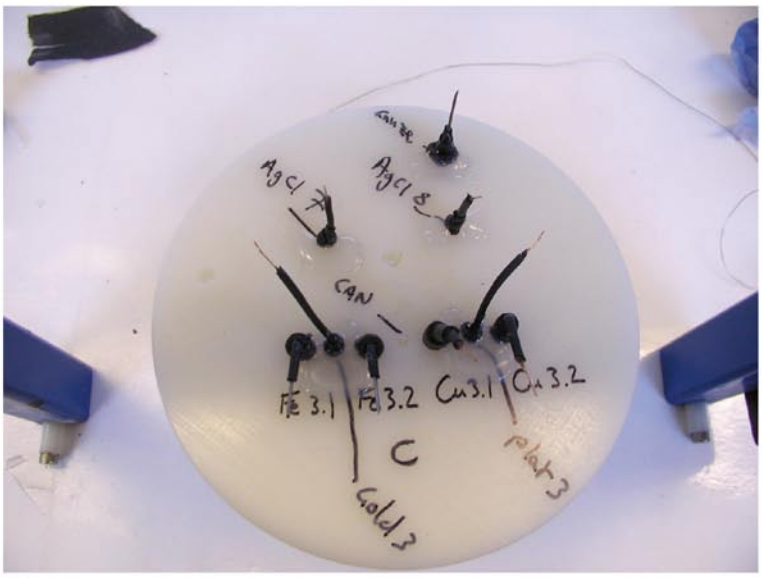

b)

Figure 4-2. *a) Nylon support rack for sensors and corrosion test pieces mounted inside support cage, b) Top view.*

4.4 Pressure

The water pressure in the boreholes was initially measured by means of an analogue pressure gauge that was attached to the flanges on each borehole. Later an electrical pressure gauge was attached to the outlet pipe on the flange and the output was recorded on the datalogging equipment.

4.5 Strain

Strain gauges were applied to measure changes in the strain on the outer surface of two of the copper canisters (Tests 1 and 4). The aim of these measurements was to provide an indication of whether expansion caused by internal corrosion has caused any dimensional changes. Standard strain gauge monitoring technology using bi-axial strain gauges was applied (e.g. Techni-Measure Ltd) using cyanoacrylate adhesives and protected with waterproof coatings (see Figure 4-3).

4.6 Corrosion coupons

A number of types of corrosion coupons were mounted within the cage used for the model canister experiments, as follows:

- *Plain corrosion coupons of copper and cast iron.* The corrosion rate of the materials will be determined from weight loss measurements at the end of experiments. Duplicate weight loss samples were installed in each experiment. These coupons were suspended from the nylon mounting rack using polypropylene thread (see Figure 4-2).
- *Coupons of copper and cast iron that are electrically connected to the exterior.* These were designed to allow the corrosion potential of the electrodes to be measured. It was also possible to carry out electrochemical measurements of the corrosion rate of these coupons using linear polarisation resistance, LPR, AC impedance, ACI, electrochemical noise, ECN. Platinised titanium gauze electrode (see Figure 4-2) was used as the counter electrode in a conventional 3-electrode electrochemical cell. Electrical connections were made to the coupons using copper wire for the copper coupons and carbon steel wire for the cast iron coupons.
- *Copper electrical resistance wire probes*. These were set up to measure the corrosion rate of copper using the technique proposed previously by VTT (e.g. /10/). Each coil consisted of a total length of 112.5 cm of 1 mm diameter copper wire (99.9% purity, Advent Cu513918). The length of wire was divided into three regions each of 37.5 cm length by applying heat shrinkable, adhesive-lined polymer tubing to the end sections, leaving the middle section exposed to the test environment. The complete wire was formed into a spiral with a diameter of ~1 cm (see Figure 4-2). The two screened lengths were used as reference resistances and the change in the resistance of the exposed length was used to calculate the corrosion rate. This information was processed by the ACM Field Machine electrochemical unit. These probes were used in Experiments 2 and 5.
- *Stress corrosion test specimens.* Four Wedge Opening-loaded (WOL) specimens with the design shown in Figure 4-4 were mounted in the boreholes. They were machined from a scrap copper lid provided by SKB and they were pre-cracked to give a range of stress intensity factors. In addition four U-bend specimens were manufactured from the same lid material, with dimensions of 2.5×80×20 mm. Two U-bend specimens and two WOL specimens were mounted in each of experiment boreholes 3 and 4, by loosely suspending them from the stainless steel push rod using plastic connectors. They were thus exposed directly to the groundwater. They will be examined for any indications of SCC at the end of the experiments.
- *Copper-cast iron-copper sandwich specimens to investigate jacking effects.* These specimens were based on the multi-crevice assembly specimen used in previous galvanic corrosion experiments /11/, in which cast iron castellated nuts were tightened against sheets of copper. The aim of these specimens was to investigate a number of possible corrosion mechanisms, including crevice corrosion, galvanic corrosion and expansive corrosion. They consisted of a sheet of copper which was clamped against a block of cast iron using a ring of nylon bolts. To investigate the effect of separation distance between mating surfaces a series of steps was machined into the surface of the cast iron to give separation distances between the mating surfaces ranging from direct contact around the edges of the specimens, increasing in steps of 10 µm to 30 µm (see Figure 4-5). The materials used for the sandwich specimens were prepared from copper sheet and the same type of cast iron used for the insert in the model canisters. The specimens will be removed and examined at the end of the exposure period.

Figure 4-3. *Strain gauges mounted on model canister.*

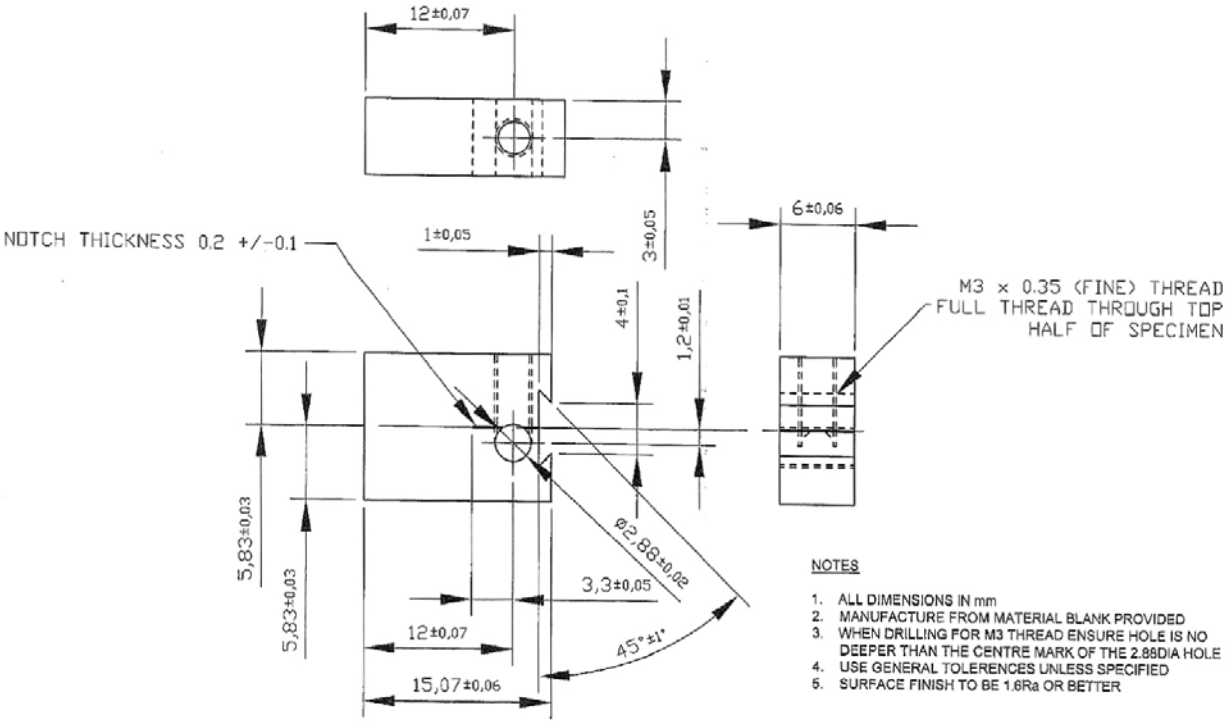

Figure 4-4. *Design of Wedge Opening-loaded (WOL) specimens.*

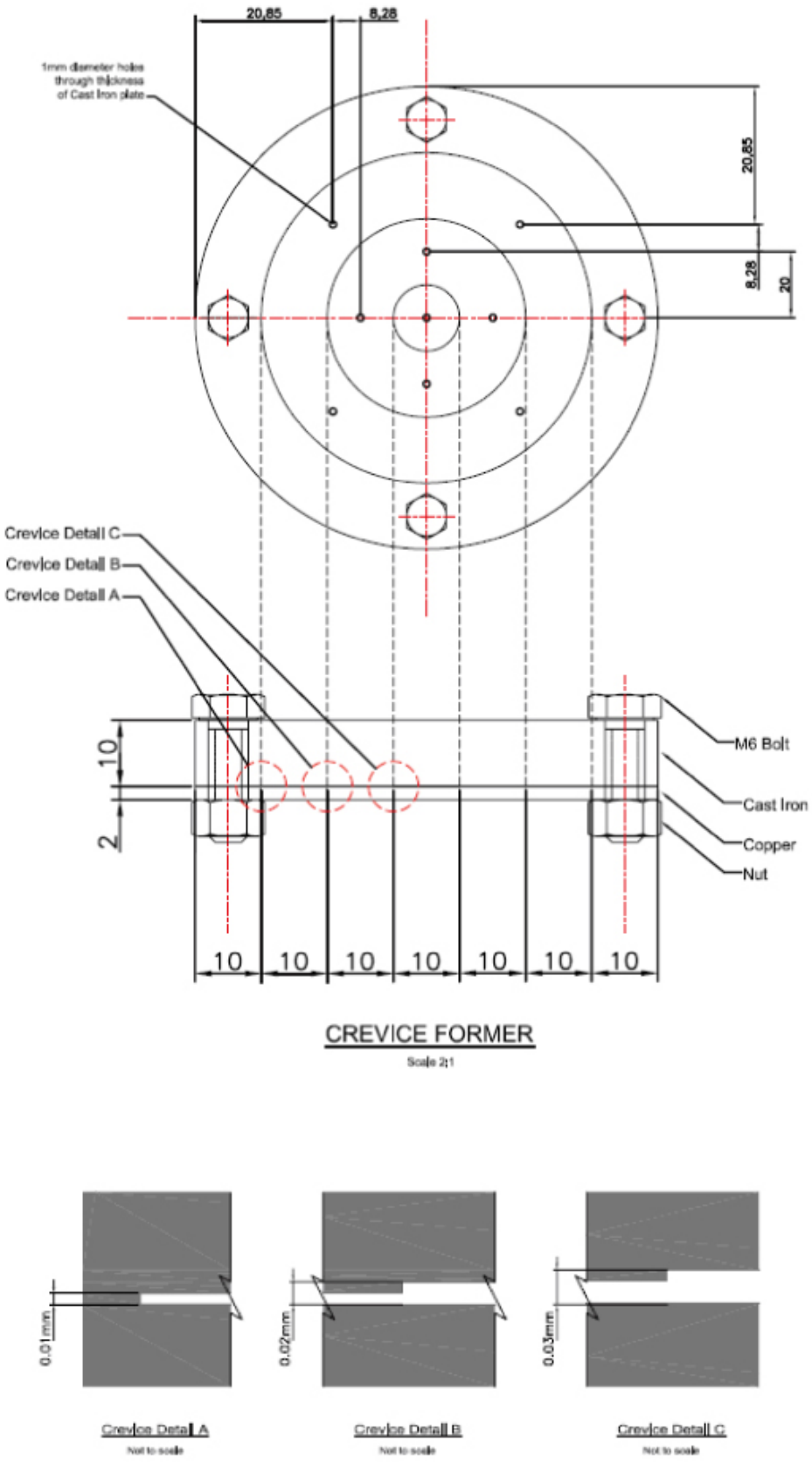

Figure 4-5. *Design of copper-iron sandwich (crevice expansion) specimens.*

4.7 Mounting system for sensors and corrosion test pieces

The corrosion coupons and environmental sensors were supported in a nylon rack (see Figure 4-2) which was placed inside the stainless steel support cage above the model canisters before the support cage was sealed. It rested on the top of the model canisters by means of support legs. Electrical connections were taken out through Conax compression fittings in the support cage lid. For Test 4, where the model canister was embedded in compacted bentonite, the corrosion coupons and sensors were placed in slots that were machined into the compacted bentonite before it was loaded into the supporting cage.

4.8 Electrical connections

A summary of the sensors in each of the experiments and the conduits required for the connecting cables is given in Table 4-1 to Table 4-3 and a summary of the outputs from each experiment is given in Table 4-4. Connecting wires from metal samples inside the canister cage (i.e. corrosion coupons and the model canister itself) were passed through compression glands (316L stainless steel Conax fittings) and connected to cables that were taken out to the external environment through stainless steel tubes which were attached to the supporting cages using Swagelok-type pressure fittings. All connections were made using soldered joints which were then sheathed in heat shrink. It should be noted that the electrochemical measurements rely on the integrity of the sheathing system throughout the experiments and the success of the sheathing will only be confirmed when the experiments are dismantled and the sheathing can be examined. The tubes were passed through the stainless steel flange at the entrance to the boreholes using bulkhead compression fittings.

Table 4-1. Summary of sensors in Experiments 1 to 3 (low density bentonite in supporting cage) and connections at borehole flange.

Experiment Number	Sensors	Location of sensor	Connections	Conduit
1 to 3	Reference electrode 1	Next to model canister, inside inner chamber	1 lead	A
1 to 3	Reference electrode 2	Next to model canister, inside inner chamber	1 lead	A
1 to 3	Reference electrode 3 (CP type)	Outside model canister support cage	1 lead	B
1 to 3	Model canister	Inside supporting cage	1 lead	A
1 to 3	Iron corrosion coupon for electrochemical monitoring	Next to model canister, inside inner chamber	1 lead	A
1 to 3	Copper corrosion coupon for electrochemical monitoring	Next to model canister, inside inner chamber	1 lead	A
1 to 3	Gold wire (×2) for redox measurements	Next to model canister, inside inner chamber	2 leads	A
1 to 3	E_h probe	Next to model canister, outside supporting cage	1 lead	B
1	Strain gauges	2 rosette gauges on surface of model canister	12 leads	C
2	Copper electrical resistance wire probe	Next to model canister, inside inner chamber	6 leads	A
1 to 3	Water sampling	Next to model canister, from inside supporting cage	1 pipe	
1 to 3	Gas purge/bleed		1 pipe	

Table 4-2. Summary of sensors in Experiment 4 (compacted bentonite in supporting cage) and connections at borehole flange.

Sensors	Location of sensor	Flange connections	Conduit
Reference electrode 1 (solid state)	Next to model canister, inside inner chamber	1 lead	A
Reference electrode 2 (solid state)	Next to model canister, inside inner chamber	1 lead	A
Reference electrode 3 (CP type)	Outside model canister support cage	1 lead	B
Model canister	Inside supporting cage	1 lead	A
Iron corrosion coupon for electrochemical monitoring	Next to model canister, inside inner chamber	1 lead	A
Copper corrosion coupon for electrochemical monitoring	Next to model canister, inside inner chamber	1 lead	A
Gold wire (×2) for redox measurements	Next to model canister, inside inner chamber	2 leads	A
E_h probe	Next to model canister, outside supporting cage	1 lead	B
Strain gauges	2 rosette gauges on surface of model canister	12 leads	C
Water sampling	Next to model canister, outside supporting cage	1 pipe	
Gas purge/bleed		1 pipe	

Table 4-3. Summary of sensors in Experiment 5 (no bentonite in supporting cage) and connections at borehole flange.

Sensors	Location of sensor	Flange connections	Conduit
Reference electrode 1	Next to model canister, inside inner chamber	1 lead	A
Reference electrode 2	Next to model canister, inside inner chamber	1 lead	A
Reference electrode 3 (CP type)	Outside model canister support cage	1 lead	B
Model canister	Inside supporting cage	1 lead	A
Iron corrosion coupon for electrochemical monitoring	Next to model canister, inside inner chamber	1 lead	A
Copper corrosion coupon for electrochemical monitoring	Next to model canister, inside inner chamber	1 lead	A
Gold wire (×2) for redox measurements	Next to model canister, inside inner chamber	2 leads	A
E_h probe	Next to model canister, outside supporting cage	1 lead	B
Copper electrical resistance wire probe	Next to model canister, inside inner chamber	6 leads	A
Water sampling	Next to model canister, inside supporting cage	1 pipe	
Gas purge/bleed		1 pipe	

Table 4-4. Summary of outputs from each experiment.

Experiment	Output	External equipment
1 to 5	Corrosion potential of model canister	Electrochemical monitoring equipment
1 to 5	Corrosion potential of copper coupon	Electrochemical monitoring equipment
1 to 5	Corrosion potential of cast iron coupon	Electrochemical monitoring equipment
1 to 5	Gold wire (×2) for redox measurements	Electrochemical monitoring equipment
1 to 5	Redox potential of Eh probe (MOx)	Electrochemical monitoring equipment
1 to 5	Corrosion rate of copper and cast iron coupons (1 of each)	Electrochemical monitoring equipment
1, 4	Strain gauge output	Strain gauge datalogging equipment
2, 5	Copper electrical resistance wire probe	Electrochemical monitoring equipment

4.9 Monitoring equipment

The electrochemical monitoring is being performed using an ACM Ltd Field Machine and an Agilent datalogger. The ACM equipment is being used to carry out the electrochemical measurements of corrosion rate (10 channels) and measurements of electrical resistance of the copper wire electrodes (2 channels), and the Agilent datalogger is used to monitor the potentials of the various electrodes, together with monitoring the strain gauges. The datalogging equipment is located in a control room near the boreholes and data is then transmitted via the Internet to Serco's Culham laboratory for analysis.

4.10 Preliminary laboratory trials of sensors

A set of trial experiments was carried out on the sensor and monitoring equipment (i.e. reference electrodes, strain gauges, electrical connections to coupons) to check that they operated successfully prior to installation in the boreholes at Äspö.

4.10.1 Reference electrode testing

Three reference electrode systems were selected for evaluation in Äspö groundwater at pressures simulating those expected in the HRL. These were: the Silvion WE10 electrode, which was developed for seawater pipeline cathodic protection systems, the World Precision Instruments (WPI) Dri-Ref silver/silver chloride electrode encased in plastic and used in the biological research community, and a plain silver/silver chloride disc reference electrode (WPI EP8, 8 mm diameter, 20 mm long Ag wire). The latter was reinforced with two-part epoxy cement at the wire to disc connection, to give added strength. An iridium-platinum oxide reversible oxygen electrode (Cumberland Scientific Ltd) was also selected for evaluation as an Eh probe.

The pressure system for the trials was a modified Parr autoclave. The electrodes were placed in a polycarbonate liner which was filled with a sample of Äspö groundwater provided by SKB. The system was pressurised to 50 bar using nitrogen at room temperature. The potentials of the electrodes were then recorded using a HP 34970 datalogger.

4.10.2 Strain gauge testing

The bonding systems for the strain gauge adhesives were tested by exposing bonded strain gauges to Äspö groundwater under pressurised conditions.

Two copper coupons were cut from a 1 mm thick stock sheet and the surface was prepared for the application of two strain gauge sensors. The coupons were sequentially soaked in acetone, dried in air, treated in 25% HCl solution for 12 hours, abraded with an abrasive pad (Scotch Brite) and stainless steel wool, followed by a final acetone dip. The strain gauge sensors tested were water proof Technimeasure Ltd WFCA-6-17-3LT gauges, which have two-gauge elements mounted at 90° to each other on a PVC backing pad. Two types of sealing system were evaluated. Type 1 was a cyanoacrylate-based adhesive (Technimeasure Ltd CN) and the other was a polyester (Technimeasure Ltd P-2). These were allowed to cure. The edges of the PVC pads were treated with a small amount of 50/50 mix of methyl-ethyl-ketone and nitrile rubber (Technimeasure Ltd M-Coat B). Another layer of M-Coat B was placed over the top and allowed to cure. M-Coat J (Technimeasure Ltd), a liquid poly-sulphide rubber was then prepared and applied over the whole sensor pad. A small sample of the cured rubber coating was placed in a tube containing copper and Äspö water to determine whether the polysulphide could leach copper. The solution with the polysulphide turned blue suggesting that copper leaching was accelerated.

5 Installation of model canisters in Äspö underground laboratory

5.1 Boreholes

The location for the model canister experiments was determined by staff at Äspö. The aim was to find a location with a plentiful supply of ground water since it was important that the corrosion experiments were not limited by the supply of water. This was achieved by reference to the fracture mapping that had been carried out within the Äspö HRL and by carrying out test drillings using small diameter drills to locate areas of high water flow. The water would be expected to become anoxic within a week of sealing the boreholes, due to reaction with rock minerals and microbial activity /12, 13/.

Five 300 mm boreholes, each 5m long, were drilled by SKB staff (Figure 5-1). The boreholes were given the following SKB code numbers (the Serco experiment numbers are shown in parentheses): KA3386A02 (Experiment 1), KA3386A03 (Experiment 2), KA3386A04 (Experiment 3), KA3386A05 (Experiment 4), KA3386A06 (Experiment 5). The boreholes were drilled at a downward incline of ~10 degrees. This angle was chosen to ensure that any gas trapped in the borehole rises towards the mouth of the borehole so that it can be bled off. The borehole was sealed using a stainless steel flange which was fixed into the boreholes using an epoxy resin grouting technique that has been successfully used before for other experiments at Äspö. Electrical connections were taken out through the flanges. The flanges were designed by staff at Äspö. All fittings used stainless steel compression joints. The boreholes were sufficiently deep to be away from the zone affected by the tunnel drilling operations (the engineered disturbed zone, EDZ).

The rock face around the boreholes was sealed using a silica sol technique, but there was still considerable flow of water from the rock face. This was probably because the silica sol was only injected to a depth of ~0.4m, whereas recent experience suggests that an injection depth of at least ~2m would be required to seal the rock faces completely.

5.2 Installation of the model canister experiments

The model canisters were assembled in their respective support assemblies at Serco's Culham laboratories and then shipped to Äspö for installation into the boreholes. In Experiments 1 to 3 the annulus within the support cage was filled with bentonite pellets and bentonite powder (see Figure 5-2) to give an overall density of bentonite (based on the weight of a mixture of bentonite pellets and powder provided by Clay Technology) as follows: Experiment 1: 1,160 kg $m^{-3;}$ Experiment 2: 1,165 kg m^{-3}; Experiment 3: 1,361 kg m^{-3}, which is designed to give a high water permeability. Electrical connections were taken out through the top flange of the support cage (Figure 5-3) and the model canister was lowered into the support cage (Figure 5-3).

To insert the model canister assemblies into the boreholes a lifting device was attached to the walls of the tunnel above the mouth of the holes so that the assemblies could be lifted into position before they were slid into the holes. A stainless steel rod was attached to the lid of each of the canister assemblies to enable them to be pushed into the boreholes. The walls of the boreholes were quite smooth and wet, so it was possible to slide the model canister assemblies into the holes using the push rod. The push rods were left in place to enable the experiments to be withdrawn at the end of the required exposure time. After installation of the experiments the boreholes rapidly filled up with water (Figure 5-4). The layout of the complete experiments is shown schematically in Figure 5-5 and the complete installation is shown in Figure 5-6. There are indications of microbial activity on the tunnel walls, with the formation of a brown sludge coating in places (see Figure 5-7). A gas bleed valve was left open on all the flanges to prevent accumulation of gas released from the groundwater during depressurisation inside the metal casing near the outer flange. A few drops of water per minute were also lost from the gas bleed lines.

Figure 5-1. *Preparation of boreholes for miniature canister experiments.*

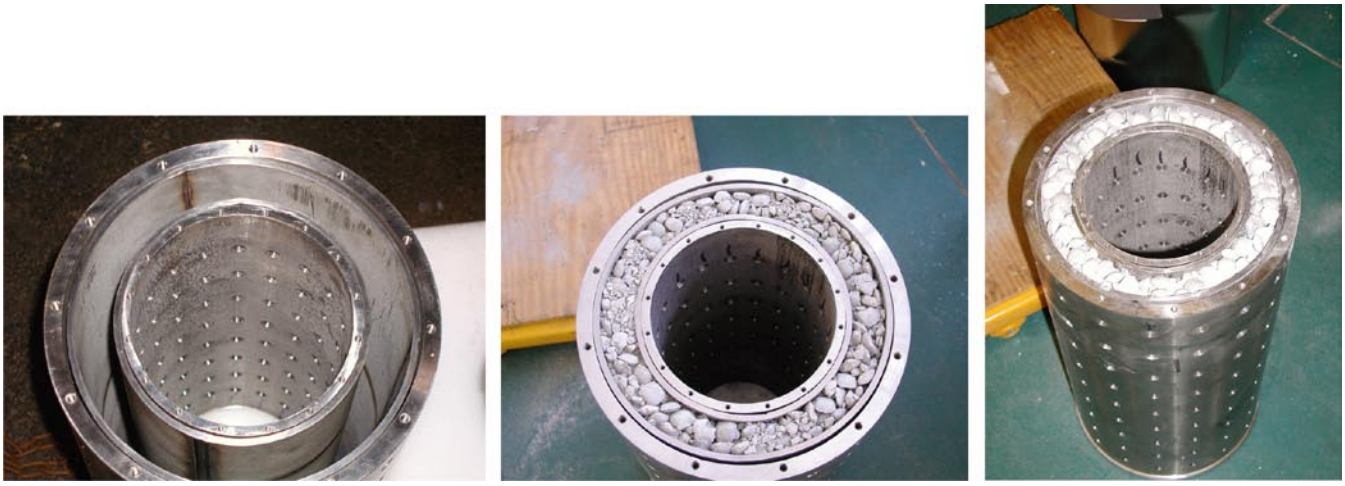

Figure 5-2. *Positioning of bentonite pellets inside annulus of support cage.*

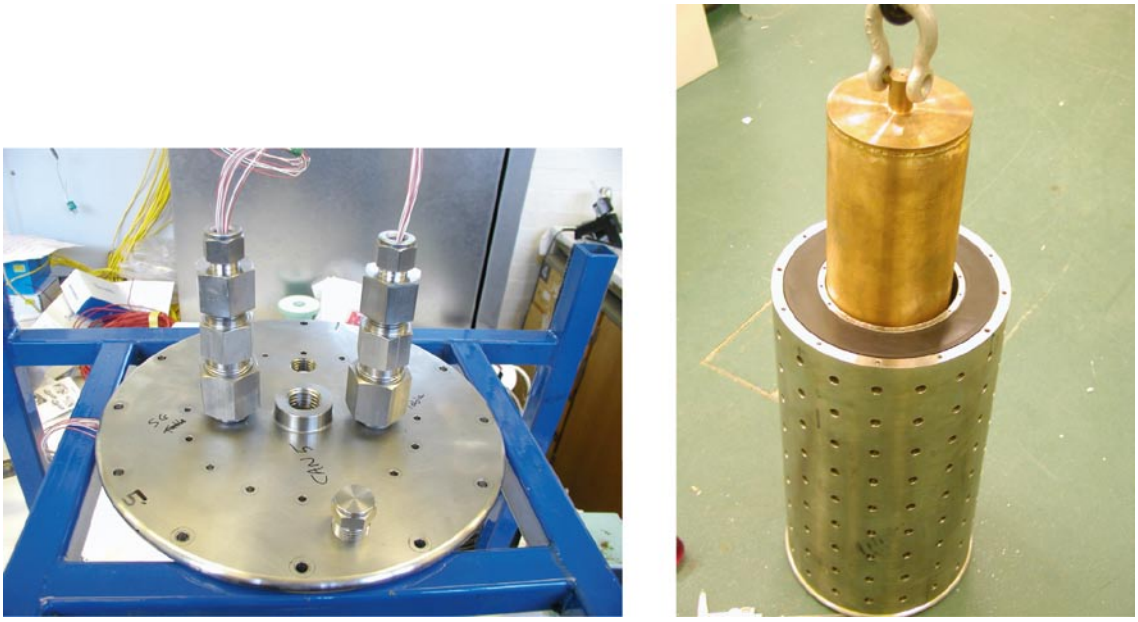

Figure 5-3. *Left: top flange for support cage. Right: insertion of model canister assembly into support cage.*

Figure 5-4. *Installation of first model canister assembly.*

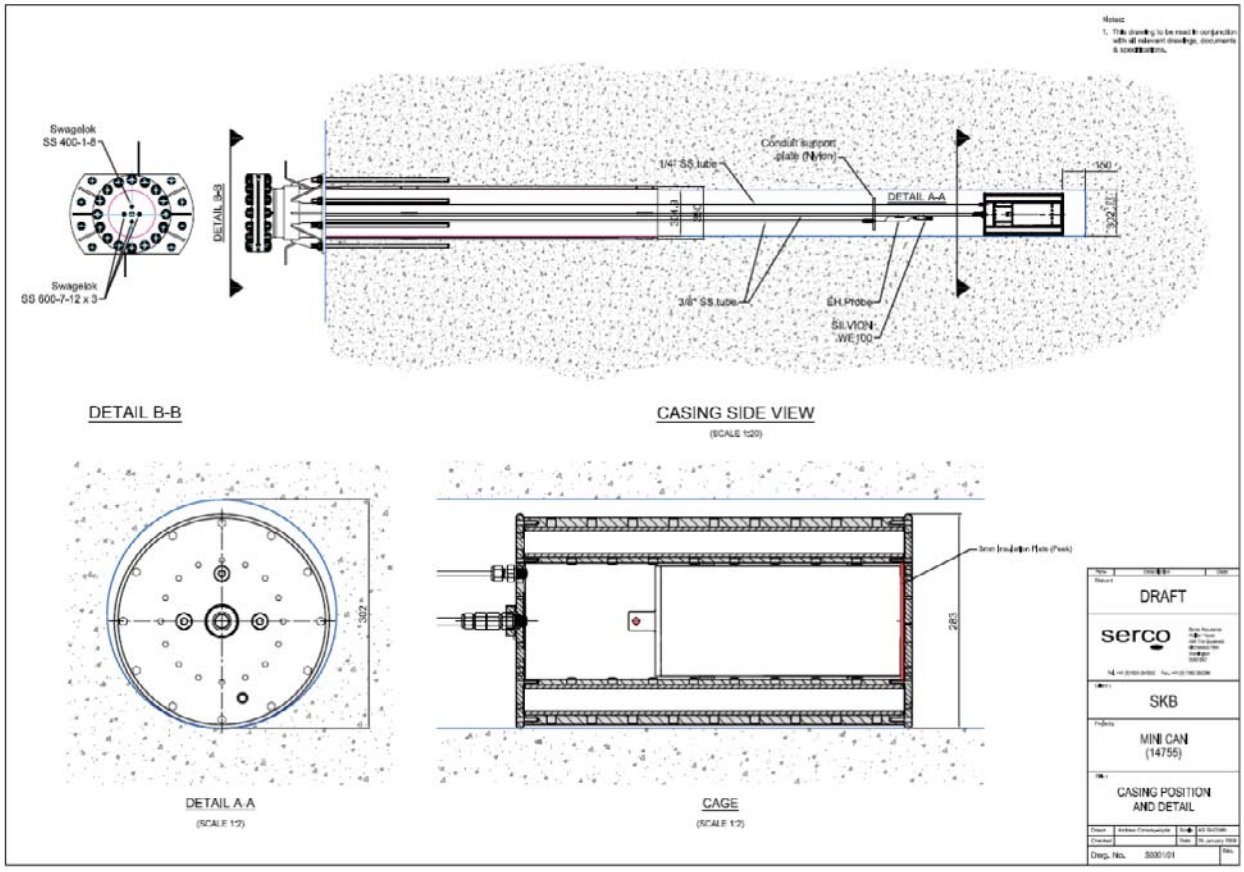

Figure 5-5. *Layout of model canister experiments in borehole.*

Figure 5-6. *Complete Minican experimental installation at Äspö Hard Rock Laboratory, showing water samples being collected for analysis. The experiments are installed in five separate boreholes, with a control room located in an ISO container at the rear left hand corner of the tunnel.*

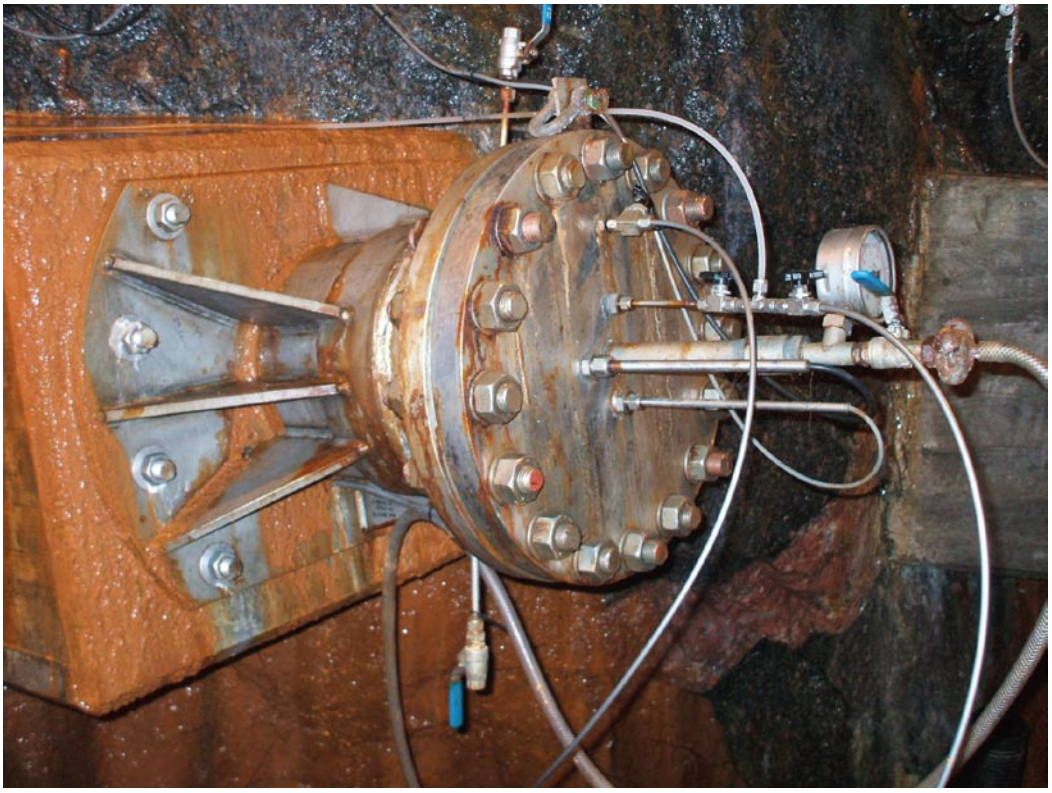

Figure 5-7. *Brown slime around experiment on rock face around borehole.*

6 Results

6.1 Laboratory trials

6.1.1 Reference electrodes

The results from the laboratory trials of the candidate reference electrodes for use in the model canister experiments are summarised in Figure 6-1, where it can be seen that none of the reference electrodes were affected by pressure. When they were disassembled after pressure testing some small amounts of solution had penetrated the rear of the Silvion ref electrode and consequently this void was filled with silicone rubber prior to insertion into the Minican housing. As a result of these experiments it was decided to use two silver chloride disc electrodes inside the model canister support cages and a Silvion reference electrode outside the support cages, but inside each borehole, to provide a back up to the disc electrodes in case of failure. If all the reference electrodes failed it would be possible to have an external reference electrode, which would be placed either in ground-water issuing from the rock face, or mounted in an additional vessel attached to the water outlet on the borehole flange.

The mixed metal oxide Eh electrode was mounted inside each borehole near the Silvion electrode, by strapping the leads to the push rods, and using plastic insulation to avoid metal contact with the Eh probes.

6.1.2 Strain gauges

The pressure had little effect on either bonding system (see Figure 6-2 and Figure 6-3). The CN bonded system showed a slight susceptibility to pressure but it still functioned after the pressure was removed. The CN bonding agent was not thought to be the reason for the pressure sensitivity. Both strain gauges were examined and found to be intact. It was decided to use the CN bonding agent and the nitrile rubber coating (M-Coat B) only on the strain gauges attached to the model canisters for use in Äspö, as the thick PVC coating already on the sensors was sufficient protection.

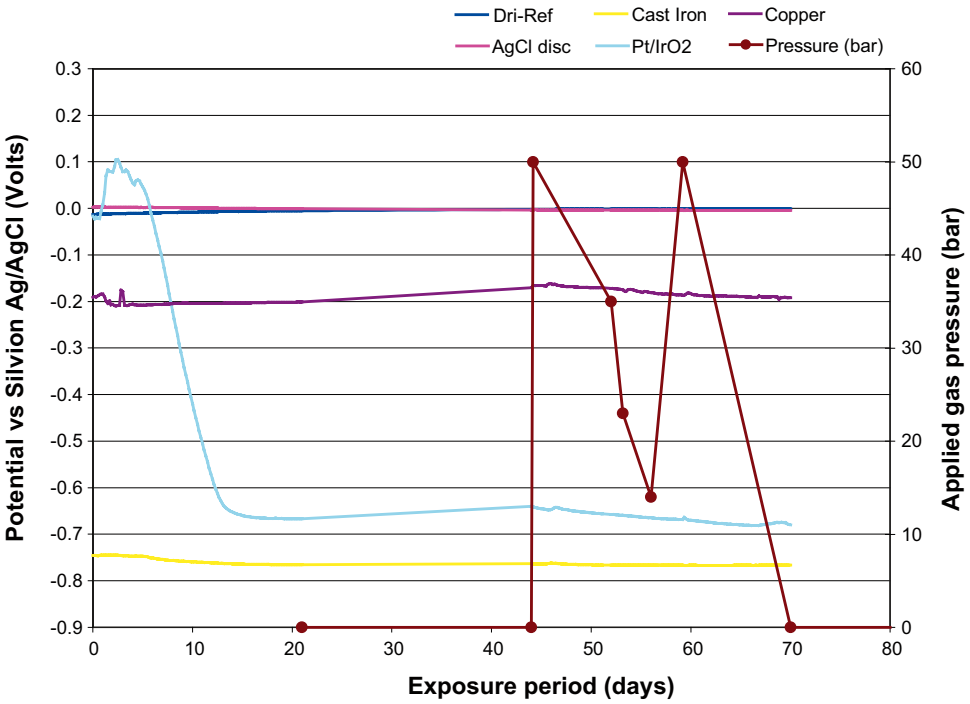

Figure 6-1. *Results of preliminary laboratory trials on reference electrodes, Eh electrode, copper and cast iron in an autoclave containing Äspö groundwater that was pressurised with nitrogen.*

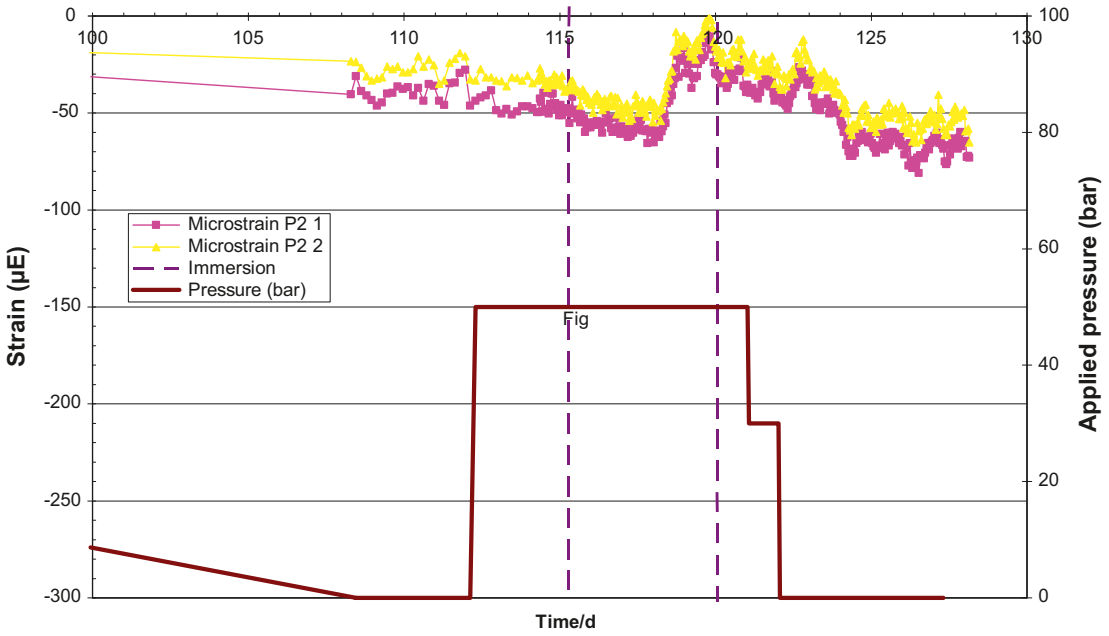

Figure 6-2. *Results of preliminary laboratory trials on strain gauges mounted on copper coupons using polysulphide rubber adhesive (Technimeasure Ltd P-2) in an autoclave containing Äspö groundwater that was pressurised with nitrogen.*

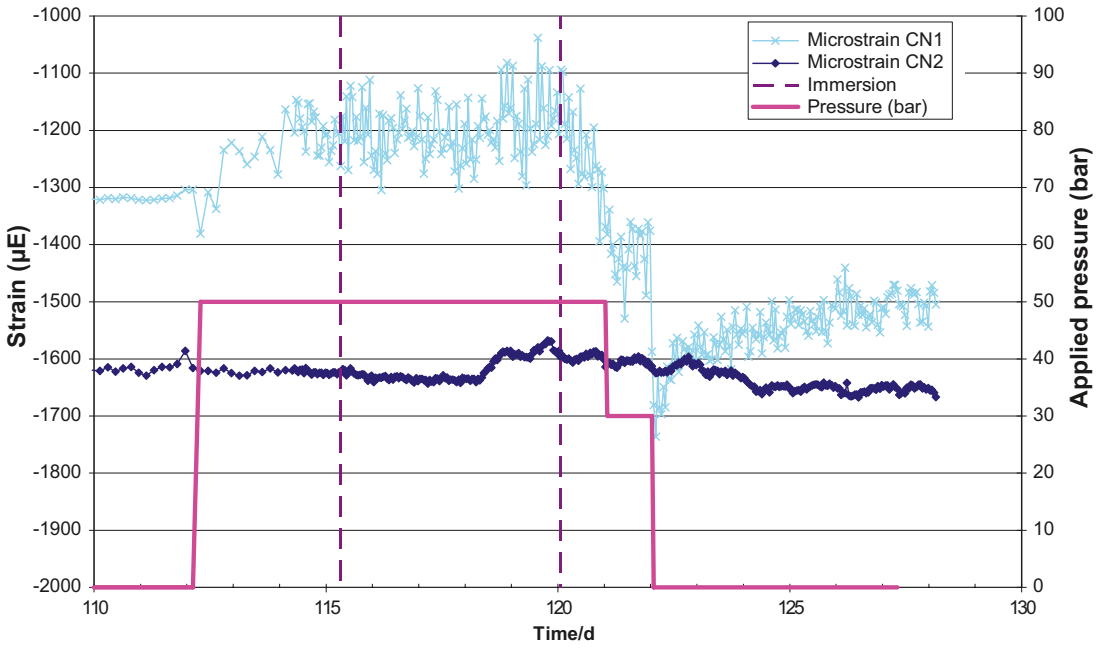

Figure 6-3. *Results of preliminary laboratory trials on strain gauges mounted on copper coupons using a cyanoacrylate adhesive (Technimeasure Ltd CN) in an autoclave containing Äspö groundwater that was pressurised with nitrogen.*

6.2 Water analysis

6.2.1 Inorganic analysis

The results from the water analyses for the five boreholes are shown in Figure 6-4 to Figure 6-8. These plots are a compilation of analyses for water samples taken from both within the support cage and external to the support cage in the borehole. A slight variation in the internal and external water compositions was observed. The plots do not show the barium concentrations, which were in the range 70–100 µg/L in all the measurements. The sulphide concentrations were in the range 0.006 to 0.223 mg/L (see Figure 6-9); the values are generally low (at least three orders of magnitude less than the sulphate concentration). The greatest variation between the internal and external ion concentrations was found in the dissolved iron analyses and these data are presented separately in Figure 6-10. They show that in the case of the experiments with low density bentonite (Experiments 1 to 3), or no bentonite at all (Experiment 5), the dissolved iron concentration inside the support cages was greater than external to the support cage. The pH of the water samples taken from inside and outside the support cages are shown in Figure 6-11. These data show a decrease in the pH of water inside the support cages compared to the water in the boreholes. The conductivity of the water was in the range 1,690 to 3,050 mS/m (i.e. 16,900 to 30,500 µS/cm), as shown in Figure 6-12. These conductivity values can be compared to that of seawater, which has a conductivity of approximately 5,300 mS/m. It is interesting to note that there are variations in conductivity between the boreholes and also between the conductivity of the water inside the support cage and the corresponding borehole outside the support cage (this is particularly pronounced in Experiment 5).

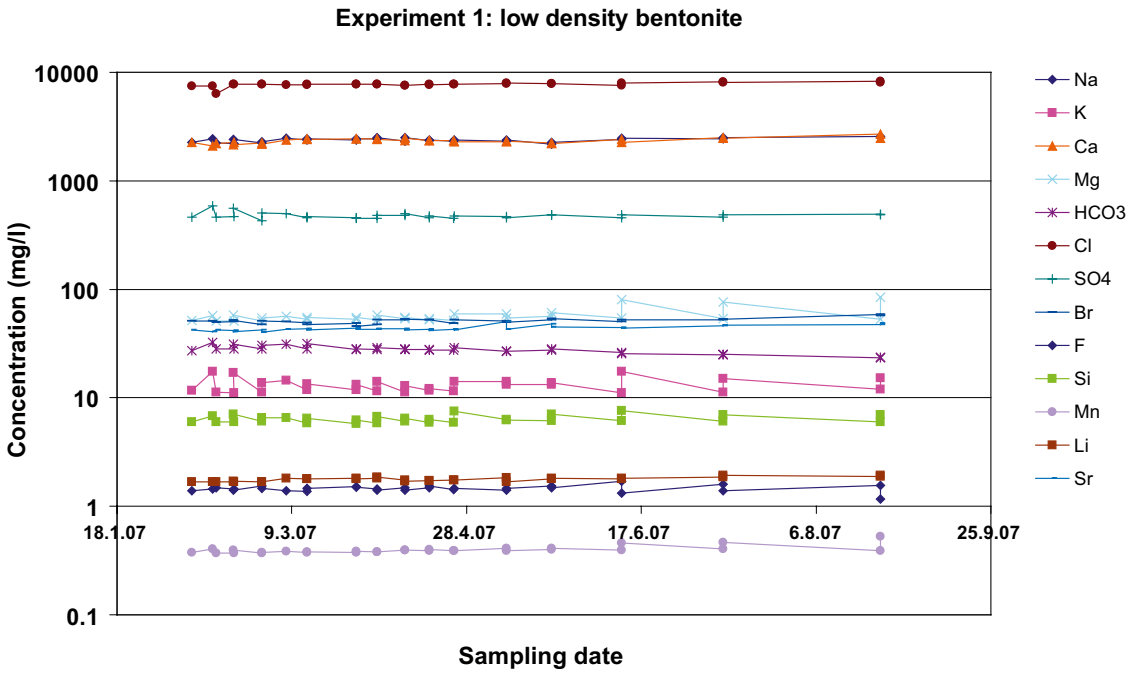

Figure 6-4. *Summary of water analyses: Experiment 1. For any given sampling date the first concentration shown when approaching along the line from the left hand side of the diagram refers to the analysis in the borehole, but outside the support cage, and the second point refers to the concentration on the inside of the support cage. The results of the iron analyses are shown in Figure 6-10.*

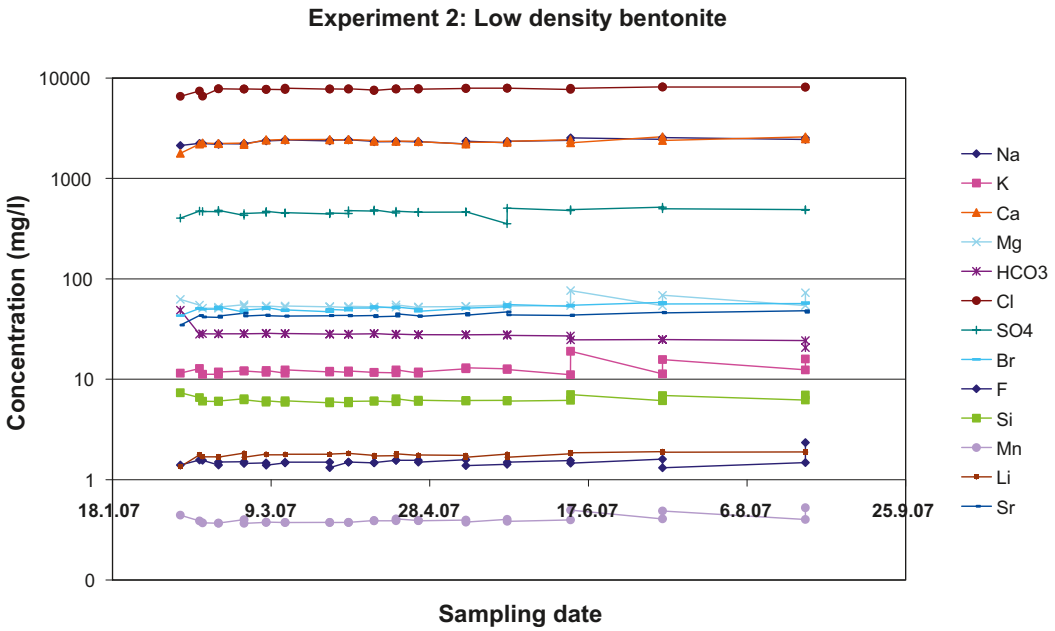

Figure 6-5. *Summary of water analyses: Experiment 2. For any given sampling date the first concentration shown when approaching along the line from the left hand side of the diagram refers to the analysis in the borehole, but outside the support cage, and the second point refers to the concentration on the inside of the support cage. The results of the iron analyses are shown in Figure 6-10.*

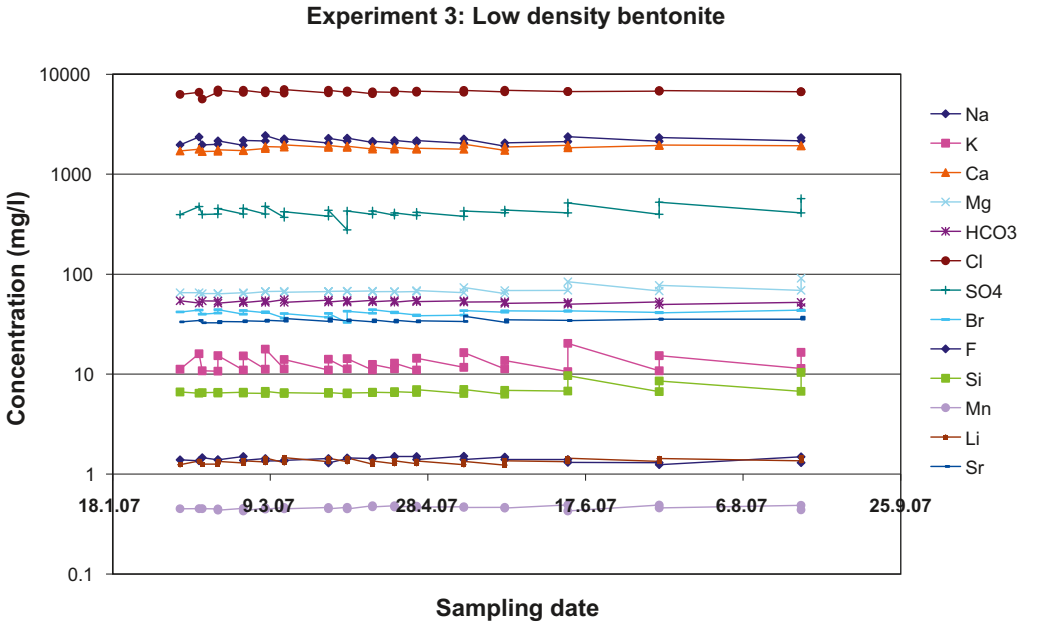

Figure 6-6. *Summary of water analyses: Experiment 3. For any given sampling date the first concentration shown when approaching along the line from the left hand side of the diagram refers to the analysis in the borehole, but outside the support cage, and the second point refers to the concentration on the inside of the support cage. The results of the iron analyses are shown in Figure 6-10.*

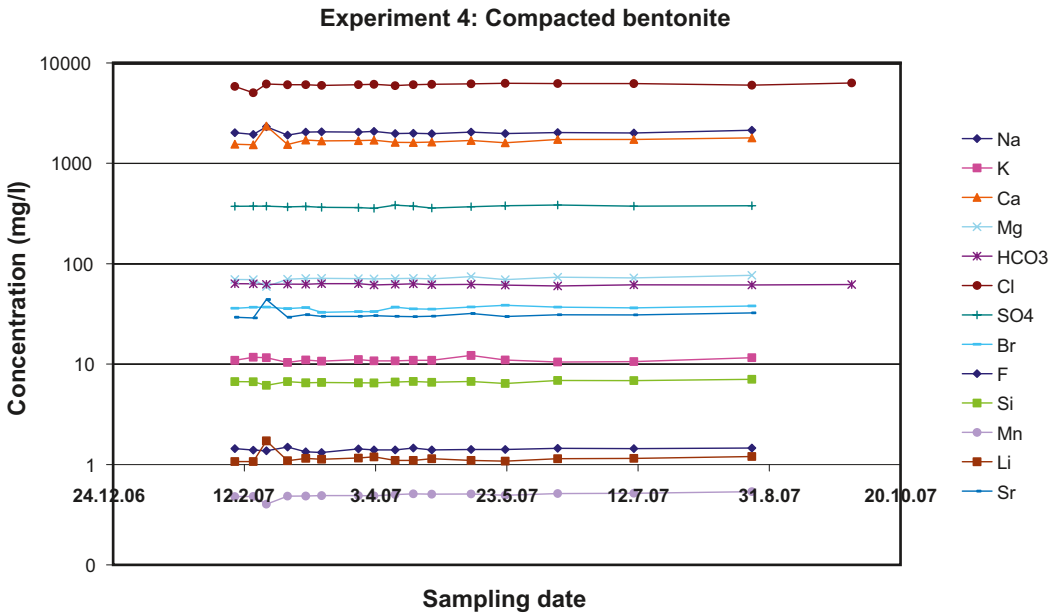

Figure 6-7. *Summary of water analyses: Experiment 4. It was not possible to remove any water from inside the support cage for analysis, so al data refer to a water sample taken from the borehole outside the support cage. The results of the iron analyses are shown in Figure 6-10.*

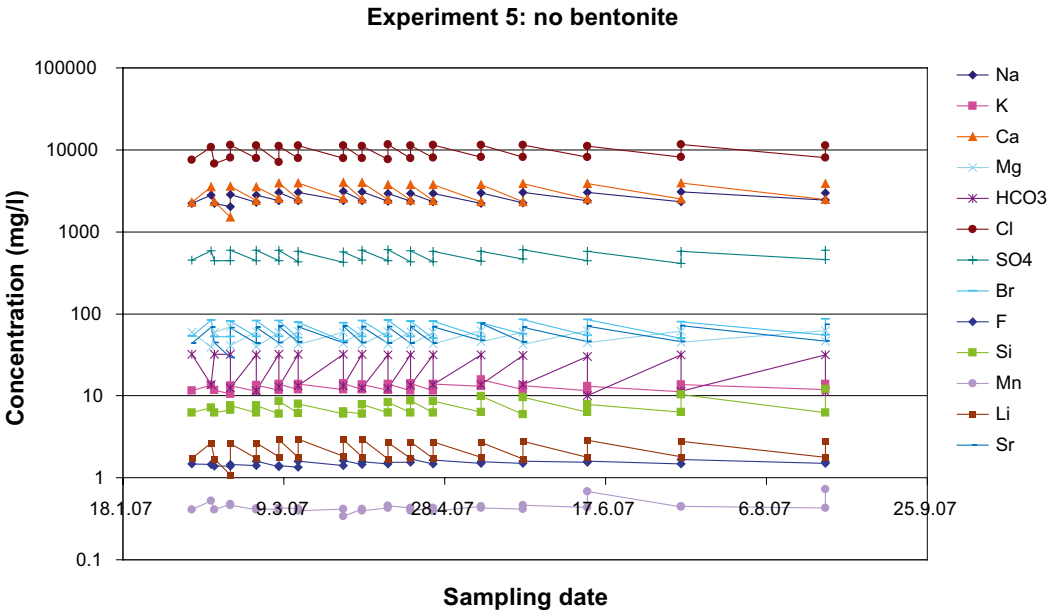

Figure 6-8. *Summary of water analyses: Experiment 5. For any given sampling date the first concentration shown when approaching along the line from the left hand side of the diagram refers to the analysis in the borehole, but outside the support cage, and the second point refers to the concentration on the inside of the support cage. The results of the iron analyses are shown in Figure 6-10.*

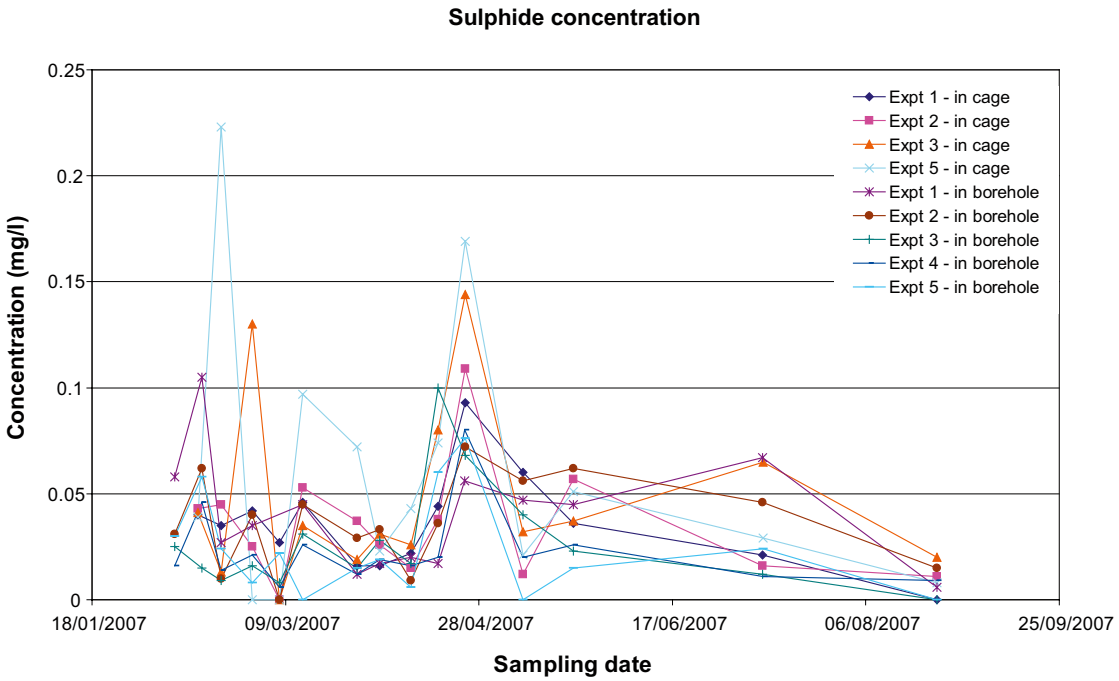

Figure 6-9. *Summary of sulphide concentration in water samples.*

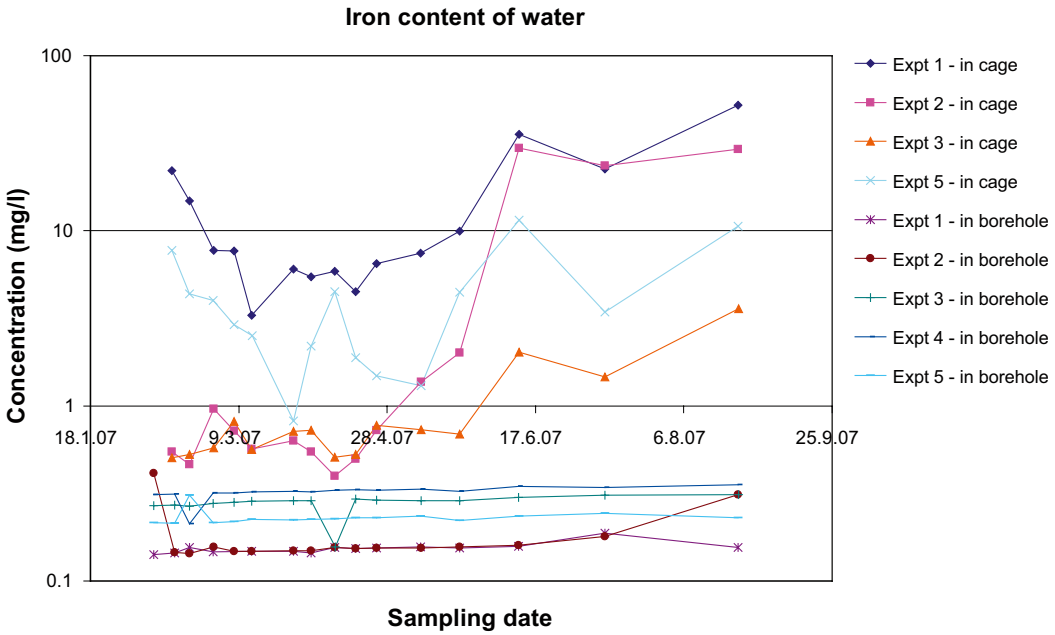

Figure 6-10. *Summary of iron analysis in water samples.*

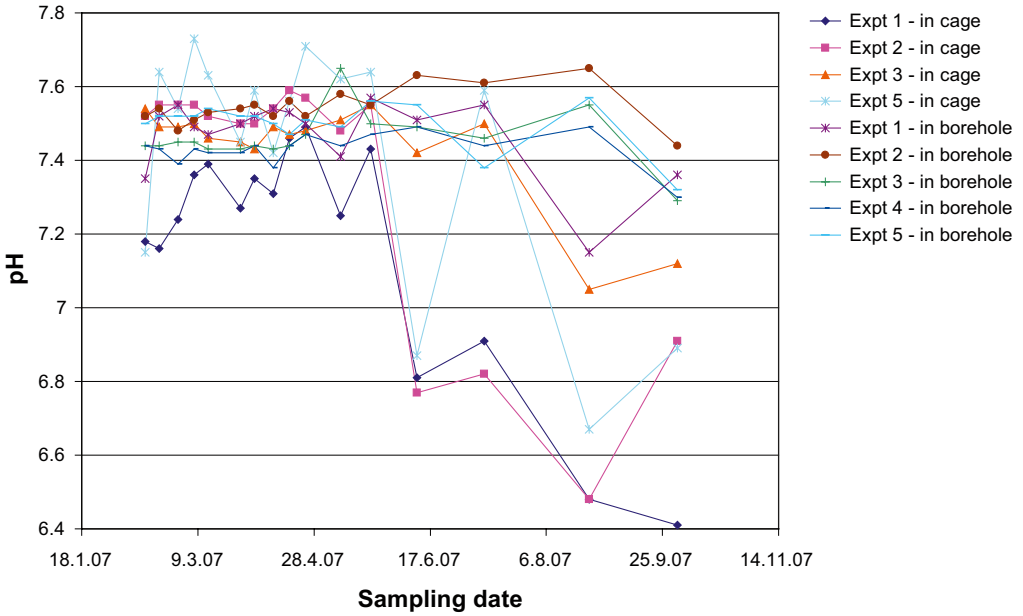

Figure 6-11. *pH of water samples taken from model canister experiments.*

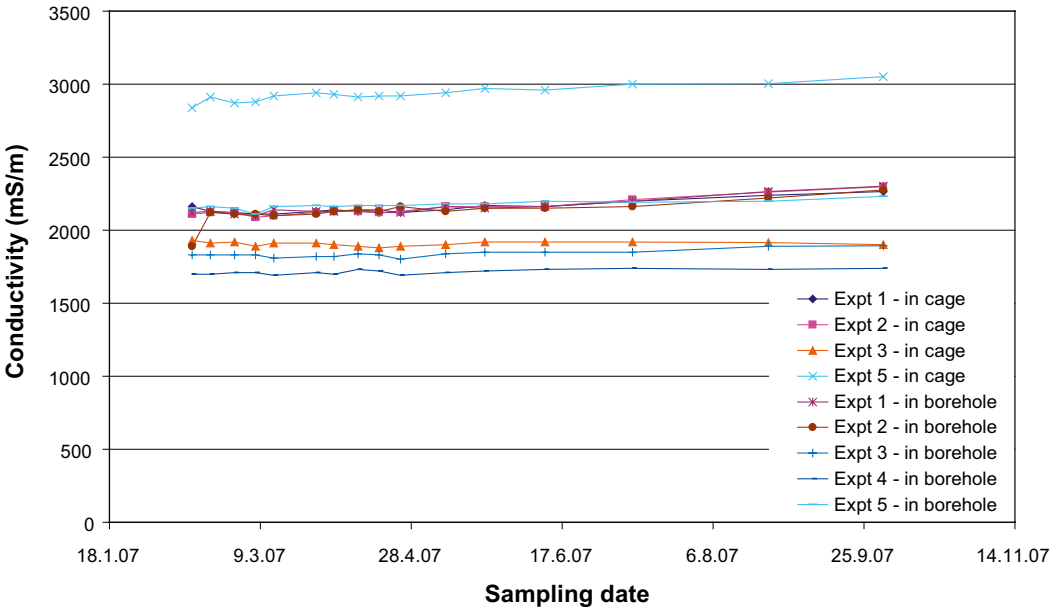

Figure 6-12. *Conductivity of water samples.*

The results of the trace element analyses (copper, nickel and chromium) are shown in Figure 6-13 to Figure 6-17. The concentration of these elements outside the support cage was very low (typically less than 5 µg/L). However, raised concentrations of nickel and chromium were observed inside the support cage. Although the actual levels are still low, they are significantly higher than external to the support cages and this is an indication of enhanced corrosion of the stainless steel support structure. Most copper measurements were below the detection limit of the analytical technique (0.5 µg/L), but measurements slightly above the detection limit were observed near the start of the experiments, suggesting that copper corrosion (i.e. corrosion of the model canisters) was slightly more active while residual oxygen was still present.

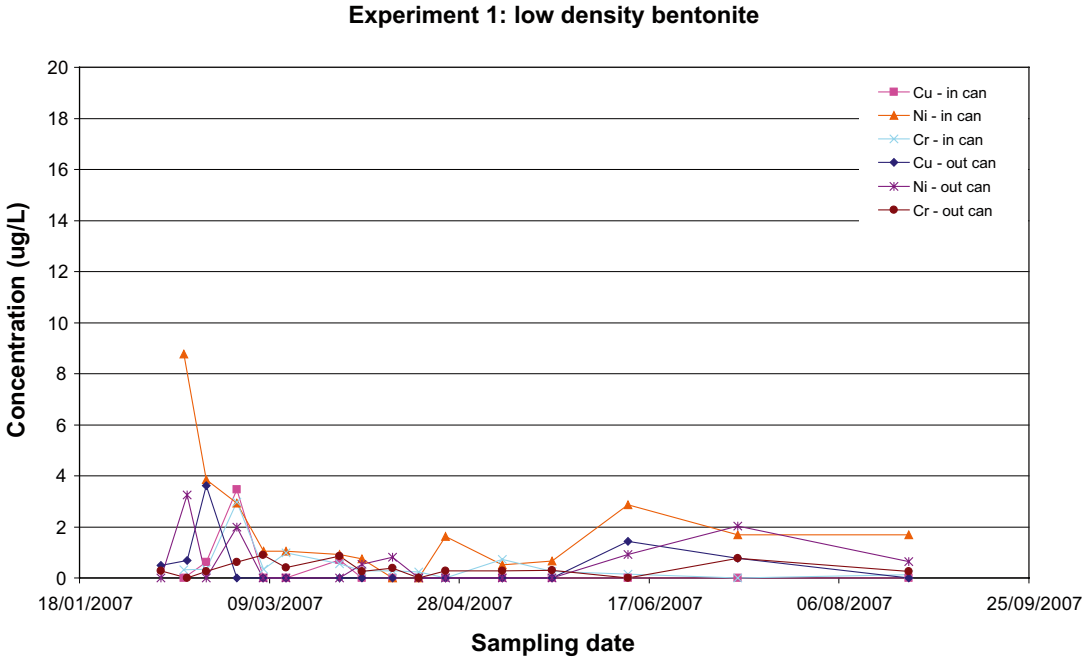

Figure 6-13. *Results of trace element analyses in Experiment 1 (low density bentonite).*

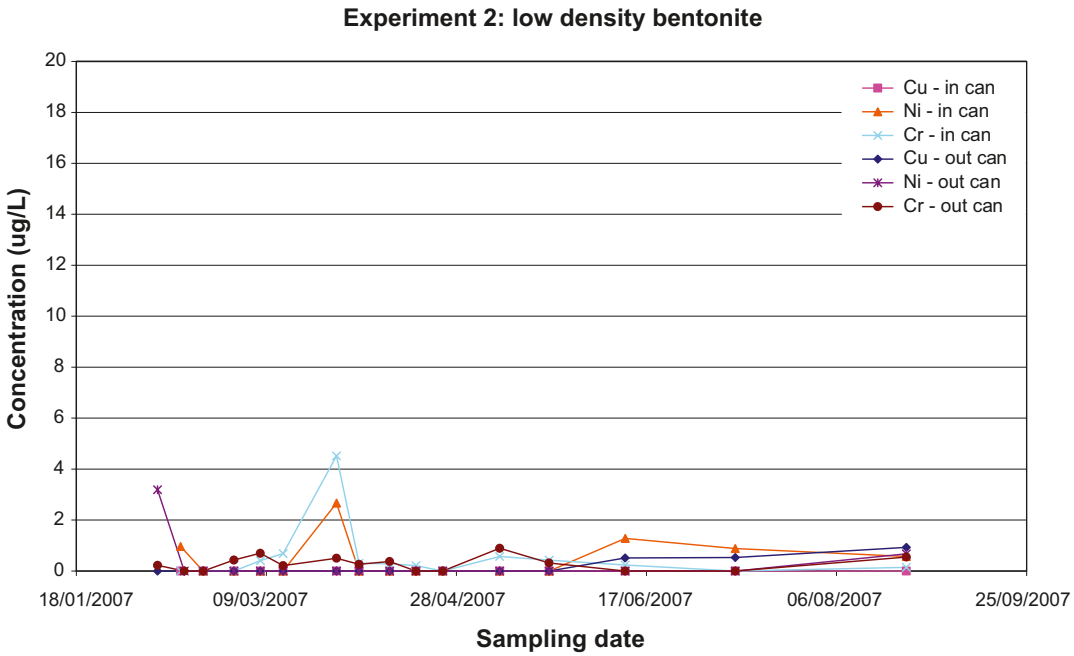

Figure 6-14. *Results of trace element analyses in Experiment 2 (low density bentonite).*

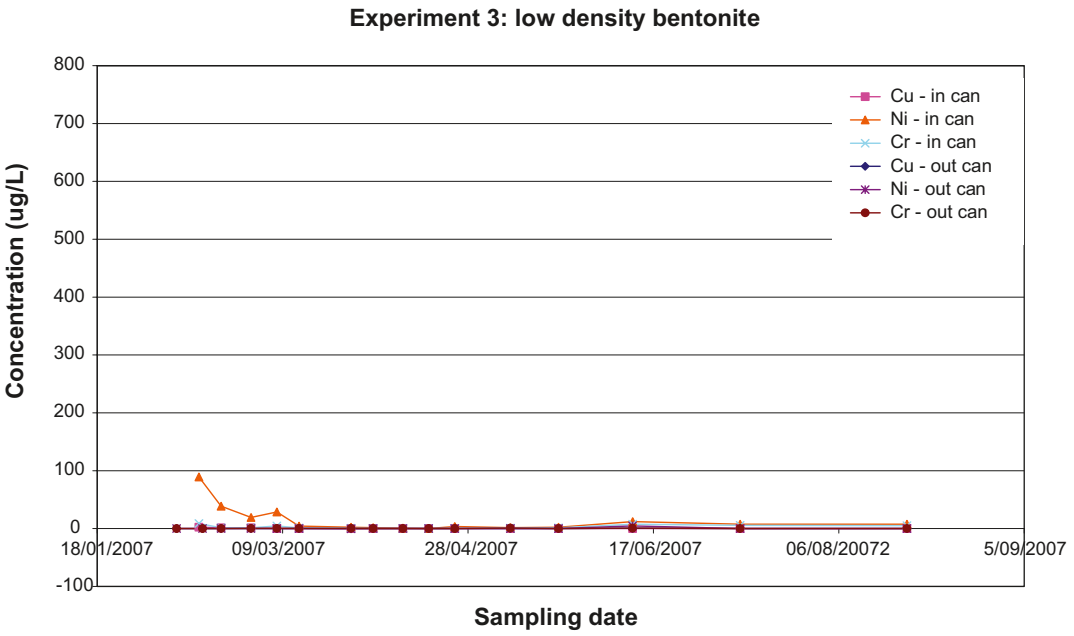

Figure 6-15. *Results of trace element analyses in Experiment 3 (low density bentonite).*

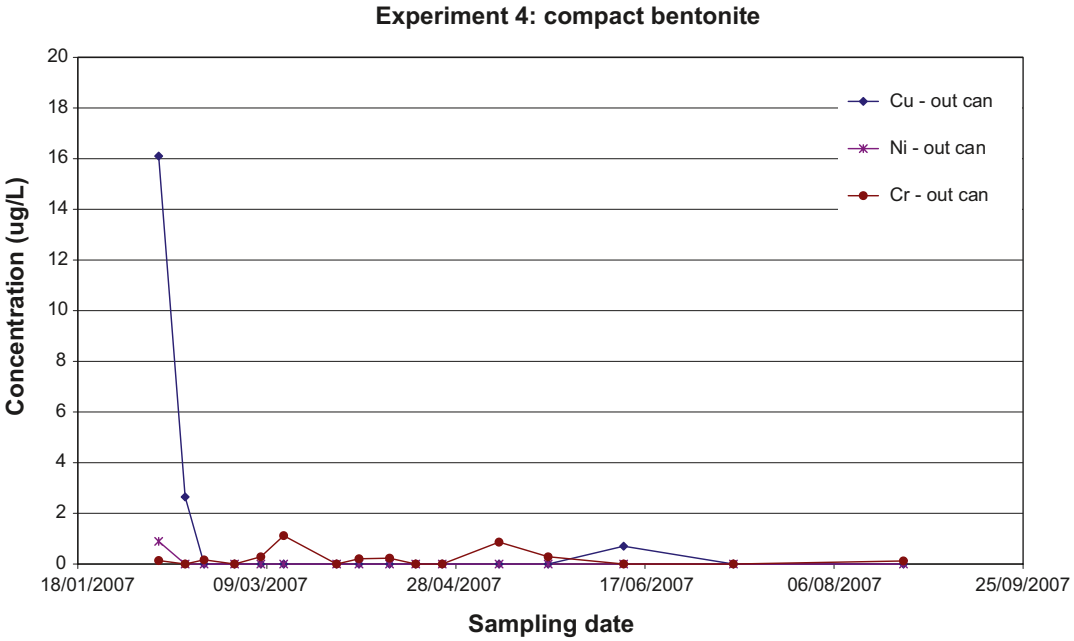

Figure 6-16. *Results of trace element analyses in Experiment 4 (compact bentonite).*

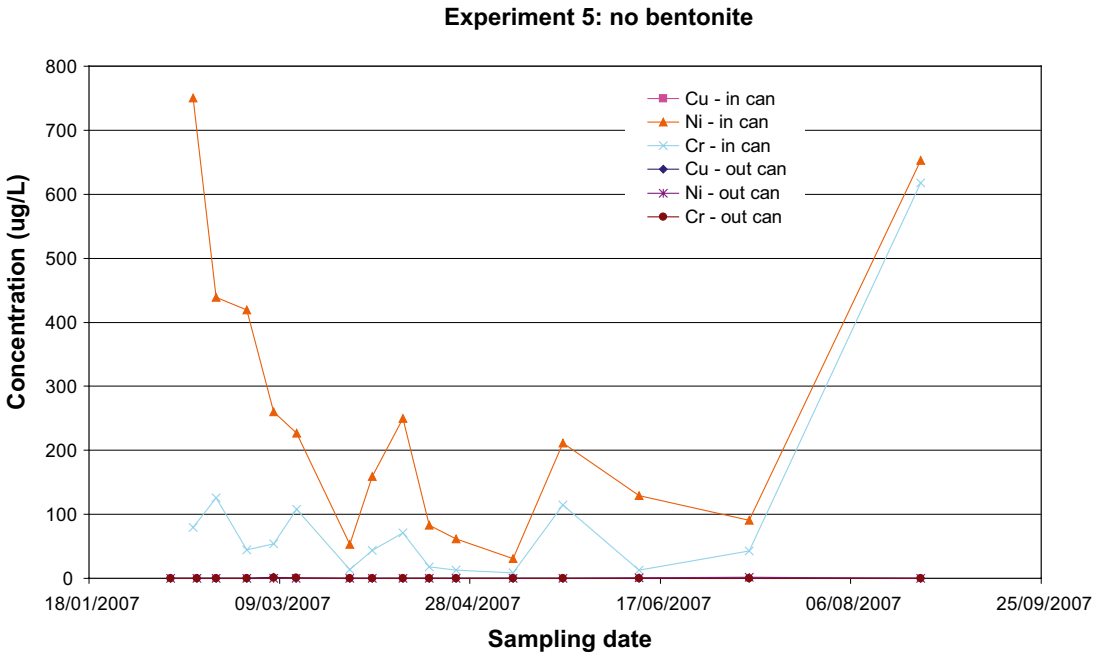

Figure 6-17. *Results of trace element analyses in Experiment 5 (no bentonite).*

The total organic content (TOC) measurements are shown in Figure 6-18. In Experiments 1 and 3 the TOC was slightly higher inside the support cage than outside the cage.

The results of the dissolved gas analyses are shown in Table 6-1. These data show that the oxygen concentration in the groundwater is essentially zero. The dominant dissolved gas is nitrogen, with significant quantities of helium, argon, carbon dioxide and methane also present. The concentration of hydrogen was particularly high in Experiment 5 (no bentonite); this may be due to anaerobic corrosion of the cast iron insert.

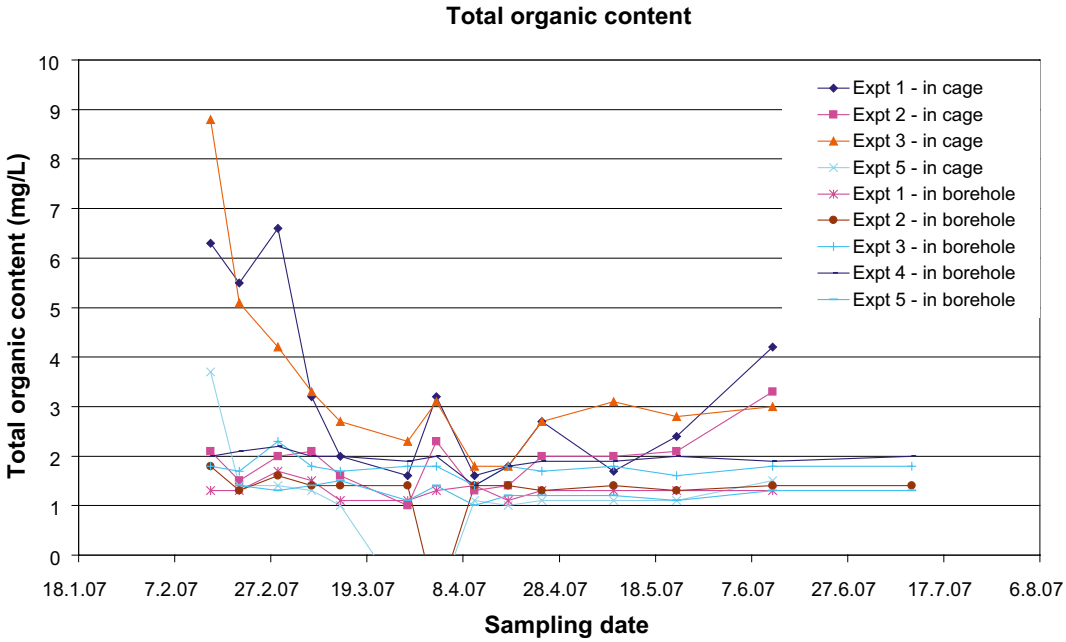

Figure 6-18. *Results of total organic content analysis.*

Table 6-1. Concentration of dissolved gases in water samples taken from the boreholes.

Expt	He ml/l	Ar ml/l	N_2 ml/l	CO_2 ml/l	O_2 ml/l	CH_4 ml/l	H_2 µl/l	CO µl/l	C_2H_2 µl/l	C_2H_6 µl/l
1 - inside cage	7.98	0.838	57.80	0.913	0.000	0.326	0.200	0.580	0.140	0.330
2 - inside cage	8.42	1.060	118.0	0.786	0.000	0.317	0.500	1.080	0.070	0.200
2 - outside cage	8.11	0.649	67.10	0.186	0.000	0.210	0.200	3.390	0.000	0.090
3 - inside cage	4.92	0.842	61.10	1.850	0.000	0.245	0.100	0.720	0.020	0.120
5 - inside cage	14.20	0.710	95.60	0.843	0.000	0.177	215.0	1.140	0.000	0.650

6.2.2 Microbial analysis

The results of the microbial analyses for sulphate reducing bacteria and autotrophic acetogens are summarised in Figure 6-19. The samples were taken between August 25 2007 and November 5 2007. These data show that the autotrophic acetogens were the dominant species, but that sulphate reducing bacteria were also present in significant numbers. No other types of microbes were analysed, because these two species are believed to be the most significant in relation to corrosion. The following analyses were carried out:

- Most probable numbers (MPN) and metabolites produced by sulphate-reducing bacteria (SRB) and autotrophic acetogens (AA),
- biomass measured as adenosine-tri-phosphate (ATP) content,
- total number of cells,
- number of cultivable heterotrophic aerobic bacteria (CHAB), and
- molecular biology analyses which investigate the RNA and DNA pools in the samples.

The results of the microbial investigations will be discussed in detail in a subsequent report.

6.2.3 Pressure readings

The results from the pressure gauges in the boreholes are shown in Figure 6-20. Unfortunately there was a loss of data due to a fault with the datalogging system during the winter of 2007/8. The data show that there is a general tendency for the pressure to fall with time. The low pressure is mainly due to water loss through the rock face surrounding the boreholes.

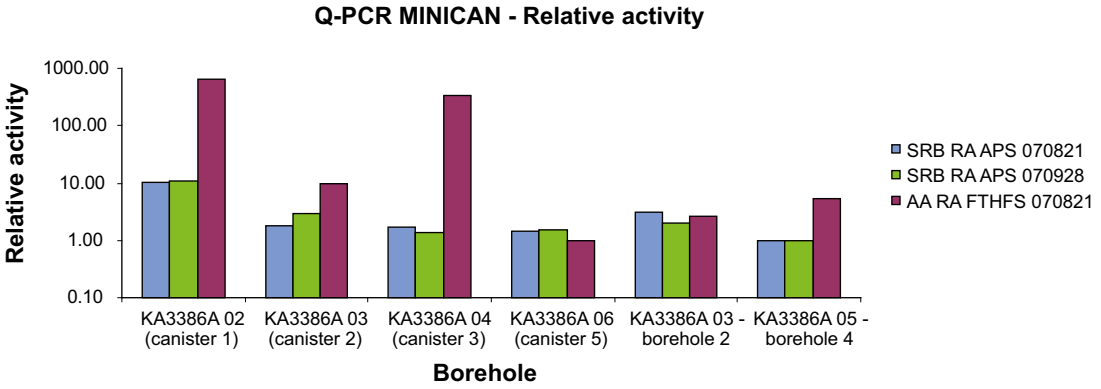

Figure 6-19. *Summary of results from microbial analysis (SRB = sulphate reducing bacteria; AA = autotrophic acetogens).*

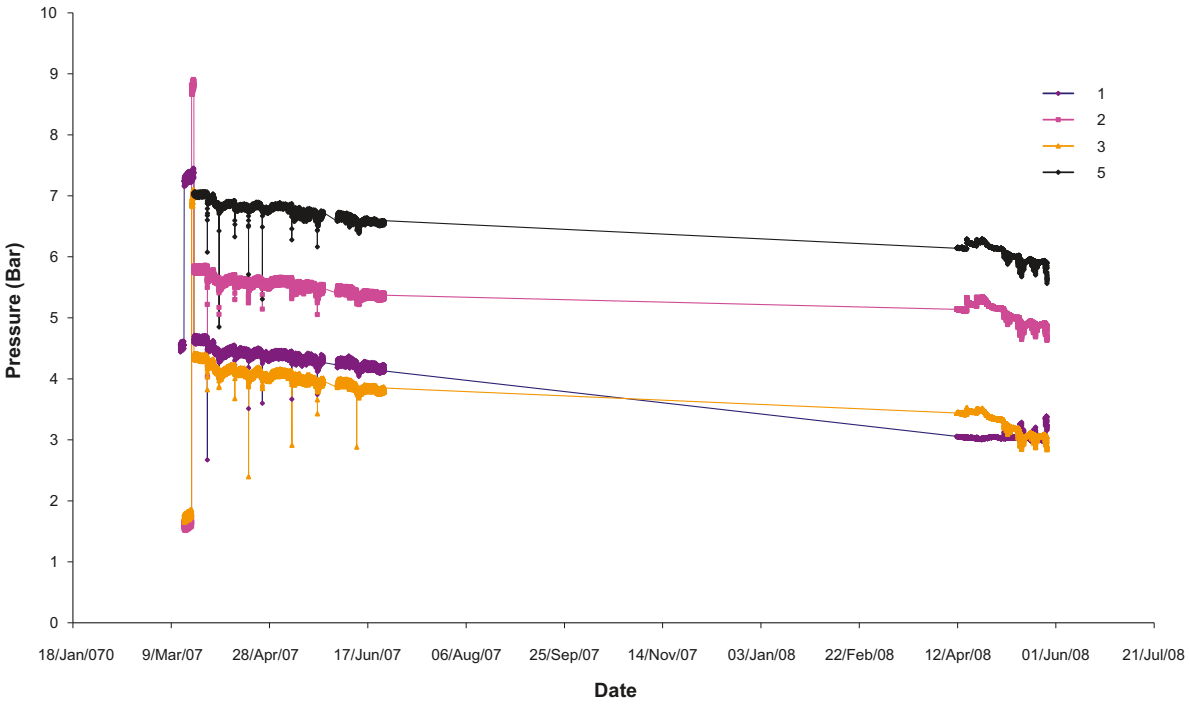

Figure 6-20. *Pressure readings for boreholes 1 to 5.*

6.3 Results of electrochemical potential measurements

This section presents the electrochemical potential measurements for each of the model canister experiments.

6.3.1 Experiment 1: Low density bentonite

In this experiment the defect in the outer copper shell (located near the top cap weld), is pointing vertically upwards. Figure 6-21 shows the results from the potential measurements for gold, platinum, Eh probe and the miniature canister. These data show the Eh values using gold and platinum, which are inside the support cage, and the Eh measured using the mixed-metal oxide electrode outside the support cage. Initially the internal silver-silver chloride reference electrodes were used for the Au and Pt electrodes, but these failed and it was necessary to switch to the Silvion reference electrode, which was mounted in the borehole outside the support cage (see change at 4,000 hours). The Au, Pt and Minican potential data up to 4,000 hours should be discounted. It is not clear why the Ag-AgCl disc electrodes failed in these experiments, since they had behaved satisfactorily during the laboratory autoclave tests. To date, the Silvion reference electrodes have performed satisfactorily.

The mixed metal oxide Eh values are reliable and show a decrease in the Eh with time. This is expected, since oxygen is consumed by microbial activity and mineral reactions. The Eh value is lower inside the cage than outside, indicating more reducing conditions, possibly due to the ongoing corrosion reactions.

The electrochemical potential for the model canister represents a mixed potential for the copper canister itself and the inner cast iron insert, which would probably have been partially wetted by water passing through the 1 mm defect in the outer copper can.

Figure 6-22 shows the potentials for the iron and copper coupons inside Experiment 1. Again there was a problem with the reference electrodes up to 27.6.07, but after the measurements were changed to being with respect to the Silvion reference electrode, reasonable values were obtained of about –450 mV vs NHE, for both iron and copper. The iron and copper potentials are consistent with anoxic conditions existing in the boreholes.

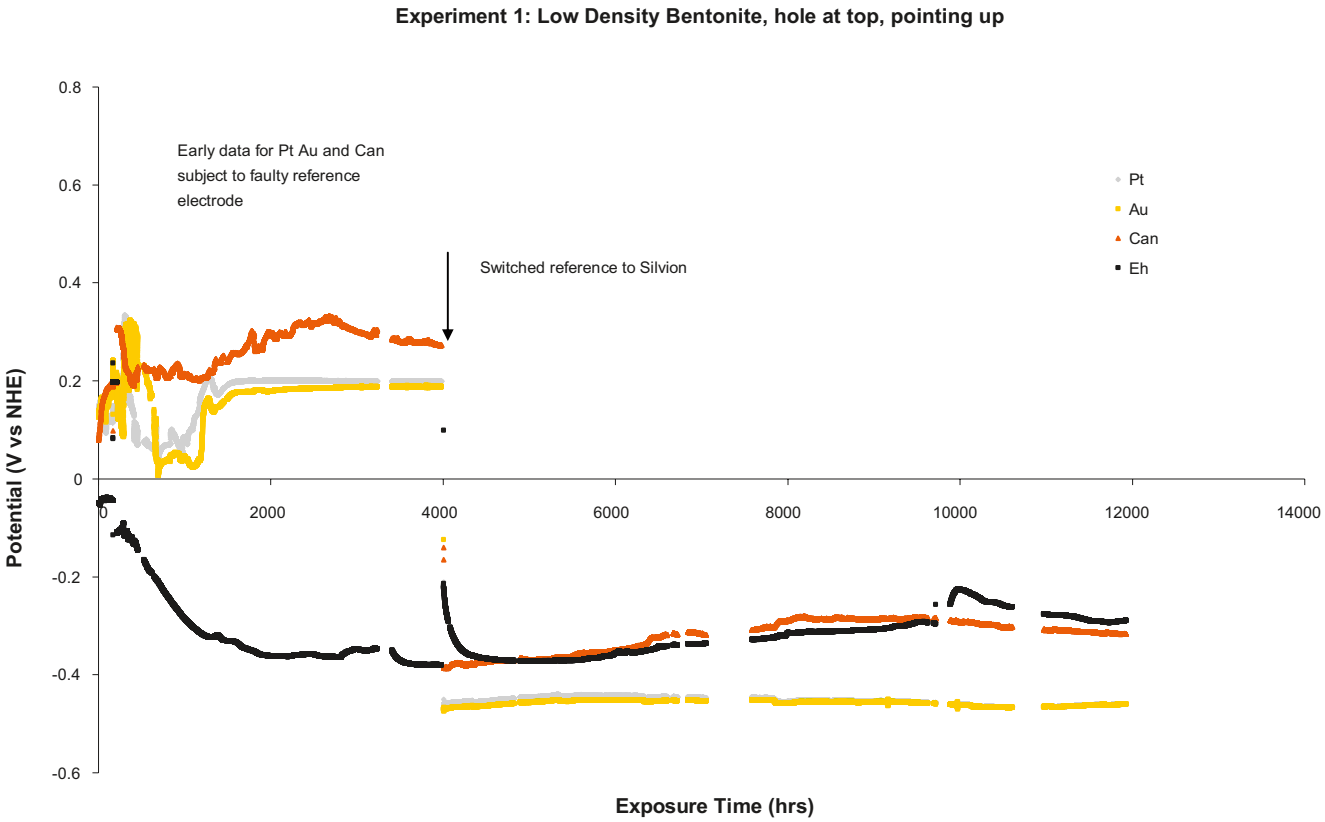

Figure 6-21. *Results of Eh and can potential measurements from Experiment 1 (low density bentonite).*

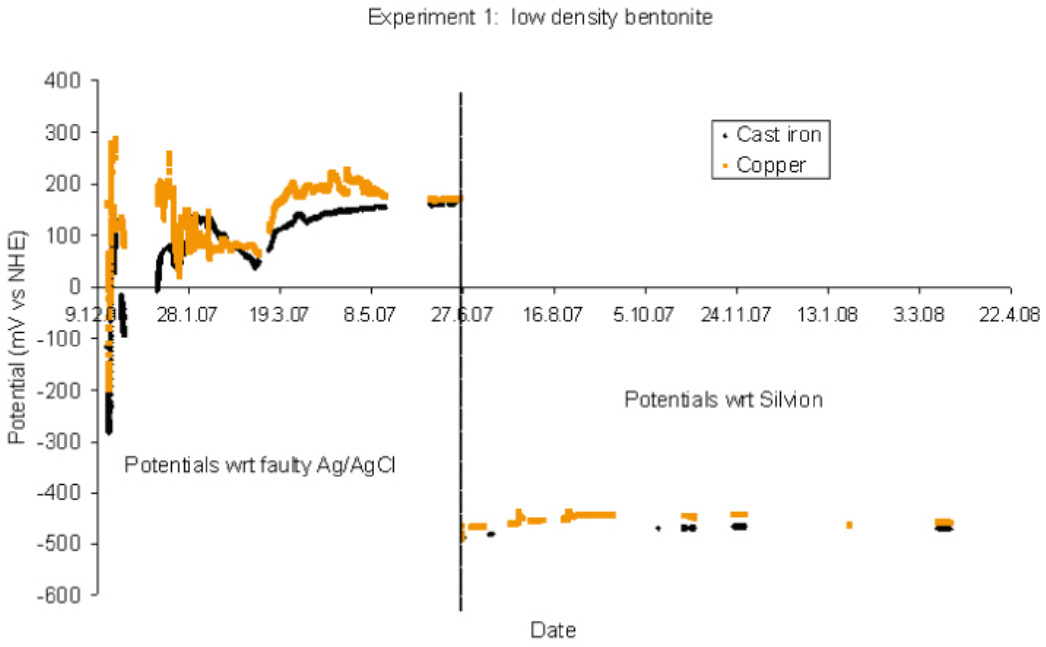

Figure 6-22. *Results of corrosion potential measurements for cast iron and copper electrodes in Experiment 1 (low density bentonite).*

6.3.2 Experiment 2: Low density bentonite

In this experiment the defect in the outer copper shell is at the top end of the canister (i.e. near the lid) but pointing downwards. Figure 6-23 shows the results from the potential measurements for gold, platinum, Eh probe and the model canister.

With Experiment 2, as for Experiment 1, there was a problem with the small Ag-AgCl reference electrodes mounted inside the support cages, but when the measurements were carried out against the external Silvion reference electrode reasonable values were obtained. The Eh value is again slightly more reducing inside the support cage than outside.

The electrochemical potential values for iron and copper are shown in Figure 6-24. As for Experiment 1 it was necessary to measure the values against the Silvion reference electrode because the internal silver-silver chloride electrodes failed. This correction was made after June 2007.

6.3.3 Experiment 3: Low density bentonite

In this experiment there are two defects present in the outer copper shell; the defect near the top lid is pointing upwards, while the defect near the bottom cap is pointing downwards. Figure 6-25 shows the results from the potential measurements for gold, platinum, Eh probe and the model canister. In Experiment 3 the internal Ag-AgCl electrodes worked properly until approximately 8,000 hours had elapsed, when it was necessary to change to the Silvion reference electrode. The fluctuations in Eh inside the support cage appear to be genuine. The Eh value external to the support cage stabilised at ~–300 mV after 3,500 hours.

The electrochemical potential values for iron and copper in Experiment 3 are shown in Figure 6-26. These data show a decrease in the corrosion potential of the copper initially, stabilising at highly negative values. The potentials were subsequently measured against Silvion after failure of the internal silver-silver chloride reference electrodes after approximately 7,500 hours.

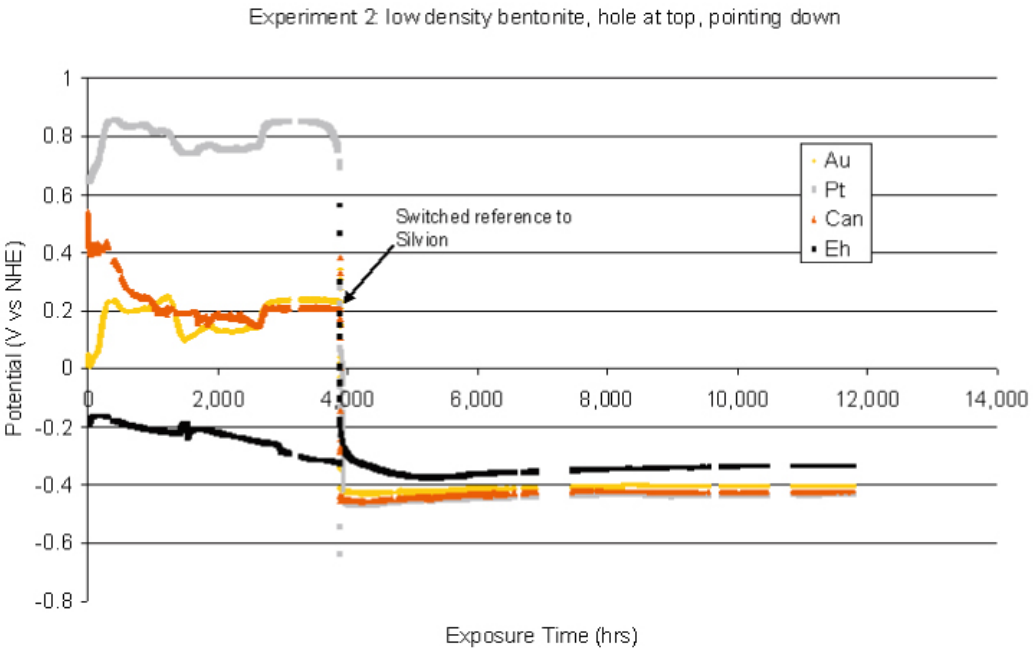

Figure 6-23. *Results of Eh and can potential measurements from Experiment 2 (low density bentonite).*

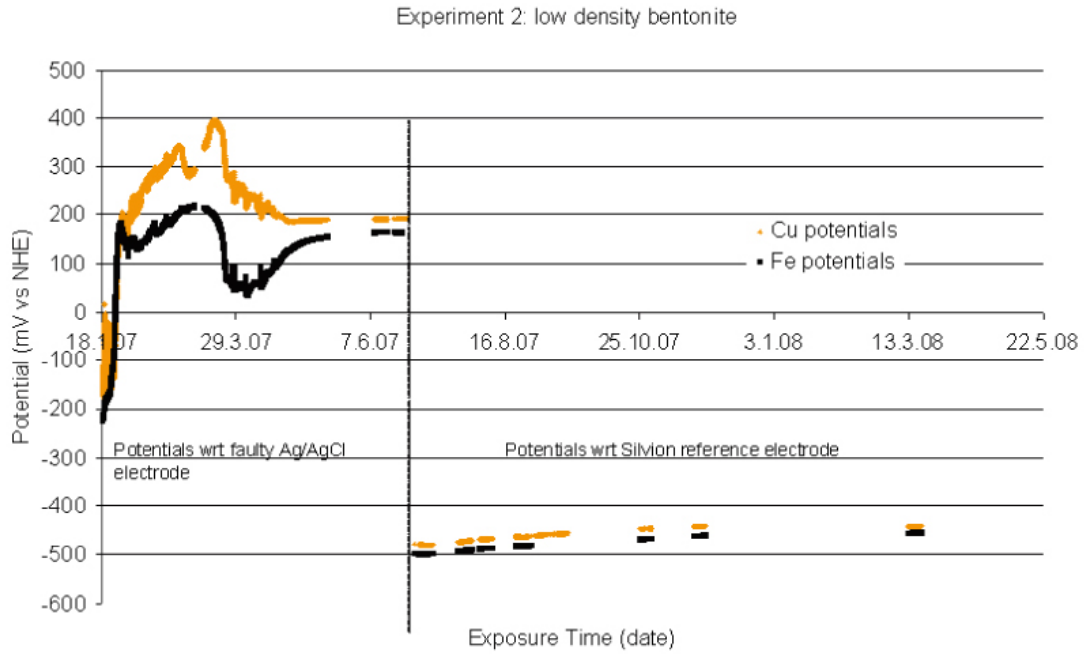

Figure 6-24. *Results of corrosion potential measurements for cast iron and copper electrodes in Experiment 2 (low density bentonite).*

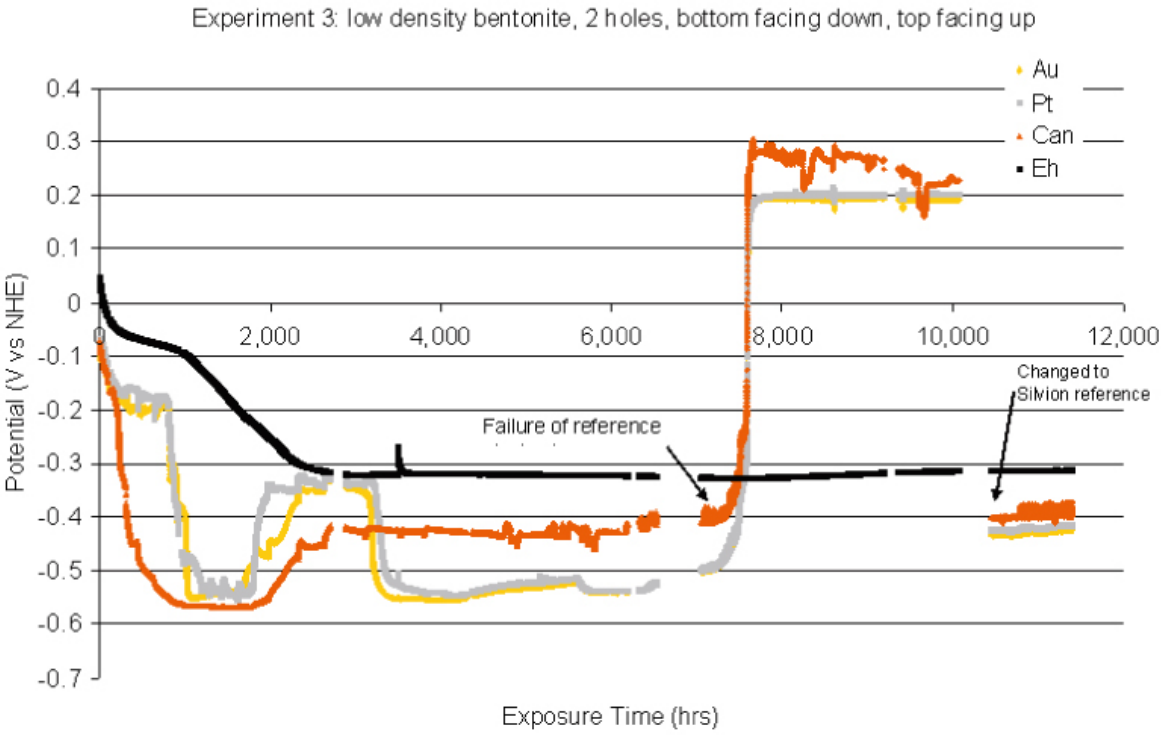

Figure 6-25. *Results of Eh and can potential measurements from Experiment 3 (low density bentonite).*

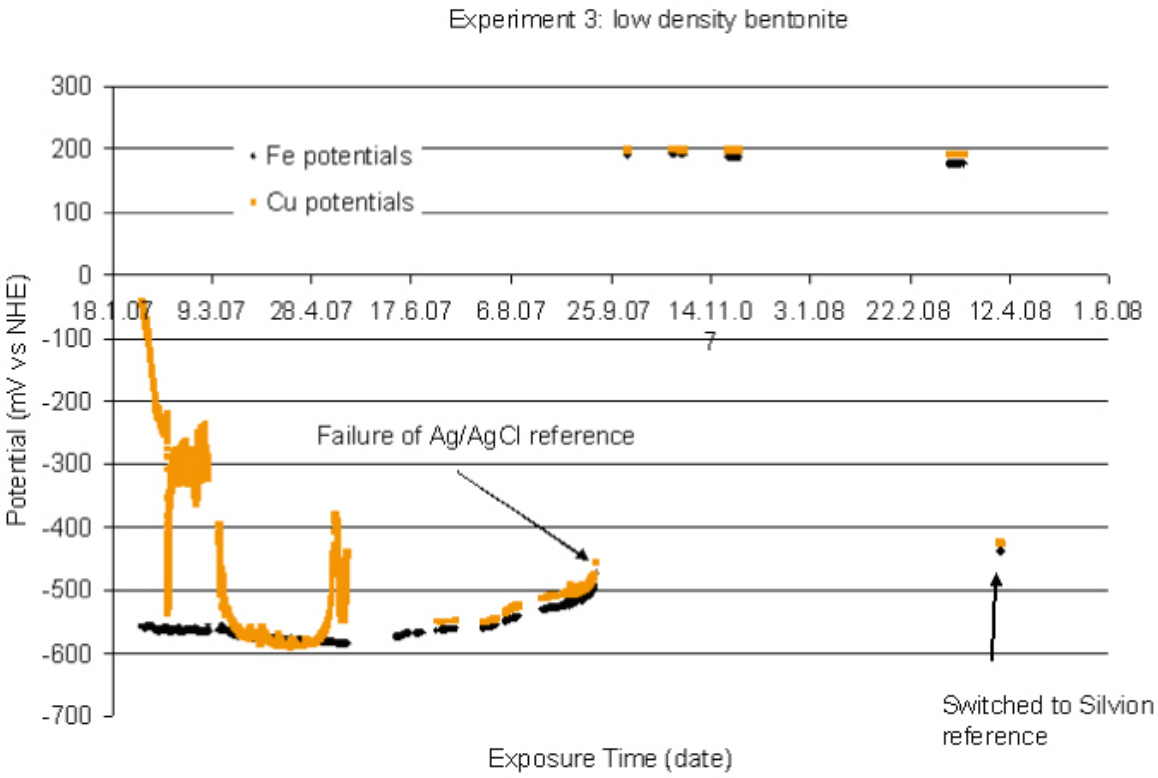

Figure 6-26. *Results of corrosion potential measurements for cast iron and copper electrodes in Experiment 3 (low density bentonite).*

6.3.4 Experiment 4: Compacted bentonite

In Experiment 4 the defect in the outer copper shell is near the top lid but pointing downwards. The whole model canister is surrounded by compacted bentonite, with the test electrodes placed in slots cut into the compacted bentonite. Figure 6-27 shows the results from the potential measurements for gold, platinum, E_h probe and the model canister. The potentials for the platinum exhibited a considerable amount of noise. It was necessary to use the external Silvion reference electrodes to measure the potentials after about 3,500 hours. It is noticeable that the E_h values are not as negative as in the fully saturated bentonite tests.

The electrochemical potential values for copper in Experiment 4 are shown in Figure 6-28. Contact has been lost with the iron electrode in this experiment.

6.3.5 Experiment 5: No bentonite

In this experiment there are two defects in the outer copper shell, both of which are near the top lid. One defect is pointing vertically upwards, the other is pointing downwards. In this experiment there is no bentonite around the model canister (i.e. it is in direct contact with the Äspö groundwater). Figure 6-29 shows the results from the potential measurements for gold, platinum, Eh probe and the model canister. In this experiment there was a problem with both the internal silver-silver chloride reference electrodes and the external Eh probe and the Silvion electrode and so it has been necessary to set up an external reference electrode and Eh probe, mounted on the borehole flange. The iron and copper potentials in this experiment are shown in Figure 6-30. Again there were problems with the small internal Ag-AgCl reference electrodes up to June 2007, after which it was necessary to switch to using the stainless steel flange as a pseudo reference electrode and then to an external reference electrode.

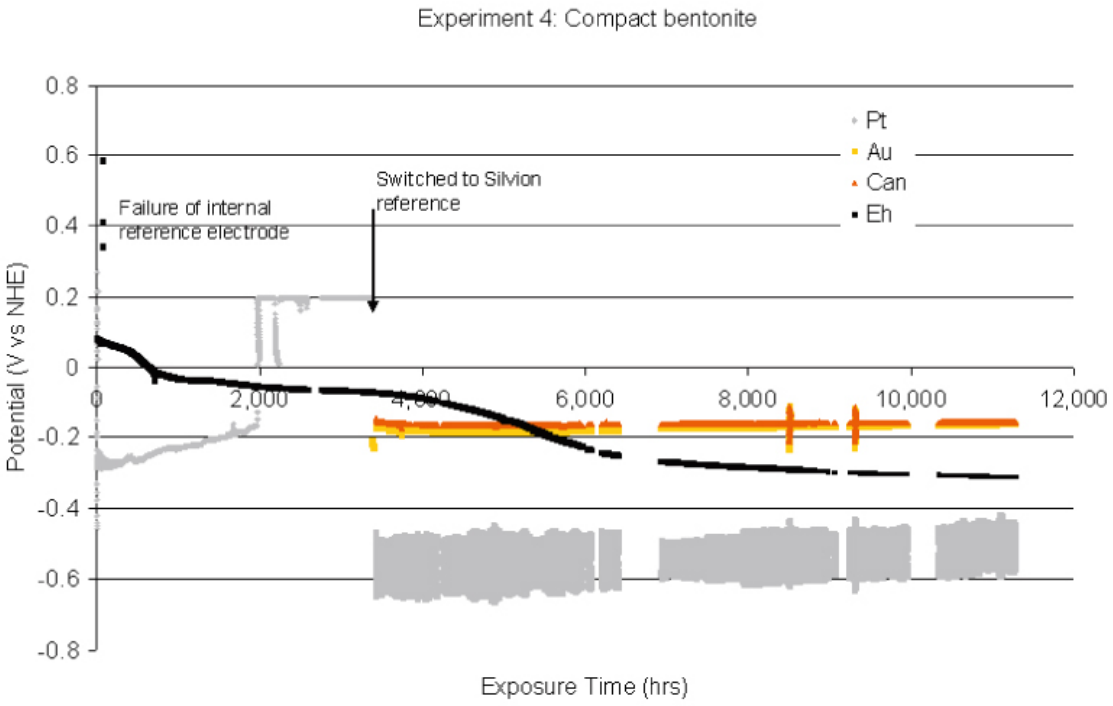

Figure 6-27. *Results of Eh and can potential measurements from Experiment 4 (compact bentonite).*

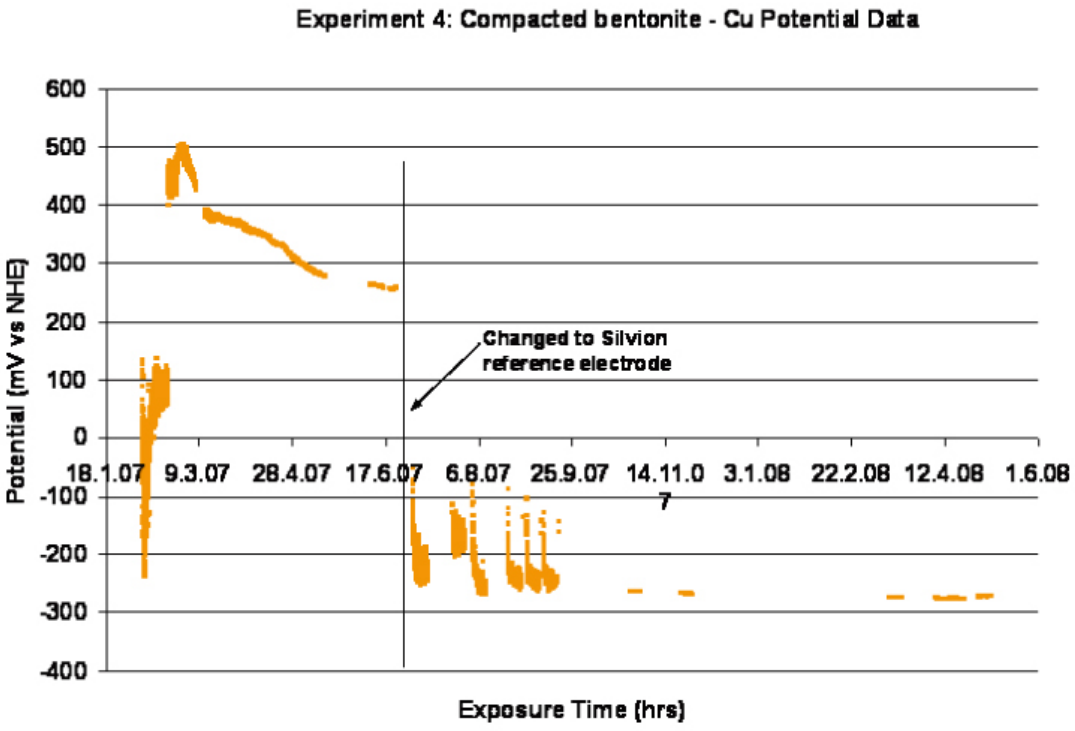

Figure 6-28. *Results of corrosion potential measurements for copper electrodes in Experiment 4 (compact bentonite).*

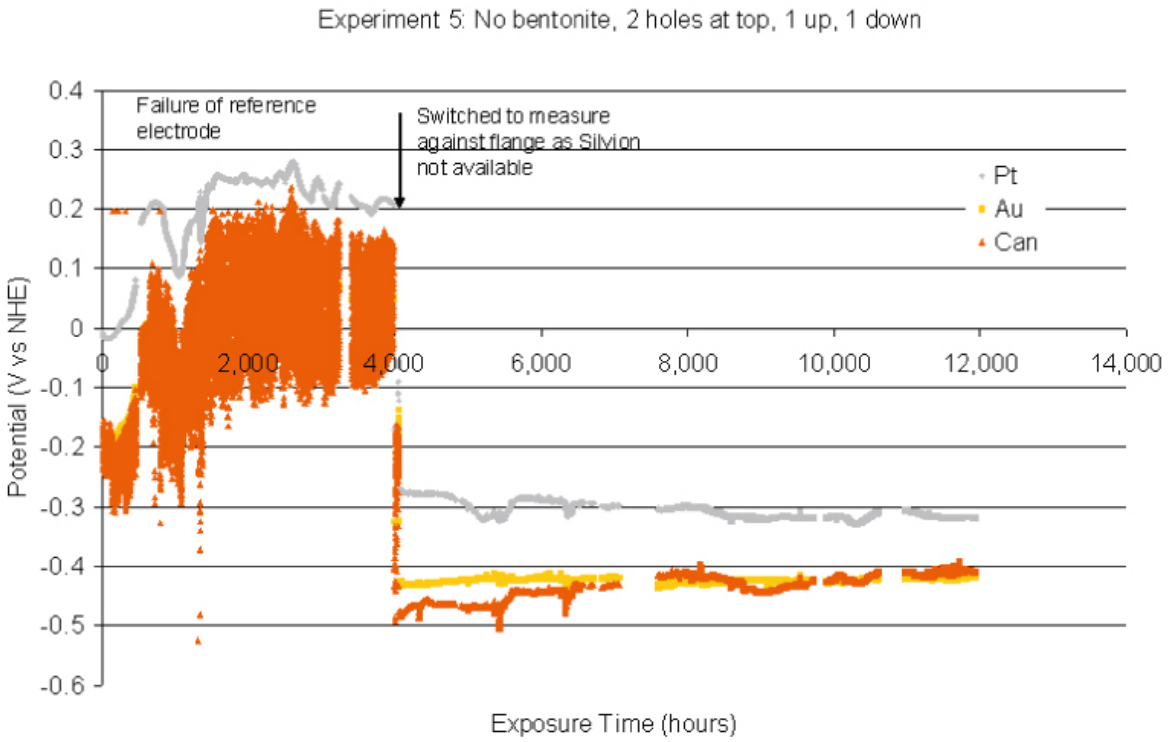

Figure 6-29. *Results of Eh and can potential measurements from Experiment 5 (no bentonite).*

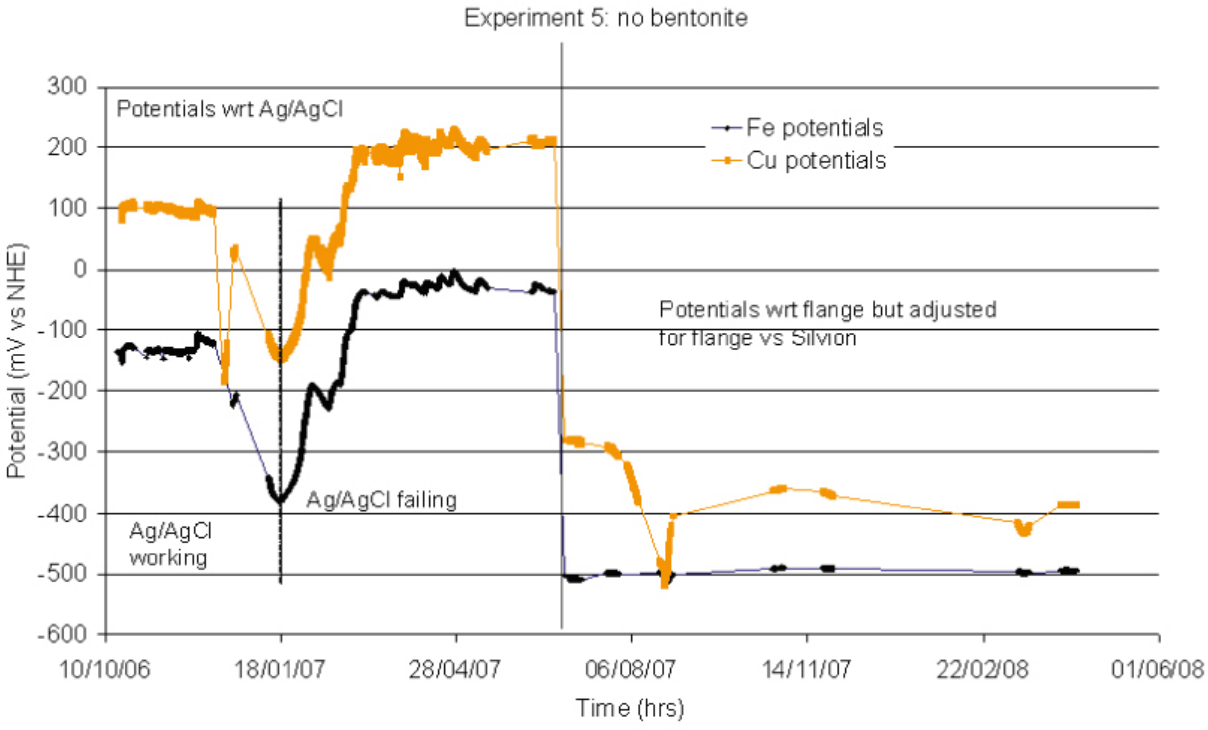

Figure 6-30. *Results of corrosion potential measurements for cast iron and copper electrodes in Experiment 5 (no bentonite; wrt = 'with respect to').*

6.4 Electrochemical corrosion rate measurements

Corrosion rate measurements were carried out using the following electrochemical techniques: linear polarisation resistance, LPR, AC impedance, ACI, and electrochemical noise, ECN. The LPR measurements were carried out over a potential range of ±10 mV with respect to the corrosion potential at a scan rate of 10 mV min^{-1} (starting with the electrode polarised to –10 mV). The corrosion rate is obtained by measuring the slopes of the plots and applying the Stern-Geary approximation /14/, with a Stern-Geary constant of 26 mV. The AC impedance measurements were carried out using a perturbation of ±10 mV, starting at an initial frequency of 10 kHz start and a final frequency of 10 mHz finish, with 100 readings taken per test. The electrochemical noise measurements were carried out at a sampling rate of ten readings per second for a period of one hour. Examples of LPR and AC impedance measurements for copper and iron electrodes in Experiment 1 are shown in Figure 6-31 and Figure 6-32. Good agreement was obtained between the corrosion rates derived from the two techniques.

The corrosion rate values obtained for copper in the five experiments are summarised in Figure 6-33. The values from electrochemical measurements on cast iron are shown in Figure 6-34. Electrochemical noise is a technique used to look for indications of localised corrosion; an example of the data acquired to date is shown in Figure 6-35. These data were obtained by coupling two copper electrodes together and measuring the current and potential noise between them. If localised corrosion was occurring transients would be expected in the results. There is no indication of localised corrosion in this case.

6.5 Copper wire resistance measurements

The results from the electrical resistance measurements on coils of copper wire are shown in Figure 6-36 and Figure 6-37. The resolution of these measurements is expected to increase with increasing measurement period. It appears that the long-term corrosion rate for copper is close to zero in these measurements, but the resolution is rather poor at the moment.

6.6 Pressure and strain gauge data

The strain gauge results for Experiments 1 and 4 are shown in Figure 6-38. Gauges 1a and 1b are showing an initial increase in tensile strain and we are not clear about the explanation for this behaviour. It seems to be too early to be due to expansion caused by a corrosion process.

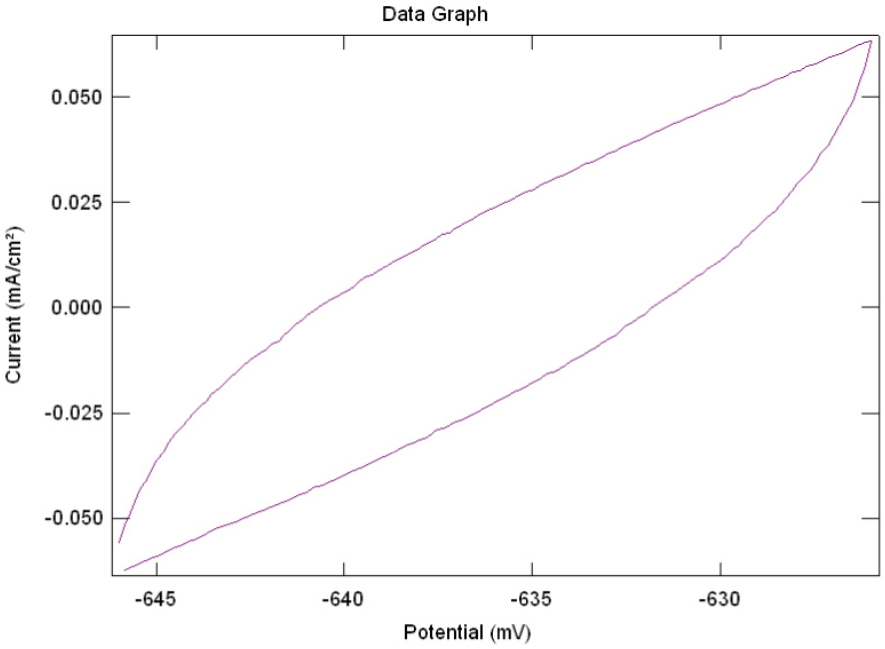

(a)

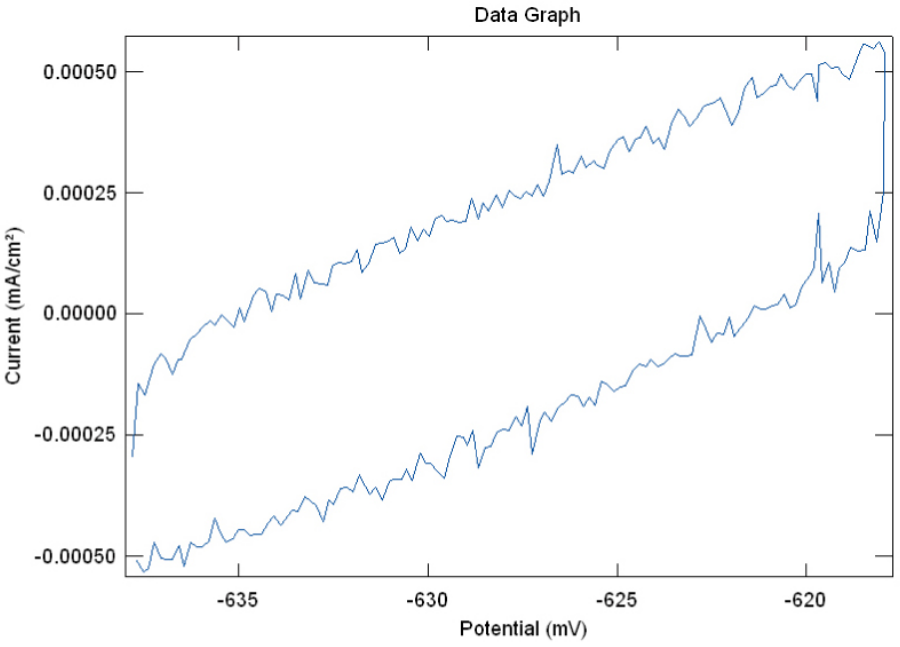

(b)

Figure 6-31. *Typical examples of linear polarisation resistance (LPR) measurements on Experiment 3 : (a) cast iron, (b) copper*

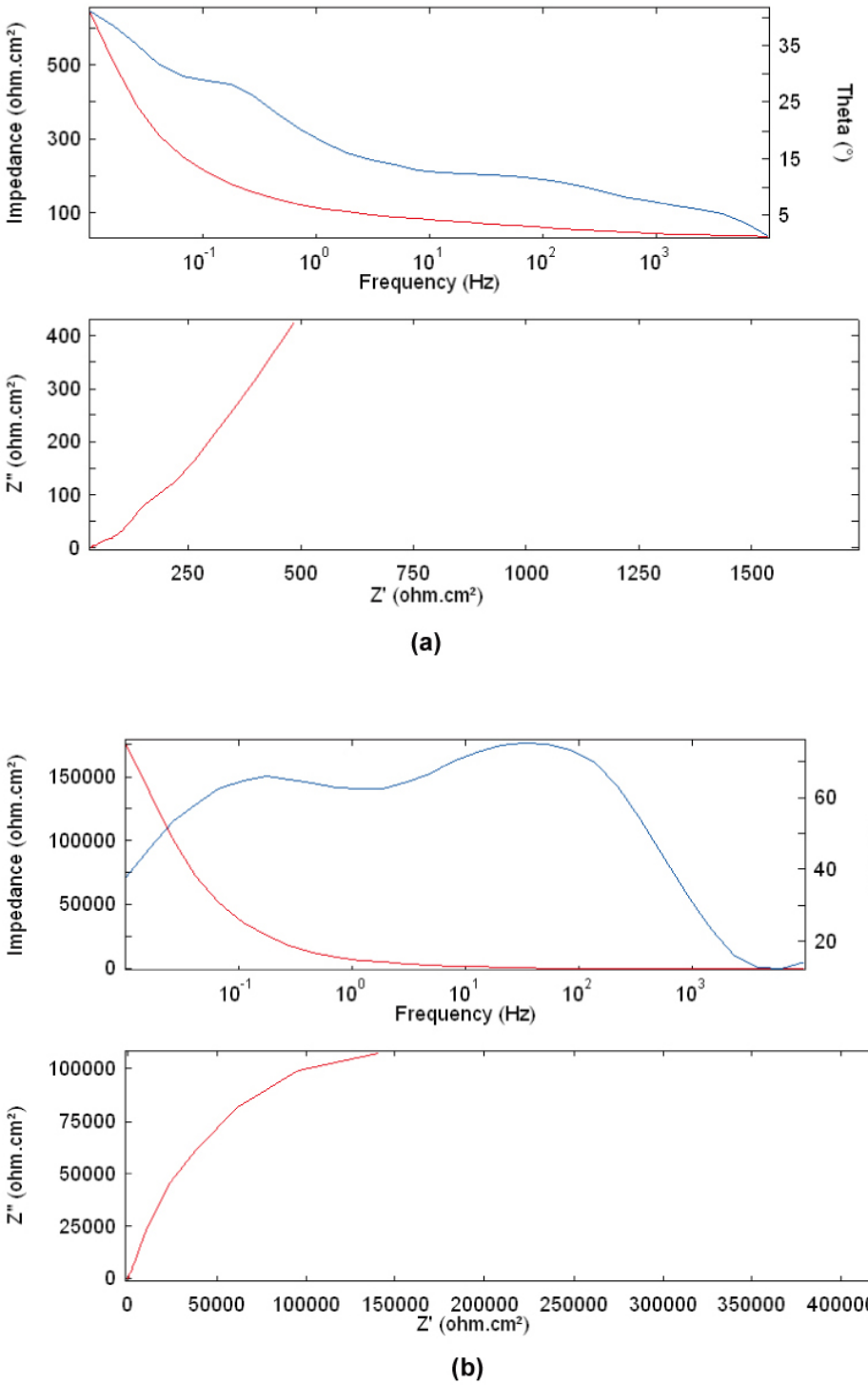

Figure 6-32. *Typical examples of AC impedance measurements (ACI) on Experiment 1: (a) cast iron, (b) copper. Top figure: blue line = theta plot; red line = impedance plot.*

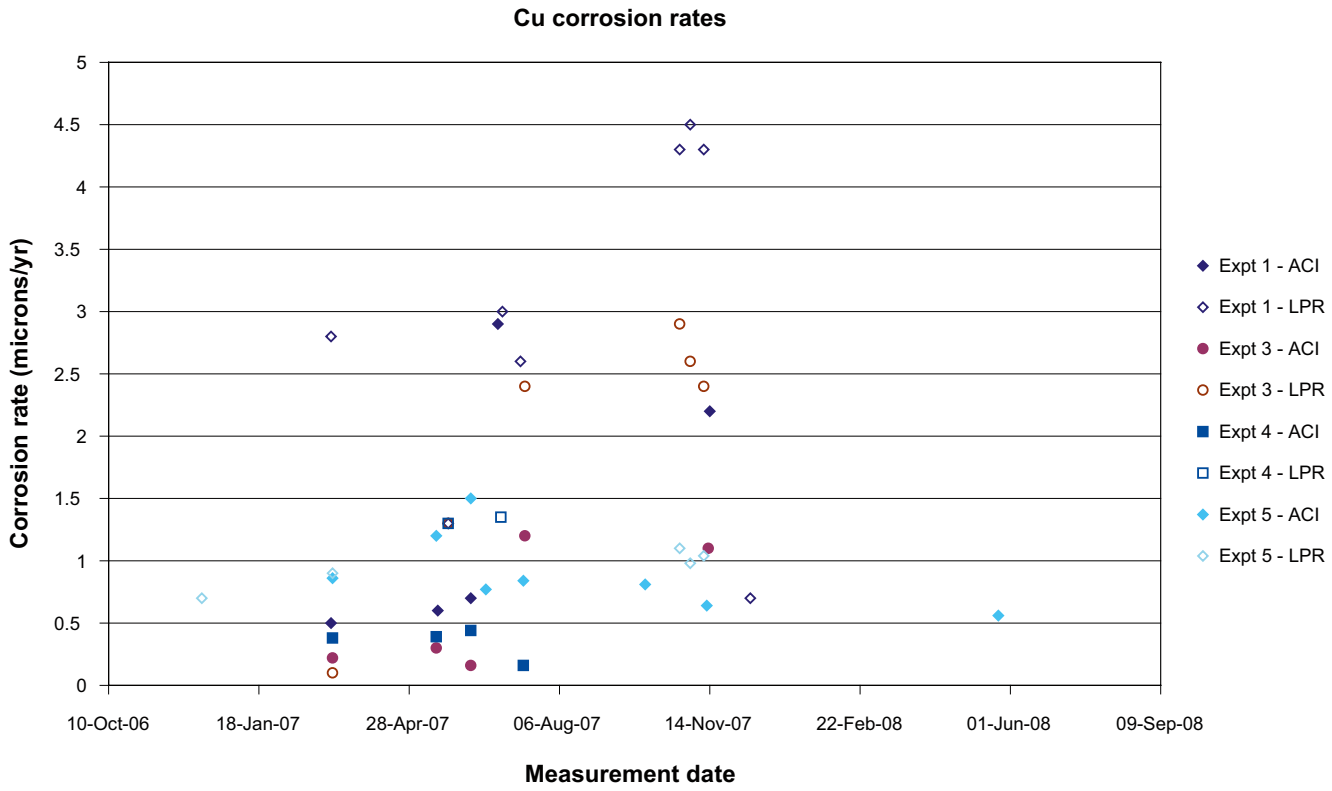

Figure 6-33. *Summary of copper corrosion rates obtained by AC impedance and LPR measurements.*

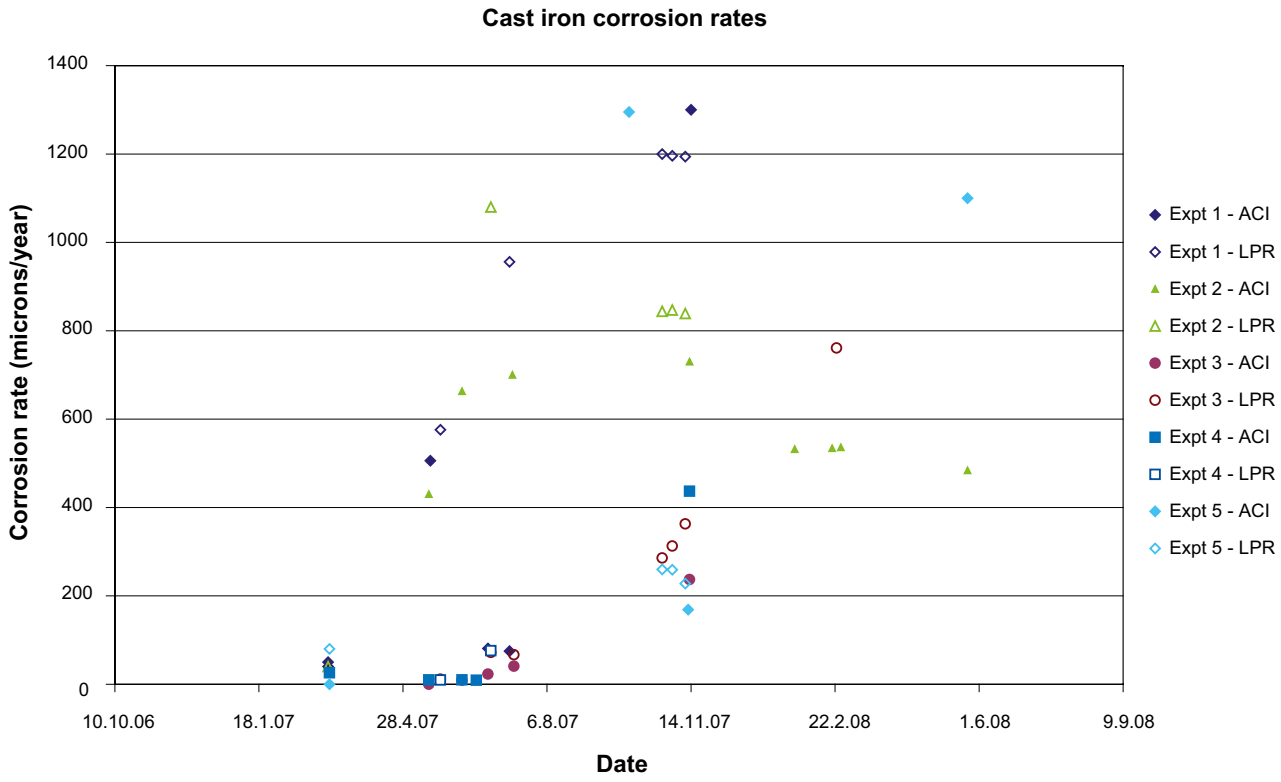

Figure 6-34. *Summary of iron corrosion rates obtained by AC impedance and LPR measurements.*

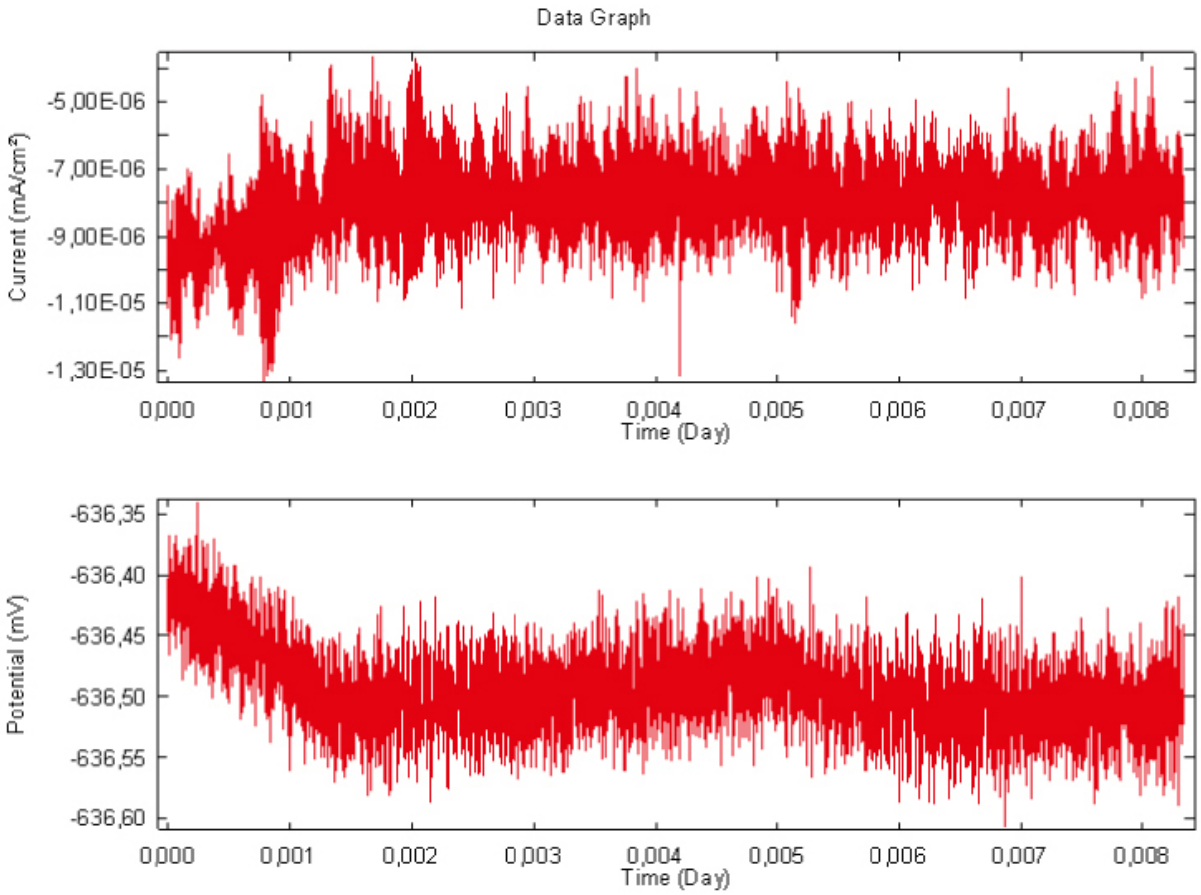

Figure 6-35. *Results from electrochemical noise measurements for a pair of copper electrodes in Experiment 2 (low density bentonite).*

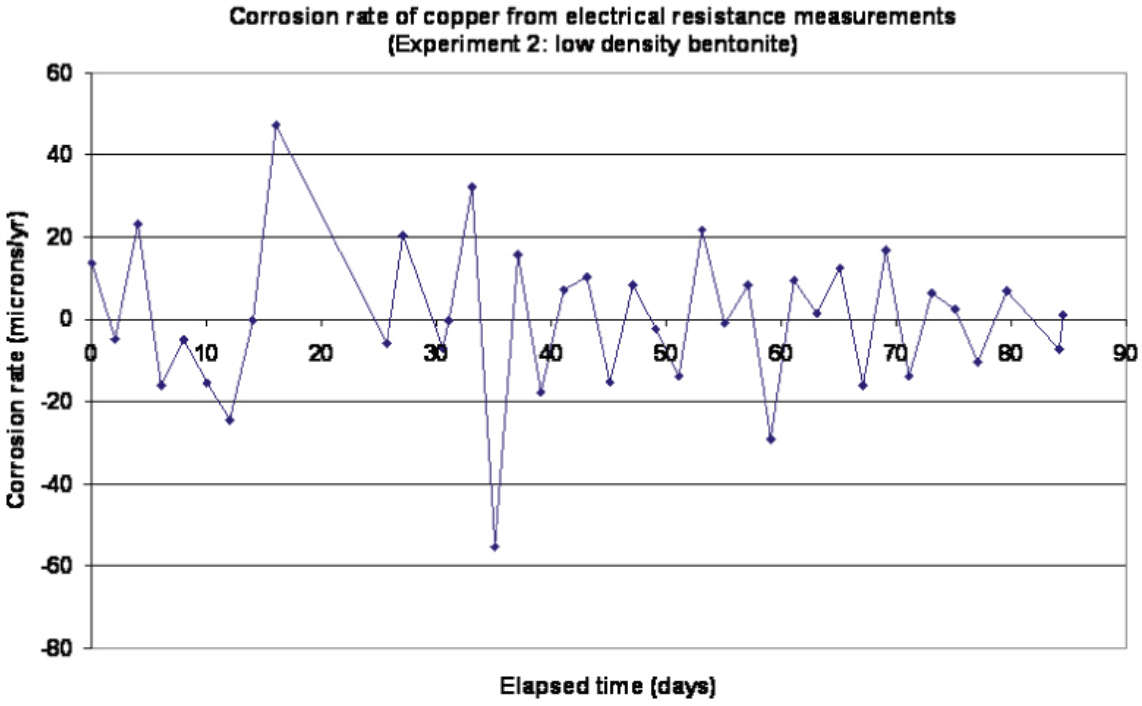

Figure 6-36. *Results of corrosion rate measurements from copper wire electrical resistance measurements (experiment 2: low density bentonite).*

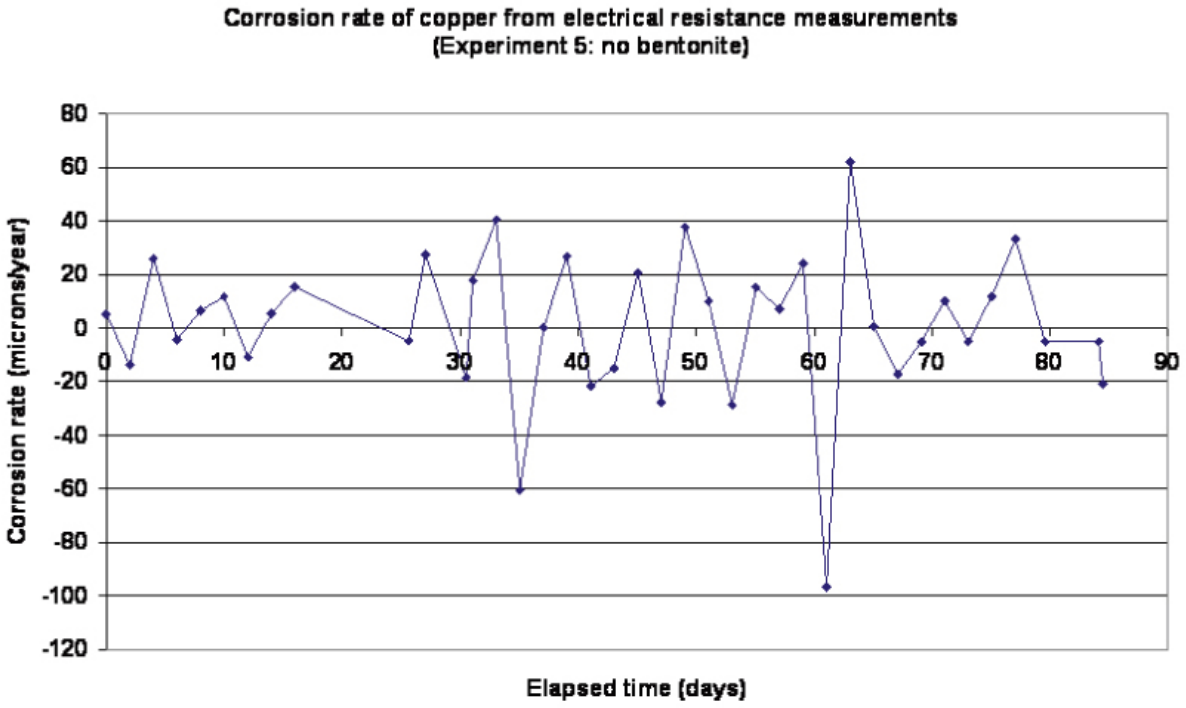

Figure 6-37. *Results of corrosion rate measurements from copper wire electrical resistance measurements (experiment 5: no bentonite).*

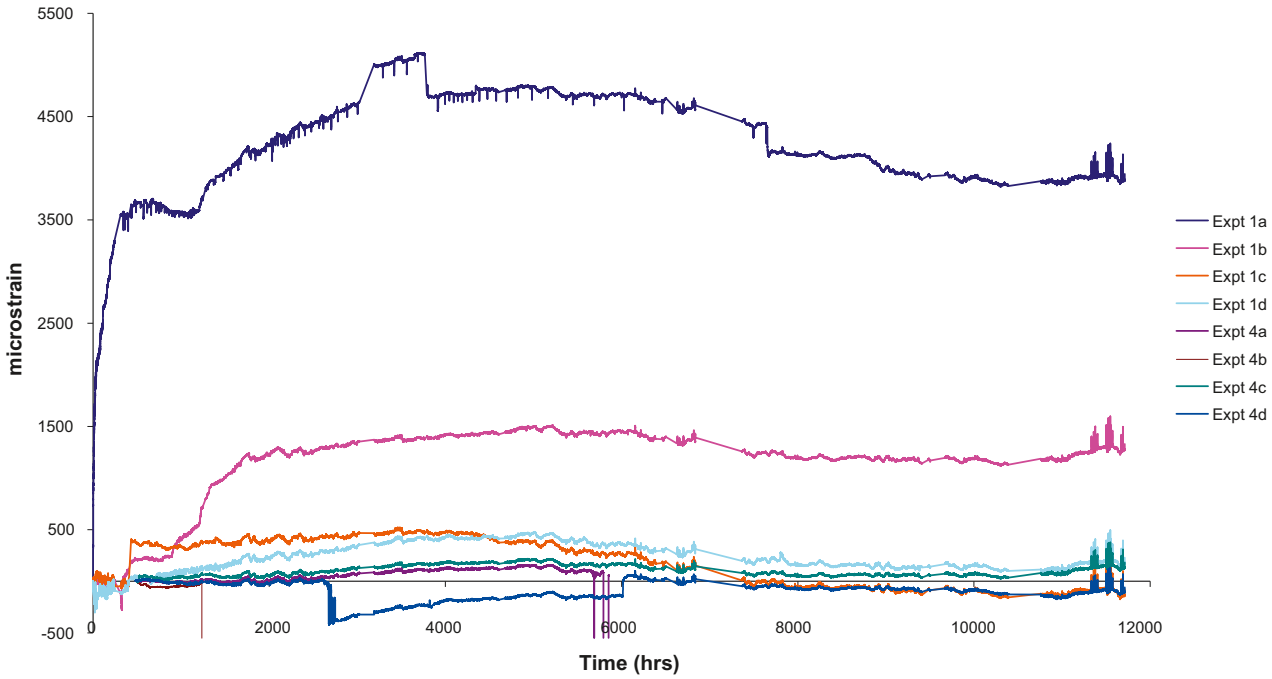

Figure 6-38. *Strain gauge results from Experiments 1 and 4.*

7 Discussion

7.1 Water analysis and microbial activity

There are a number of interesting features regarding the results of the water analysis from the model canister experiments. In general, the groundwater composition outside the support cages does not vary significantly between boreholes. Firstly, there is a marked increase in the iron concentration inside the model canister support cage (Figure 6-10) compared to the surrounding water in the borehole. This is accompanied by an increase in the concentration of nickel and chromium (Figure 6-13 to Figure 6-17). This increase in dissolved metal concentration could be due to corrosion of the stainless steel support vessel, the cast iron coupons, and/or the cast iron insert itself, which will be in contact with groundwater as a result of the defect in the outer copper canister. The concentration of chromium and nickel is much lower than the concentration of iron, suggesting that most of the iron results from corrosion of the cast iron, rather than stainless steel, unless there is some kind of selective dissolution of the stainless steel occurring.

Figure 6-11 shows that there is a decrease in the pH inside the support cage compared to outside the support cage. This could be a result of the microbial activity inside the support cage, as shown by Figure 6-19. The gas analysis data (Table 9) show the very low oxygen content of the groundwater and the presence of helium and methane from geological sources.

The enhanced corrosion of the iron and/or stainless steel, as shown by the high concentrations of dissolved metals, would not be expected in anoxic near-neutral water at low temperature, even with the high concentrations of chloride present, based on the results of laboratory experiments in the absence of microbial activity. This result suggests that the corrosion is enhanced by microbial activity. This may also account for the high corrosion rates or iron measured electrochemically. It should be noted that the concentration of dissolved copper was very low.

Figure 6-19 indicates that autotrophic acetogens and sulphate reducing bacteria, SRBs are active in the vicinity of the model canisters. The key metabolic reactions for these species are:

Autotrophic acetogens: $4H_2 + 2CO_2 \Rightarrow CH_3COO\text{-} + H^+ + 2H_2O$

Sulphate reducing bacteria: $CH_3COOH + SO_4^{2-} \Rightarrow H_2S$ and $Fe^{2+} + H_2S \Rightarrow FeS + 2H^+$

The acetogens produce acetate, which can cause stress corrosion cracking (SCC) of copper, and sulphur from SRB activity is detrimental to copper. In principle, hydrogen produced by the anaerobic corrosion of iron could drive the activity of the acetogens and hence there is a possibility of autocatalytic behaviour. The processes summarised above are consistent with the measured fall in pH and the increase in corrosion rate and release of iron observed during these experiments. A more detailed assessment of the microbial activity analysis will be presented in a subsequent report.

7.2 Electrochemical measurements

The electrochemical potentials of the gold, platinum and the miniature canisters are indicative of very low oxygen concentrations. The electrochemical potential values obtained for the gold in the Model Canister experiments are comparable to the electrochemical potential values obtained during laboratory investigations of galvanic corrosion of iron-copper couples in anoxic conditions /11, 15/, and the anaerobic corrosion of iron /16, 17/. They are also comparable to E_h values reported in the literature for the E_h value of deep Swedish groundwaters /18, 19/. The data show that for Experiments 1 to 3, with low density bentonite, the E_h outside the cage is slightly higher than inside the cage, whereas for Experiment 4, with compacted bentonite the situation is reversed.

The corrosion potential of the copper and the model canisters can be compared with other measurements and modelling activities /18/; for example the predicted long-term corrosion potential of a copper canister in compacted bentonite is shown in Figure 7-1 (NB: this calculation was for an initially aerated repository). These modelling calculations show that the predicted short-term corrosion potential for a

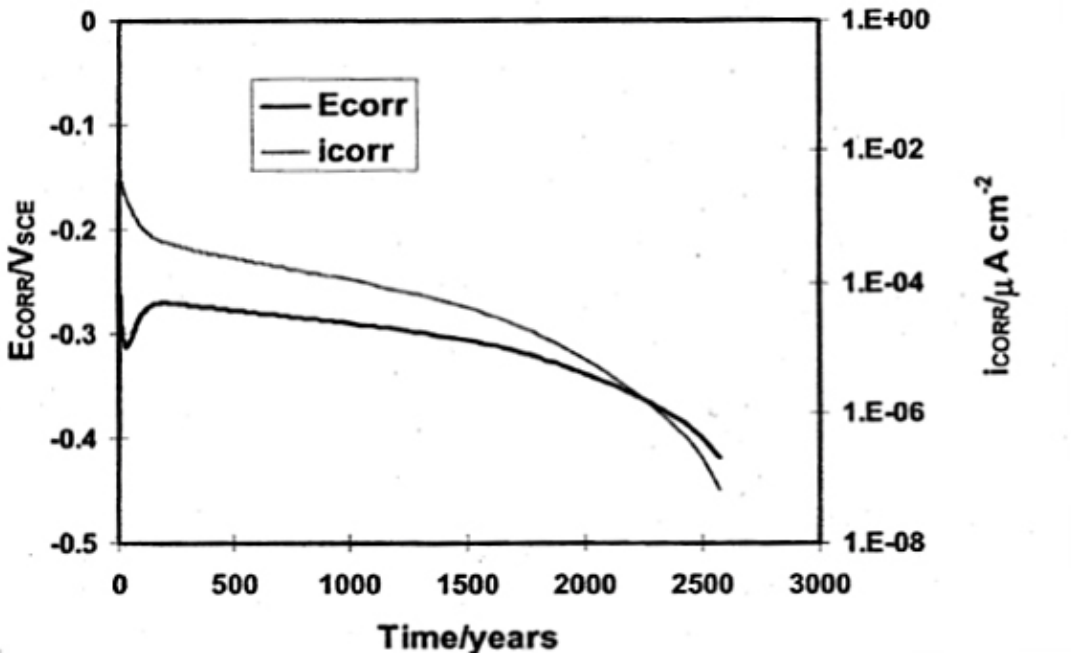

Figure 7-1. *Predicted time dependence of the corrosion potential (Ecorr) and corrosion current (Icorr) of a copper canister in a Canadian repository [18].*

copper canister is of the order of –300 mV vs SCE (i.e. ~ –50 mV vs NHE). This is more positive by approximately 100 mV than the value measured in Experiment 4 for the model canister embedded in compact bentonite (Figure 6-27). The potential of the copper electrode in the same experiment was similar to that of the copper canister (Figure 6-28).

The potentials of the iron electrodes are below the hydrogen evolution potential at pH 7 and are consistent with the occurrence of anaerobic corrosion.

7.3 Corrosion rate measurements

These corrosion rates for iron are quite high and appear to be increasing with time. They are considerably higher than would be expected from laboratory experiments on the anaerobic corrosion on iron /20, 21/. They have to be treated with some caution as electrochemical measurements tend to overestimate the true values, since they only provide an instantaneous measure of corrosion rate, which is based on a number of assumptions about the nature of the electrochemical interface. The overall corrosion rates will be checked against weight loss measurements at the end of the experiments (i.e. a long-term integrated measurement of corrosion rate). There is also a possibility that crevice corrosion might be occurring if the environmental conditions are correct, although it is normally believed that crevice corrosion is not possible in anoxic conditions. The high rates reported here may support the observation of increased iron concentrations in the water analyses. It is possible that the high rates may be a result of microbial activity inside the support cage (see Section 6.2.2).

The electrochemical measurements of corrosion rate indicate corrosion rate values for copper up to values of ~3 μm yr^{-1} (Figure 6-33). This is based on a Stern-Geary constant of 26 mV, whereas other authors (e.g. /22/) have used lower values. Thus the figures reported here are conservative values. These are consistent with the electrical resistance measurements which indicate values close to zero, but with a large scatter. The resolution of these measurements should improve with elapsed time. The derived corrosion rate values can be compared with values given in the literature for experiments on copper in compacted bentonite; for example values of up to 2.5 μm yr^{-1} have been reported by Rosborg et al. /22/ for measurements during the LOT experiment and 4.7 μm yr^{-1} by Saario et al /23/ for weight loss measurements on copper in compacted bentonite in laboratory tests.

7.4 Future programme

It is envisaged that the model canister experiments will run for a period of at least five years after which the test assemblies will be withdrawn from the boreholes for examination. There may be a rolling programme of dismantling the experiments, combined with setting up some new experiments. This would enable the design of the experiment to be modified during the course of the project, if necessary. After dismantling, detailed analysis of the container and the surrounding bentonite matrix will be carried out (e.g. to determine the profile of any iron and/or copper released from the model canisters into the bentonite).

After withdrawal from the boreholes, the model canisters will be transported to Culham, U.K. whilst sealed in an inert atmosphere, where they will be placed in a nitrogen-purged glovebox and dismantled. Appropriate surface analyses of samples cut from the model canisters will then be carried out (e.g. SEM, EMPA, Raman, etc) to address the issues listed in Section 1. Tests will be carried out to identify the type of microbes present.

Weight loss measurements will be carried out on the corrosion coupons and the copper-cast iron-copper sandwich specimens will be removed and analysed to determine the nature of the corrosion product and the extent of any ‘jacking’ effects. The coupons used for electrochemical measurements will be removed and examined for corrosion.

Until such time as the experiments are removed for examination, automated monitoring and analysis of the data will continue. A further campaign of water analysis, including gas analysis and microbial analysis, is planned for October 2008. It was decided to halt the previous water sampling campaign to allow the experiments to equilibrate without disturbance for a longer period.

8 Conclusions

The main conclusions from the work to date are as follows:

1. The model canister experiments have been successfully set up. Although failure of some of the reference electrodes has occurred, built in redundancy has enabled the experiments to continue.
2. Water analyses have shown an increased concentration of iron and a decrease in pH inside the support cages, which may be associated with microbial activity (particularly by SRBs) affecting the corrosion rate of iron-based materials in the experiment (i.e. cast iron and/or stainless steel).
3. The measured E_h values are compatible with published literature and show a fall in E_h with time as any residual oxygen is consumed. This is confirmed by dissolved gas analysis.
4. The electrochemical corrosion rate measurements are compatible with published literature, but they need to be confirmed by weight loss measurements when the experiments are dismantled.

9 Acknowledgements

The authors gratefully acknowledge assistance provided by the following:

- Serco: Paul Fennell, Geoff Knowles, Joe Deane, Bharti Reddy and David Spencer.
- SKB: Lars Werme, Richard Bäck, Mats Lundqvist, Tereseta Morales, SKB chemistry laboratory staff at Äspö.
- Clay Technology: Ola Karnland.
- Microbial Analytics: Prof. Karsten Pedersen and Sara Eriksson.

The authors also gratefully acknowledge financial support provided by SKB for conducting this project.

10 References

/1/ **Smart N R, Fennell P A H, Rance A P, 2005.** Expansion Due to Anaerobic Corrosion of Iron, SA/EIG/15031/C001.

/2/ **Smart N R, Bäck R, Fennell P A H, Knowles G, Lundqvist M, Rance A P, Reddy B, Spencer D, Werme L O, 2007.** In Situ Corrosion Testing Of Miniature Copper-Cast Iron Radioactive Waste Canisters, Corrosion, Extended abstract, Research in Progress Symposium, Nashville, March 2007.

/3/ **Smart N R, Fennell P A H, Knowles G, 2005.** Design of Model Canister Experiments, SA/EIG/11080/C001.

/4/ **C-G Andersson, 2002.** Development of Fabrication Technology for Copper Canisters with Cast Inserts, SKB TR-02-07, Svensk Kärnbränslehantering AB.

/5/ **Smart N R, Blackwood D J, Werme L, 2001.** The Anaerobic Corrosion of Carbon Steel and Cast Iron in Artificial Groundwaters, SKB TR-01-22, Svensk Kärnbränslehantering AB.

/6/ **Bond A E, Hoch A R, Jones G D, Tomczyk A J, Wiggin R M, Worraker W J, 1997.** Assessment of a Spent Fuel Disposal Canister. Assessment Studies for a Copper Canister with Cast Steel Inner Component, SKB TR-97-19, Svensk Kärnbränslehantering AB.

/7/ **Karnland O, Sandén T, Johannesson L E, Eriksen T E, Jansson M, Wold S, Pedersen K, Motamedi M, Rosborg B, 2000.** Long Term Test of Buffer Material. Final Report on the Pilot Parcels, SKB TR-00-22, Svensk Kärnbränslehantering AB.

/8/ **Gunnarsson D, Börgesson L, Hökmark H, Johannesson L E, Sandén T, 2001.** Report on the Installation of the Backfill and Plug Test, SKB IPR-01-17, Svensk Kärnbränslehantering AB.

/9/ **Johannesson L E, Gunnarsson D, Sandén T, Börgesson L, 2004.** Karlzén R, Prototype Repository. Installation of Buffer, Canisters, Backfill, Plug And Instruments in Section ll, SKB IPR-04-13, Svensk Kärnbränslehantering AB.

/10/ **Saario T, 2004.** Effect of the Degree of Compaction of Bentonite on the General Corrosion Rate of Copper, presented at EuroCorr 2004, Nice, 2004.

/11/ **Smart N R, Rance A P, Fennell P A H, 2004.** Galvanic Corrosion of Copper-Cast iron Couples, SA/EIG/13974/C001.

/12/ **Puigdomenech I, et al. 2000.** O2 Consumption in a Granitic Environment, in Scientific Basis for Nuclear Waste Management XX111, Materials Research Society Symposium Proceedings Volume 608, R.W. Smith, D.W. Shoesmith (eds.), p. 179.

/13/ **Puigdomenech I, Ambrosi J P, Eisenlohr L, Lartigue J E, Banwart S A, Bateman K, Milodowski A E, West J M, Griffault L, Gustafsson E, Hama K, Yoshida H, Kotelnikova S, Pedersen K, Michaud V, Trotignon L, Rivas Perez J, 2001.** O2 Depletion in Granitic Media. The Rex Project, SKB TR-01-05, Svensk Kärnbränslehantering AB.

/14/ **ASTM standard G59-97e1, Standard Test Method for Conducting Potentiodynamic Polarization Resistance Measurements, 2003.**

/15/ **Smart N R, Fennell P A H, Rance A P, Werme L O, 2004.** Galvanic Corrosion of Copper-Cast Iron Couples in Relation to the Swedish Radioactive Waste Canister Concept, presented at Eurocorr 2004, Nice, September, 2004; Published in a separate volume: pg. 52 in Prediction of Long Term Corrosion Behaviour in Nuclear Waste Systems, Proceedings of 2nd International Workshop, Nice, September 2004, Eurocorr 2004, published by Andra in Science and Technology Series.

/16/ **Peat R, Brabon S, Fennell P A H, Rance A P, Smart N R, 2001.** Investigation of Eh, pH and Corrosion Potential of Steel in Anoxic Groundwater, AEAT/R/PS-0028, issue 1, 2000 and SKB TR-01-01, Svensk Kärnbränslehantering AB.

/17/ **Smart N R, Fennell P A H, Peat R, Spahiu K, Werme L, 2001.** Electrochemical Measurements During The Anaerobic Corrosion Of Steel, Materials Research Society Symposium Proceedings Volume 663, Scientific Basis for Nuclear Waste Management XXIV, K.P. Hart and G.R. Lumpkin (eds.), p. 487–495.

/18/ **King F, Ahonen L, Taxen C, Vuorinen U, Werme L, 2001.** Copper Corrosion Under Expected Conditions in a Deep Geological Repository, SKB TR-01-23, Svensk Kärnbränslehantering AB.

/19/ **Puigdomenech I, Ambrosi J P, Eisenlohr L, Lartigue J E, Banwart S A, Bateman K, Milodowski A E, West J M, Griffault L, Gustafsson E, Hama K, Yoshida H, Kotelnikova S, Pedersen K, Michaud V, Trotignon L, Rivas Perez, Tullborg E L, 2001.** O2 Depletion in Granitic Media. The REX project, SKB TR-01-05, Svensk Kärnbränslehantering AB.

/20/ **Smart N R, Blackwood D J, Werme L, 2002.** Anaerobic Corrosion of Carbon Steel and Cast Iron in Artificial Groundwaters: Part 1–Electrochemical Aspects, Corrosion 58(7), 547.

/21/ **Smart N R, Blackwood D J, Werme L, 2002.** Anaerobic Corrosion of Carbon Steel and Cast Iron in Artificial Groundwaters: Part 2-Gas Generation, Corrosion 58(8), 627.

/22/ **Rosborg B, Eden D, Karnland O, Pan J, Werme L, 2004.** Real-time Monitoring of Copper Corrosion at the Äspö Laboratory, presented at Eurocorr 2004, Nice, September, 2004; Published in a separate volume: pg. 10 in Prediction of Long Term Corrosion Behaviour in Nuclear Waste Systems, Proceedings of 2nd International Workshop, Nice, September 2004, Eurocorr 2004, published by Andra in Science and Technology Series.

/23/ **Saario T, Betova I, Heinonen J, Kinnunen P, Lilja C, 2004.** Effect of the Degree of Compaction of Bentonite on the General Corrosion Rate of Copper, presented at Eurocorr 2004, Nice, September, 2004; Published in a separate volume: pg. 45 in Prediction of Long Term Corrosion Behaviour in Nuclear Waste Systems, Proceedings of 2nd International Workshop, Nice, September 2004, Eurocorr 2004, published by Andra in Science and Technology Series.

ISSN 1404-0344
CM Gruppen AB, Bromma, 2009